

STOCHASTIC MODELS OF AGE-STRUCTURED POPULATIONS

A THESIS PRESENTED FOR THE DEGREE OF

DOCTOR OF PHILOSOPHY OF IMPERIAL COLLEGE LONDON

AND THE

DIPLOMA OF IMPERIAL COLLEGE

BY

FRANCESCO PUCCIONI

DEPARTMENT OF MATHEMATICS

IMPERIAL COLLEGE

180 QUEEN'S GATE, LONDON SW7 2AZ

30 July 2024

Copyright

The copyright of this thesis rests with the author. Unless otherwise indicated, its contents are licensed under a Creative Commons Attribution-Non Commercial 4.0 International Licence (CC BY-NC). Under this licence, you may copy and redistribute the material in any medium or format. You may also create and distribute modified versions of the work. This is on the condition that: you credit the author and do not use it, or any derivative works, for a commercial purpose. When reusing or sharing this work, ensure you make the licence terms clear to others by naming the licence and linking to the licence text. Where a work has been adapted, you should indicate that the work has been changed and describe those changes. Please seek permission from the copyright holder for uses of this work that are not included in this licence or permitted under UK Copyright Law.

Declaration of Originality

I hereby certify that this thesis is the result of my own original work. Any research, ideas, or quotations sourced from collaborators or other individuals, whether published or unpublished, have been fully acknowledged and referenced in accordance with the accepted citation practices of the discipline

Francesco Puccioni

ABSTRACT

The following work is a study on population dynamics and investigates the interplay between individuals heterogeneity and randomicity in natural systems. This thesis consists of two parts: the implementation of a theoretical framework to model the stochastic evolution of structured populations and, in the second part, a set of applications to real natural scenarios.

The initial chapter, Chapter 1, provides a historical introduction to population modelling, justifies the theoretical nature of this work and alleviates the theoretical burden of Chapter 2.

In Chapter 2, a framework to quantify the stochastic evolution of age-structured populations is presented, and, at its core, it is founded on a functional Chapman-Kolmogorov Equation. The reader will also be provided (in Chapter 3) with the main Monte Carlo methods to simulate age-structured dynamics.

In the first application, an age-structured division-death process is studied, Chapter 4. Such an application aims to quantify the fractional killing of cancer cells despite drug treatment. In periodic drug environments, we discover peaks, named "survival resonance", in the survival probabilities of cells for specific configurations, unseen in unstructured populations.

An additional take on age-structured division-death models is taken in chapter 5 to investigate survival strategies exploited by bacterial or cancer cell to evade drug treatment. Modelling periodic treatments, we recovered the survival resonance and displayed additional extinction peaks.

As a last application, a compartmental epidemic model is considered. The interplay between stochastic dynamics and age heterogeneity and its consequences on the dynamics are evident in this study, where a few methods are also presented to describe such scenarios. This chapter showcases the flexibility of the theoretical framework for a model not belonging to the class of branching processes.

Acknowledgements

I have always seen mathematics and physics as invaluable tools, ones I first discovered during the challenging years of my adolescence. Despite the initial struggles, I've never wavered in my belief in the power and freedom that these fields offer. My journey was often solitary, and to most of my family and friends, it remained something of a mystery. Because of this, I am deeply grateful to the brilliant minds who joined me along the way.

First and foremost, I must thank Dr. Philipp Thomas, who supervised my research over the last four years. Without him, I would not be where I am today, and I certainly wouldn't have grown as a researcher. It was truly an honour to work alongside such a brilliant yet humble individual.

I am also indebted to Johannes Paush, my mentor and colleague. Through our collaboration, I learned how crucial work ethic is to becoming a dependable researcher. I'm grateful to Johannes for recommending so many invaluable references, now gems in my personal library. My heartfelt thanks also go to Paul, Dimitris, Zekai, Hannah, and Fern. Our group saw people come and go, but I'm confident it will continue to thrive under Philipp's leadership.

I would also like to thank Prof. Vahid Shahrezaei and Dr. Farshid Jafarpour. Their insightful feedback and honest questions made this work more coherent and polished in its presentation.

My mother and father have been a constant source of support over the past four years. Their unwavering love and encouragement have meant the world to me. While they may never have fully understood what I was doing, they have always supported me, and I will forever be grateful for that.

Finally, I want to acknowledge my long-time Italian friends, who provided welcome breaks from the intense and sometimes stressful life of a PhD student. Whether it was a BBQ in Canneto, a dinner in Turin, or a lively night out in Florence, these moments of joy were always a reminder of the balance I needed.

This has been a long and difficult journey, filled with struggles, overcoming fears, and life-changing experiences. I am immensely grateful to everyone who was part of this extraordinary and unexpected journey that led to this publication

List of Figures

1.1	Edmond Halley's Life Table, 1693	5
1.2	State of the art of age-structured analysis	19
2.1	Representation of the difference between Bellman-Harris process and the framework proposed in the thesis	46
4.1	State of the art of age-structured analysis	59
4.2	Survival probability of a newborn cell with division and death ages following Γ distributions	65
4.3	Noise-induced transitions in constant environments	66
4.4	Survival probability in a constant environment with log-normal distributed division and death times	68
4.5	Modelling alternated drug treatments	69
4.6	Survival resonances under periodic on-off treatments of length .	73
4.7	Graphical sketch of the renewal condition in deterministic reso- nances	74
4.8	Dependence of noise-induced resonances on environment shape, growth regimes and persistence probability	75
4.9	Transient behaviour of the survival probability in periodic on-off environments	77
4.10	Stochastic resonance-like behaviour of the survival probability peaks	78
5.1	Illustration of age-dependent population dynamics	84
5.2	Survival probability p_{surv} of a newborn cell with division, death, dormancy and awakening ages following Γ distributions	88
5.3	Dormancy induces a shift of the transition point between frac- tional killing and total extinction	89
5.4	Comparative analysis of models with and without persistence . .	92

5.5	Schematic representation of alternated drug treatments	95
5.6	Strategy 1: switching irrespective of environment	97
5.7	Strategy 2: the inverse tendency for awakening and dormancy .	99
5.8	Strategy 3: inverted dormancy and awakening	99
6.1	Comparison between unstructured and age-structured Susceptible-Infected-Susceptible models.	104
6.2	Age-induced fluctuations affect the epidemic asymptotic state. .	108
6.3	Simulations framework, time sampling and system size.	110
C.1	Survival resonances are absent for constant division and death rates	132

Contents

1	Introduction	1
1.1	A Historical Overview on Age-Structured Populations	5
1.1.1	Euler's Geometric Growth	6
1.1.2	Bernoulli's Epidemic Model	8
1.1.3	Euler-Lotka Equation	10
1.1.4	Galton-Watson process	11
1.1.5	McKendrick–von Foerster Partial Differential Equations .	12
1.1.6	Patrick Leslie and the Matrix Based Approach	14
1.1.7	The Integral Formulation of Bellman and Harris	15
1.2	Overview of Age-Structured Models	16
1.2.1	Unstructured Models	17
1.2.2	Age-Structured Models	18
1.2.3	Conclusions	19
2	A Stochastic Age-Dependent Theory	22
2.1	Differential Chapman-Kolmogorov Age-Structured Equations	23
2.2	Age-Structured Reaction Networks	27
2.3	Generating Functionals	33
2.4	Integral Chapman-Kolmogorov Equations	35
2.4.1	Moments	39
2.5	Age-Structured Branching Processes	40
2.5.1	Deterministic Limit	44
2.5.2	Comparison with Bellman-Harris Process	45
2.6	Conclusions	47
3	Simulations	49
3.1	Rejection-Acceptance Sampling Method	50

3.2	Thinning and Extrande Algorithm	52
3.3	Conclusions	55
4	Birth and Death of Age-Structured Populations	57
4.1	Theoretical Framework	59
4.2	Continuous Therapeutic Treatments	64
4.2.1	Persistence During Constant Treatments	66
4.3	Discontinuous Periodic Drug Treatments	69
4.4	Survival Resonances	72
4.4.1	Deterministic Resonances of Survival Probability	72
4.4.2	Noise-induced Resonances of Survival Probability	74
4.5	Conclusions	78
5	Survival Strategies of Cancer Cells	81
5.1	Theoretical Framework	82
5.2	Continuous Treatments of Cancer Cells	87
5.2.1	Theoretical Framework of a Division-Death-Dormancy Model in Absence of Persistence	87
5.2.2	Division, Death, Dormancy and Persistence	91
5.2.3	The Renewal Condition and the Inheritance Problem	93
5.3	Interrupted Drug Treatments	94
5.3.1	Survival Resonances and Dormancy	100
5.4	Conclusions	101
6	Preliminary Study of an Age-Structured SIS Model	103
6.1	Deterministic SIS Model	104
6.2	Stochastic SIS Model	110
6.3	Linear Coupled Volterra's Equations	111
6.3.1	Unstructured SIS as System of Renewal Equations	112
6.3.2	Age-Structured SIS Models Are not Renewal Processes	113
6.4	The Initial Spread	114
6.5	Peaked Distributions of Recovery and Infection Times	115
6.6	Conclusions	117
7	Conclusions	119

A Derivation of The Integral Chapman-Kolmogorov Equations	123
A.1 Integral Chapman-Kolmogorov Backward Equation	124
A.2 Forward Integral Derivation	125
A.2.1 Derivation Based on the Total Probability Theorem	127
B A Recursive Solution for the Division-Death Model	129
C Constant Rates in Time-Dependent Environments	131
D Inheritance and Dormancy	133

Chapter 1

Introduction

The complexity of biological phenomena raises novel questions and challenges, driving continuous research efforts to provide quantitative and verifiable explanations of natural scenarios. In general, specific questions and challenges vary depending on the particular biological scenario under investigation. However, a pervasive and significant issue in biophysics has been identified in the lack of robust mathematical methods to quantify population heterogeneity effectively [1, 2]. This shortcoming presents a critical barrier to capturing biological populations' heterogeneous and dynamic nature.

Variability among individuals plays a crucial role in biology, significantly affecting the dynamics of entire communities and their interactions with the external environment. In this context, the term *heterogeneity* (or *variability*) does not refer to static differences within a population, such as belonging to different species or exhibiting constant traits or properties not changing over time. Instead, it refers to a time-dependent spectrum of features exhibited by population members, such as age, size, or other characteristics that change over time. This work focuses on age (labelled with the variable x) fluctuations among individuals. Age is a dynamical trait and it allows each individual to be characterised in terms of time spent inside the system. Age-structured models associate a trait x (to each individual) that increases linearly with time $\frac{dx(t)}{dt} = 1$. Other structured models, such as those which are size-structured, can be considered a generalisation of the age-structured framework in which the dynamical trait (i.e. size) y evolves accordingly with the ODE: $\frac{dy(t)}{dt} = g(y)$, where g is a generic non-linear function. In this context, a non-stochastic evolution of the traits is assumed. In fact, ODEs are employed instead of Stochastic Differential Equation (SDE) [3] since a deterministic relation between time and internal traits

is taken into assumption. As discussed throughout this work, randomicity introduced by stochastic traits can be incorporated into the statistical properties of the age-dependent event. It will be clear in the following chapters that the hazard functions of age-structured events can be manipulated and shaped to portray a wide range of random behaviour and account for possible fluctuation induced by stochastic traits.

A short comment on the nomenclature is needed before proceeding. As the reader probably noticed, *age-structured* models can be intended as a subclass of Agent-Based models [4]; the choice of the adjective "age-structured" aims to stress the specific attributes of the agents (*age*) and not to be confused with a set of simulation-based computational methods (to which the name Agent-Based models usually refers to).

The role played by age heterogeneity is demonstrated in different areas of biology. One example is cell populations, where variations in the cell cycle strongly affect cell population growth. Numerous studies have shown the interdependence between cell division frequency and the stages of the cell cycle [5, 6, 7, 8]. This heterogeneity is also evident in drug targeting analyses of cell populations [9, 10] and theoretical models lead to several validated pharmacological interventions currently in clinical trials [11, 12, 13]. Narrowing down the attention to cancer cells and bacteria, the role played by cell-cycle variation appears to be essential in comprehending the growth of bacterial and cancer populations. In fact, under adverse conditions such as repeated drug treatments, most cells in a population die while few cells survive, a phenomenon called *fractional killing* [9, 10, 14]. The short timescale of drug exposure often excludes the evolution of drug resistance but requires non-genetic mechanisms underlying fractional killing, which are still not fully understood [15, 16]. A well-accepted view is that heterogeneous survival arises from fluctuations in intracellular pathways influencing cell division, growth and apoptosis in coordination with the cell cycle [16, 17]. Recent advances in single-cell imaging allow tracking heterogeneity in individual lineages to drive insights into persistence against antimicrobial or anti-cancer treatments aided by quantitative stochastic models [18, 19].

Beyond cell populations, the macroscopic effects induced by age variability at individual levels are also evident in demographic models [20]. Age heterogeneity is a natural characteristic of a population within a country or region, and it

closely influences birth rates, death rates and migration patterns [21, 22, 23, 24]. The age structure of a population, which refers to the proportionate numbers of people in different age groups at a given time, is essential in understanding demographic dynamics. In the context of evolutionary demographic dynamics, the role of natural selection is affected by the way in which fecundity and survival depend on age [25]. De facto, the chances of survival in dying and dividing populations are an age-dependent stochastic quantity. From another standpoint in evolution theory, it is widely accepted that deleterious mutations depend upon their age of expression; specifically, the deleterious effects of novel mutations tend to decrease with age, as does the variation among mutational effects [26, 27]. This and the latter instances testify to the broad applicability of age-structured demographic models.

One last example can be found for epidemic scenarios where the role of age-heterogeneity influences the spread of pathogens [28, 29, 30, 31]. Curiously, age-structured epidemic models were the first to be developed [32]. The spread of disease is strongly influenced by population heterogeneity, especially age variability (as shown during the 2020-2022 COVID-19 pandemic [33]). Infections and deaths are closely related to the immune system of individuals, which is heavily influenced by age [34]. Thus, the probability of infection or mortality correlates with the age of the members of a community [35]. The importance of age distribution in epidemic scenarios is also underlined by the relations holding between the growth rate of the populations and the infections dynamics [20]. The growth rate of the population is clearly a quantity depending on the age distribution of the population [36], and its interdependence with the infection spread was also reported in several works on the COVID-19 epidemic [33, 34].

The paragraphs above represent a brief overview of the research attention on the role of heterogeneity in population models. The necessity to account for age-related heterogeneity arises whenever an individual's ability to perform actions is not constant but depends on their age. In competition scenarios, understanding how age impacts performance can shape strategies and outcomes [37, 38]. In fact, age variability tremendously increases the number of degrees of freedom of the system, and a wide phase space follows as a consequence, where even counterintuitive configurations might appear, as the ones where a higher reproduction rate can be less beneficial for a population growth [39, 40]. Economic models increasingly incorporate age-dependent variables to predict market be-

haviours and workforce dynamics more accurately [41, 42, 43]. In quantitative sociology and psychology, age-related variability is essential for understanding social behaviours, mental health trends and developmental processes [44, 45, 46]. Information spreading theory also benefits from considering age heterogeneity, as different age groups may adopt and disseminate information at heterogeneous rates [45, 46, 47, 48, 49]. Additionally, ecological models encode age-dependent traits which can influence the interactions between species, population growth, and ecosystem stability [50, 51, 52, 53].

In general, the current state of the art in population models can be divided into two distinct mathematical approaches. When the evolution of a biological scenario is not significantly affected by individual variability, the standard approach is to ignore population heterogeneity. This method is known as the *unstructured* approach. Conversely, when the aim is to encode the role of heterogeneity, the *structured* (e.g. *age-structured*) approach is exploited. Therefore, investigating a biological scenario can exhibit two levels of detail: the *unstructured* approach considers only variations within the number of individuals in each species, while the *age-structured* approach also accounts for variability induced by age heterogeneity among individuals.

It must be noted that models increase their complexity under a *structured* analysis, as the degrees of freedom in the system expand. This added complexity, while challenging, is necessary for developing accurate and effective models that reflect the heterogeneous nature of biological systems. The following Sec. (1.1) contains a brief historical overview of the main theoretical milestones leading to establishing the current age-structured framework in population models. A portion of these results only aims to provide historical background, while the ones presented in the conclusive part of Sec. (1.1), still represent the pillars of the current age-structured theory. These theories were developed by McKendrick [54], von Foerster [55], Bellman, Harris [56] and Leslie [57]. The following presentation is inspired by a comprehensive work on the history of population modelling proposed by Nicolas Baca   in *A Short History of Mathematical Population Dynamics* [32].

In Sec. 1.2, I then provide a detailed contemporary overview of age-structured models, highlighting the most significant recent findings and pinpointing critical areas in which additional research efforts are required. This thesis aims

Age.	Per- sons															
Curt.		Curt.														
1	1000	8	680	15	628	22	585	29	539	36	481	7	5547			
2	855	9	670	16	622	23	579	30	531	37	472	14	4584			
3	798	10	661	17	616	24	573	31	523	38	463	21	4279			
4	750	11	653	18	610	25	567	32	515	39	454	28	3564			
5	732	12	645	19	604	26	560	33	507	40	445	35	3504			
6	710	13	640	20	598	27	553	34	499	41	430	42	3178			
7	692	14	634	21	592	28	546	35	490	42	427	49	2709			
Age.																
Curt.																
43	417	50	348	57	272	64	202	71	141	78	58	63	1694			
44	407	51	335	58	262	65	192	72	120	79	49	77	1244			
45	397	52	324	59	252	66	182	73	105	80	41	84	692			
46	387	53	313	60	242	67	172	74	92	81	34	100	253			
47	377	54	302	61	232	68	162	75	88	82	28	107	34000			
48	367	55	292	62	222	69	152	76	78	83	23					
49	357	56	282	63	212	70	142	77	68	84	201				Sum Total.	

Figure 1.1: **Edmond Halley’s Life Table of 1693.** [59] The table displays the age-structured categorisation of Breslau’s population abundances

to address gaps in the literature and contribute meaningfully to advancing our understanding of age-structure dynamics.

1.1 A Historical Overview on Age-Structured Populations

The first research on age-variability in statistic demographic analysis was carried out in the last decades of the 17th century when, in 1693, Edmond Halley published a dataset on the number of deaths and births in the population of Breslau (Germany) for a given age range. In an article titled *An estimate of the degrees of the mortality of mankind, drawn from curious tables of the births and funerals at the city of Breslaw, with an attempt to ascertain the price of annuities upon lives* [58] (see Fig. 1.1), Halley defined the annual number of births as P_0 , the population aged k as P_k and the annual number of deaths at age k : D_k . This framework is still considered the first age-structured analysis, see Fig. 1.1. In Halley’s framework, the quantities P_k, D_k are assumed to be constant for all $k \in \mathbb{N}$. From the data, Halley computed the annual mean D_k of the number of deaths among people aged k for all $k \geq 0$. Exploiting the formula: $P_{k+1} = P_k - D_k$, Halley’s life table allowed him to determine the probability of surviving until age $k + 1$, knowing that one had already reached age k , using the ratio $\frac{P_{k+1}}{P_k}$. The same tables served as a reference for various demographic works in the eighteenth century proposed by Christiaan Huygens, Gottfried Wilhelm von Leibniz and Abraham de Moivre [32].

Halley’s work can be considered the first milestone in the development of age-structure modelling. His work stands as the introduction of age-structured data categorisation inferred to derive mainly qualitative observations. The lack of a

more general set of methods to quantitatively study population dynamics was later addressed by Euler, who proposed a more solid framework to investigate age heterogeneity and its effects on population growth.

1.1.1 Euler's Geometric Growth

Leonhard Euler developed the first quantitative results on age-structured populations at the end of the 18th century. Euler was known in the scientific community for his work on population dynamics and geometric growth (1748) [60]. In basic terms, the growth rate of the population was labelled with x , and the population size P_n in a given year n was given by:

$$P_{n+1} = P_n(1 + x) \quad (1.1)$$

Recursively, the population size in year n can be expressed in terms of the initial population P_0 as $P_{n+1} = (1 + x)^n P_0$.

In 1760, Euler presented a second paper entitled *A general investigation into the mortality and multiplication of the human species* [61]. This work was a kind of synthesis of his previous analysis of geometric growth and the earlier studies of Halley on life tables. Euler considered, for example, the problem:

Knowing the number of births and burials which happen during the course of one year, to find the number of all the living and their annual increase, for a given hypothesis of mortality.

In Euler's framework, the following quantities are given: the number of births during year n (B_n), the number of deaths during year n (D_n) and the proportion of newborns that reach age $k \geq 1$ (q_k). Euler also assumed that the population increases geometrically ($P_{n+1} = rP_n$) and the ratio between births and population size is constant: $\frac{B_n}{P_n} = m$. Euler then considered the state of the population at a hundred-year interval, say between the years $n = 0$ and $n = 100$, assuming that nobody survives beyond the age of a hundred years. To clarify, he defined $P_{k,n}$ (with $k \geq 1$) as the population alive at the beginning of year n (born in the year $n - k$) and $P_{0,n} = B_n$ as the number of births during year n . From the definition of the survival coefficient q_k (i.e. the proportion of newborns reaching age k), follows that $P_{k,n} = q_k P_{0,n} - k = q_k B_n - k$. Via trivial arithmetic manipulations, Euler obtained the following constraint for the

growth rate r :

$$1 = m \left(1 + \frac{q_1}{r} + \frac{q_2}{r^2} + \dots + \frac{q_{100}}{r^{100}} \right). \quad (1.2)$$

This is the equation which is sometimes called *Euler's equation* in demography, and it will be extended for a continuous unbounded age-spectrum by Lotka at the beginning of the 20th century (Sec. 1.1).

Counting births and deaths separately, Euler derived the following recursive equation:

$$rP_n = P_{n+1} = P_n - D_n + B_{n+1} = P_n - D_n + rB_n, \quad (1.3)$$

and under the assumption that the number of deaths also increases geometrically: $D_{n+1} = rD_n$, he derived:

$$\frac{1}{m} = \frac{P_n}{B_n} = \frac{\frac{D_n}{B_n} - r}{1 - r}. \quad (1.4)$$

Finally, he combined Eq. (1.2) and Eq. (1.4) to obtain:

$$\frac{\frac{D_n}{B_n} - 1}{1 - r} = \frac{q_1}{r} + \frac{q_2}{r^2} + \dots + \frac{q_{100}}{r^{100}}, \quad (1.5)$$

where there is only one unknown variable left: r . This is what is usually called an implicit equation because r cannot be expressed as a function of the other parameters. However, it is possible to compute the left- and right-hand sides of Eq. (1.5) for a fixed value of r and let r vary until the two sides are equal. The value of r thus obtained provides the growth rate $x = r - 1$ of the population. Therefore, using Eq. (1.2) and (1.4), the population size P_n can be described as:

$$P_n = B_n \left(\frac{q_1}{r} + \frac{q_2}{r^2} + \dots + \frac{q_{100}}{r^{100}} \right). \quad (1.6)$$

Note that, if the population is stationary ($r = 1$), the latter expression coincides with the one proposed by Halley to estimate the population of Breslau.

Euler's contributions represent a crucial step towards the development of age-structured modelling and, encoded in a different formalism (see Euler-Lotka Equation, Eq. (1.1.3)), stand as the core of current age-structured growth analysis. Euler's main accomplishment was encoding the age-structured dynamics within the broader context of geometric growth. The lack of a continuous vari-

ability range of age-heterogeneity was later filled by Bernoulli who proposed a modern approach in which the abundances of a population were expressed as continuous functions of age.

1.1.2 Bernoulli's Epidemic Model

Bernoulli presented the first age-structured epidemic model in 1760 in a work entitled *An attempt at a new analysis of the mortality caused by smallpox and of the advantages of inoculation to prevent it* [62]. The aim was to understand if inoculation of the first form of vaccine should be encouraged within the population. The driving motivation behind this study was that the first vaccine prototypes could frequently result in a deadly outcome. Bernoulli provided quantitative and qualitative insights about the long-term benefits of inoculation compared to the likely alternative: imminent death. Bernoulli defined p as the probability of dying (so that $1 - p$ is the probability of surviving) after the first inoculation. He also introduced an infection rate q so that qdx is the probability of being infected in the age range $[x, x + dx]$. One of the significant novelties was the introduction of a continuous range for age, leading to the consideration of a continuous rate function $m(x)$ for the mortality at age x due to causes other than smallpox. This formulation would be later encoded in the theory of Non-Homogeneous Poisson Process (N.H.P.P.) [63] such that $m(x)dx$ represents the mortality probability in the infinitesimal age range $[x, x + dx]$.

Bernoulli assumed a fixed number of people born the same year (P_0) while $S(x)$ was the number of “susceptible” people still alive at age x without ever having been infected with smallpox. The number of people alive at age x and who survived smallpox is represented by $R(x)$, while the total number of individuals is labelled by $P(x) = S(x) + R(x)$. Moreover, birth corresponds to age $x = 0$ and the initial conditions are fixed such that: $S(0) = P(0) = P_0$ and $R(0) = 0$.

Applying the methods of calculus developed at the end of the seventeenth century by Newton and Leibniz, Daniel Bernoulli noticed that, between age x and age $x + dx$ (with dx infinitely small), each susceptible individual had a probability qdx of being infected with smallpox and a probability $m(x)dx$ of dying from other causes. Therefore, the variation of the number of susceptible

people is $dS = -Sqdx - Sm(x)dx$, leading to the differential equation:

$$\frac{dS}{dx} = -qS - m(x)S. \quad (1.7)$$

During the infinitesimal age interval $[x, x + dx]$, the number of people dying from smallpox is $pS qdx$, and the number of people who survived smallpox is given by: $(1 - p)S qdx$. In addition, $R(x)m(x)dx$ is the number of deaths from causes other than smallpox (in the age interval $[x, x + dx]$). This leads to a second differential equation for $R(x)$:

$$\frac{dR(x)}{dx} = q(1 - p)S(x) - m(x)R(x). \quad (1.8)$$

Adding the two equations ((1.7) and (1.8)), an ordinary differential equation for a total number of individuals $P(x) = S(x) + R(x)$ at age x can be obtained:

$$\frac{dP(x)}{dx} = -pqS(x) - m(x)P(x). \quad (1.9)$$

From Eqs. (1.7) and (1.8), Bernoulli was able to show that the fraction of people who are still susceptible at age x is:

$$\frac{S(x)}{P(x)} = \frac{1}{(1 - p)e^{qx} + p}. \quad (1.10)$$

Bernoulli's work is not a milestone only in epidemic modelling but also in the more general class of age-structured models. In fact, it is the first case in which the heterogeneous abundances are encoded in age-dependent continuous functions, and the evolution is expressed in terms of rate functions as for NHPP.

Bernoulli's contributions may be considered the first concrete attempt to model the effects of continuous age variability on dynamics in terms of NHPPs. Nevertheless, Bernoulli's epidemic model only incorporates a continuous age-structure dependence for the death events ($m(x)$). At the same time, recovery and infection rates were age-independent, following an exponential distribution for the event times. A comprehensive general framework to study age-structured dynamics emerged with the work of McKendrick and Foerster in the early 20th century. However, an important intermediary step was provided by Lotka, who generalised Euler's work to incorporate continuous age variability in a deterministic framework to quantify a population's growth.

1.1.3 Euler-Lotka Equation

In 1907 and 1911, Lotka took up the study of the dynamics of age-structured populations without knowing about Euler's work on the same subject [35]. In contrast to Euler's work, Lotka considered time and age as continuous variables. He defined $B(t)$ as birth rate (the number of births per unit of time) at time t , $p(x)$ as the probability of still being alive at age x and $h(x)$ as fertility at age x (so that $h(x)dx$ is the probability for a man to have one newborn son between age x and $x + dx$). Lotka noted that the quantity $B(t - x)h(x)dx$ is the number of males born between time $t - x$ and $t - x + dx$, who are still alive at time t . These males have $B(t - x)p(x)h(x)dx$ sons per unit of time at time t . Therefore, the total male birth rate at time t can be expressed as follows:

$$B(t) = \int_0^\infty B(t - x)p(x)h(x)dx. \quad (1.11)$$

Lotka also assumed that if the population follows an exponential growth (with rate r), the growth rate can be encoded in the following integral equation:

$$1 = \int_0^\infty e^{-rx}h(x)p(x)dx. \quad (1.12)$$

Eq. (1.12) is usually known as the *Euler-Lotka Equation* due to its similarity to Euler's work. The *Euler-Lotka Equation* still represents (in the modern era of modelling) a useful tool to quantify the growth rate of age-structured populations. The deterministic framework first proposed by Euler and then implemented by Lotka, can be considered an implicit representation of age-structured dynamics. In other words, it still lacks an explicit notation to quantify the number of individuals for a given age range. This gap was later filled by McKendrick and von Foerster who encoded the state of heterogeneous populations in two variables (x, t) functions representing the density of individuals with age x and at a given time t .

1.1.4 Galton-Watson process

In the second half of the 19th century, a landmark development in stochastic analysis emerged, and although not displaying an age-structured framework, it plays a crucial role in the analytical derivations presented in this thesis, which is why it is discussed in detail. The Galton-Watson process was initially developed by Francis Galton in 1889 to model the propagation of family names [64, 65]. Here, I mainly focus on the extinction probability and its recursive formulation in the asymptotic regime. In its modern formulation, the Galton-Watson process is defined as a branching process $\{Z_n\}_{n \geq 0}$ (where n labels the discrete time steps), which generates k -offspring with probability $\{\{p_k\}_{k \geq 0}\}$ (offspring distributions); in mere terms, it is a discrete Markov chain where the state values are natural positive numbers with transition probability $P(Z_{n+1} = m + k | Z_n = n) = p_k$. Given the probability of observing a state (n, t) given the initial condition $(1, t_0)$, we observe that the Chapman-Kolmogorov integral equation allows to state:

$$P(n, t|m, t_0) = \sum_{q=0}^{\infty} P(n, t|q, t') P(q, t'|m, t_0) \quad (1.13)$$

Moreover, we can also introduce the generating function [66] Z associated with the probability of reaching a state given an initial condition (P) as:

$$Z(h, t) = \sum_{n=0}^{\infty} h^n P(n, t|m, t_0) \quad (1.14)$$

which allows to express Eq.(1.13) as:

$$Z(h, t|m, t_0) = \sum_{q=0}^{\infty} Z(h, t|q, t') P(q, t'|m, t_0) \quad (1.15)$$

Eq.(1.15) can be manipulated simply by observing that each branch is independent in a branching process:

$$P(n, t|m, t_0) = \underbrace{(P(n, t|1, t_0) * P(n, t|m, t_0) * \dots * P(n, t|m, t_0))}_{m-\text{times}} (t - t_0) \quad (1.16)$$

and, due to the Convolution Theorem [3], the generating function can be factorized as: $Z(n, t|m, t_0) = Z^m(n, t|1, t_0)$. In fact, Eq.(1.15) can be manipulated

as follows:

$$\begin{aligned}
Z(n, t|m, t_0) &= \sum_{q=0}^{\infty} Z(n, t|q, t') P(q, t'|m, t_0) \\
&= \sum_{0}^{\infty} Z^q(n, t|1, t') P(q, t'|m, t_0) \\
&= Z(Z(h, t|1, t')|m, t_0)
\end{aligned} \tag{1.17}$$

It follows that the evolution over the discrete time steps can be expressed by embedding generating functions as:

$$Z_n(Z_k(h)) = Z_{n+k}(h) \tag{1.18}$$

Since the extinction probability can be defined as $Z_k(h = 0)$ at each time-step k , the asymptotic extinction probability $p = \lim_{k \rightarrow \infty} Z_k(h = 0)$ can be encapsulated in a fixed point equation via a recursive approach [56, 64, 65]:

$$p = Z_1(p) \tag{1.19}$$

The latter equation shows that the asymptotic extinction probability can be expressed via a compact recursive equation given the generating function over one-time step. This formulation works as a powerful tool in the study of the extinction of stochastic branching processes as the chromosome transmission in genetics [67] or the family names extinction [64]. As reported in Ch. 2, the Galton-Watson formulation can be extended to heterogeneous populations via a functional representation, and it was exploited to derive a crucial portion of the results presented in this thesis.

1.1.5 McKendrick–von Foerster Partial Differential Equations

Despite the efforts of Lotka, Euler and Bernoulli, the 20th century began without a comprehensive deterministic framework to quantify the evolution of age-structured populations. To overcome this shortcoming, the so-called McKendrick–von Foerster Equation was first proposed by Anderson Gray McKendrick in *Applications of Mathematics to Medical Problems* (1926) [68]; the same equation was later developed in 1959 by the Austrian-Hungarian physicists

Heinz von Foerster. While McKendrick's work was meant to model epidemic scenarios, von Foerster aimed to account for cell-cycle variability to model growing cell populations [55]. This brief presentation of the von Foerster McKendrick framework is mainly based on the results proposed by von Foerster.

The McKendrick-von Foerster Equation encodes the density of individuals with age x , at time t , in a function $n(x, t)$. The ageing process was represented via continuity equation and the division and death rates were labelled by $\gamma(x)$ and $d(x)$ so that the probabilities of division or death in the age range $[x, x+dx]$ are $\gamma(x)dx$ and $d(x)dx$:

$$(\partial_x + \partial_t)n(x, t) = -(\gamma(x) + d(x))n(x, t), \quad (1.20)$$

The latter partial differential equation is coupled with a set of initial conditions:

$$\begin{aligned} n(0, t) &= 2 \int_0^t \gamma(x)n(x, t)dx, \\ n(x, 0) &= \Phi(x), \end{aligned} \quad (1.21)$$

where $\Phi(x)$ is the initial age distribution and $n(0, t)$ labels the density of individuals with age $x = 0$ at time t and is equal to the probability of dividing at age $[x, x+dx]$ multiplied and integrated over the number of individuals $n(x, t)$. As displayed by the initial condition (upcoming equation, Eq.(1.21)), the division process is encoded in the substitution of the mother via two newborns. This constrain is crucial for this formulation, and a large portion of this thesis (Ch. 2 and 5) illustrates the difference with the more realistic case where an individual with age x leads to the creation of two newborns, still not dying.

The name *McKendrick-von Foerster Equation* is nowadays used to refer to a deterministic age-structured equation of the following form:

$$(\partial_x + \partial_t)n(x, t) = F[n; x, t], \quad (1.22)$$

where the functional F depends on the state n , the age of abundances and time. The shape of RHS of Eq. (1.22) determines the possible reactions affecting the state of the population.

The deterministic age-structured dynamics is now mainly modelled using McKendrick's and von Foerster's Partial Differential Equations (PDEs). However, around the mid-20th century, Patrick Leslie introduced an alternative

approach whereby the age-structured dynamics was modelled discretely rather than continuously [57]. This approach was encapsulated in a compact matrix notation known as the Leslie matrix. While this might appear as a step backwards, Leslie's work coincided with the advent of the first computational tools. The matrix-based approach allowed for faster numerical implementation, particularly advantageous given the computational limitations of the time [69].

1.1.6 Patrick Leslie and the Matrix Based Approach

Patrick Holt Leslie published an article in 1945 in a journal (*Biometrika*) founded by Galton, Pearson and Weldon in 1901. In this article titled *On the use of matrices in certain population mathematics* [57], Leslie developed a model for the growth of the number of females in an animal population (e.g. a population of rats).

The population was divided into $K + 1$ age groups where $P_{k,n}$ is the number of females aged k at time n ($k = 0, 1, \dots, K$ and $n = 0, 1, \dots$). In this framework, f_k is the fertility at age k , i.e. the number of daughters born per female between time n and time $n + 1$. Note that K is the maximum age with nonzero fertility ($f_K > 0$). The quantity s_k is defined as the probability for an animal aged k to survive at least until age $k + 1$, therefore the population dynamics can be encoded in the following set of equations:

$$\begin{aligned} P_{0,n+1} &= \sum_{k=0}^K f_k P_{k,n} \\ P_{1,n+1} &= s_0 P_{0,n} \\ P_{2,n+1} &= s_1 P_{1,n} \\ &\vdots \\ P_{K,n+1} &= s_{K-1} P_{K-1,n}. \end{aligned} \tag{1.23}$$

All the numbers f_k are non-negative, while s_k satisfies $0 < s_k < 1$. At the end of the nineteenth and beginning of the twentieth centuries, mathematicians developed the habit of writing such systems of equations in the abbreviated form

$$P_{n+1} = M P_n, \tag{1.24}$$

where P_n is the column vector $(P_{0,n}, \dots, P_{K,n})$ and M is the square matrix. Leslie's matrix formulation of problems in population dynamics is still used by many biologists and biophysicists [69, 70]. The dominant eigenvalue allows for determining long-term population growth, and the eigenvector (related to the dominant eigenvalue) represents the age distribution in an asymptotic regime. Modern computers greatly simplify the computations and scientific software that can compute eigenvalues and eigenvectors of any matrix.

The crucial novelty in Leslie's framework is the simplicity with which deterministic age-structured dynamics can be encoded simply using basic concepts in Linear Algebra. Leslie's matrix model still imposes a discrete representation of age heterogeneity. In the same years, Bellman and Harris developed and published the first solid work on stochastic age-structured dynamics.

1.1.7 The Integral Formulation of Bellman and Harris

Leslie's approach to age-dependent process was set aside in 1948 when Bellman and Harris proposed to the National Academy of Sciences a work with the title *On age-dependent binary branching processes*. [71]. Any specific biological application or scenario was investigated in their original work, the two authors were *interested in the following problem which is of possible biological, chemical, and physical interest* [71]. A more comprehensive theoretical work was then proposed by Harris in *Theory of branching process* [56] in 1963.

In the standard Bellman-Harris process, each individual exhibits a continuous lifetime trait (age) labelled with τ . The lifetimes are non-negative random variables with arbitrary distributions, and a single ancestor is born at time $t = 0$. Each individual lives for time τ which is a random variable with cumulative distribution function $G(\tau)$. At the moment of death, the individual produces two progenies and each of the first-generation progeny behaves independently of each other and the ancestor (i.e., it lives for a random time distributed according to $G(\tau)$ and produces two newborn individuals) [56].

The variable $N(t)$ is used to denote the total number of individuals at time t and it is assumed to be a stochastic process $\{N^t, t \geq 0\}$. The original framework [72] states that the generating function associated to the stochastic variable N^t :

$$Z(h, t) = \sum_{N=0}^{\infty} h^N P[N, t] \quad (1.25)$$

evolves following the renewal equation:

$$Z(h, t) = h(1 - G(t)) + \int_0^t Z^2(h, t-u)dG(u). \quad (1.26)$$

The latter equation is usually called *Bellman-Harris Equation* and can be manipulated to obtain a wide set of results regarding the state of age-structured population; the versatility of the Bellman-Harris Equation is thoroughly discussed in [56] and later in Ch. 2. It must be remembered that Feller also made significant contributions by demonstrating how Euler's, Lotka's, and McKendrick's results can be derived from the integral representation of Bellman and Harris; moreover, Feller provided a comprehensive framework for both exact and asymptotic moment calculations [73, 74].

The integral representation is still the core method in investigating stochastic age-structured branching processes [3]. However, the Bellman-Harris formulation exhibits several limitations related to the constraints on the lifetime distributions, the initial conditions and other quantities, which are extensively addressed throughout this thesis (Ch. 2). Here, just a few limitations are mentioned. First, the natural passage from the deterministic McKendrick-von Foerster theory to a stochastic age-structured theory would require considering the abundances $n(x, t)$ as stochastic functions. Instead, Bellman and Harris considered the total abundances as stochastic variables. Second, due to the mechanistic derivation [56] of Eq. (1.26), the process is constrained to a single newborn at time $t = 0$, neglecting the effects of different initial age conditions. These and other shortcomings of the Bellman-Harris Equation are outlined in detail in Sec. 2.5.2.

1.2 Overview of Age-Structured Models

The role played by heterogeneity has proven crucial in understanding countless biological phenomena ranging from cell-cycle dynamics to the spread of epidemics [20, 75]. Although models encoding age-variability can be traced back to the end of the 17th century, a comprehensive recipe (deterministic and stochastic) to model age-structured dynamics is still missing. This is in contrast with unstructured models, in which all individuals are considered indistinguishable and for which the general theoretical framework is clear [32, 35].

In the next subsections, the level of description available for *unstructured* and *age-structured* populations is compared (Subsec. 1.2.1 and 1.2.2). Finally, I introduce the core concepts (Sec. 1.2.3) on which this research project was developed, I discuss the current shortcomings of stochastic models and propose a theory to overcome them.

1.2.1 Unstructured Models

Based on the current nomenclature, a herd or a group of individuals is considered *unstructured* when all the individuals are indistinguishable by no means other than for the species to which they belong. In other words, the state of an *unstructured* population at a given time is defined solely by the number of species it is made of and the abundances of individuals for each species [35, 76]. The levels of description for *unstructured* models are well established in contrast to *age-structured* models. Despite the stochastic nature of these systems, their deterministic description is frequently employed and is usually expressed in terms of Ordinary Differential Equations (O.D.E.) like the deterministic compartmental models [35, 75, 77], the Logistic map model [78, 79] or the Lotka-Volterra models [35].

Moving on to the stochastic characterisation of *unstructured* populations, their evolution can be simulated by *Stochastic Simulation Algorithms* (S.S.A.s) which are usually based on the well-known *Gillespie Algorithm* [80, 81, 82, 83]; SSAs have been widely used to simulate a variety of scenarios, such as the stochastic spreading of infectious diseases [82, 84, 85], genetic regulatory networks [80, 86, 87] and chemical reactions [80, 88].

Furthermore, the same stochastic evolution can be described theoretically by Chemical Master Equation [63], which lies on the same level as the simulations description since they both approximate the evolution as a jumping process. As for the deterministic approach and the stochastic simulations, the Chemical Master Equations have been numerically solved or analytically manipulated to describe various contexts ranging from cell populations [88, 89] to the behaviour of ecological communities [90, 91].

Despite its wide range of applications and well-established levels of description, the *unstructured* approach presents two main limitations due to the fact that the individuals are considered indistinguishable. To begin with, the *unstructured* description might not provide realistic forecasts about popula-

tion dynamics since it neglects the role of individual-to-individual heterogeneity [35, 72, 75, 78, 79, 92, 93]. Other two shortcomings arise from the fact that the *unstructured* approach might not provide information about the heterogeneous composition of the systems and the reaction times are constrained to follow an exponential distribution. All these limitations may lead to approximated predictions on different applications as the growth of cell population [72, 94], the equilibrium size distribution for an ecological community [50] or the abundances of agents with a certain position and/or age in SIR models [75, 95].

1.2.2 Age-Structured Models

Sec. 1.1 provided the reader with a brief overview of the historical development of age-structured theories. Although a broader and more articulated set of methods is available nowadays to model age-structured dynamics [3, 20], the works discussed in Sec. 1.1 still stand as the main pillars for the major part of current age-structure models.

The majority of modern deterministic age-structured results are built using drifting (transport) Partial Differential Equations (similar to McKendrick-von Foerster PDE) or by evaluating an integral equation to model age-structured dynamics as exponential growth (as in Euler-Lotka theory) [20, 96]. In addition, even Leslie's framework is frequently exploited to encode the age-structured dynamics in discrete computational-friendly form.

It follows that *age-structured* deterministic descriptions still revolve around McKendrick, von Foerster's, Euler's and Lotka's results, and it is usually expressed in terms of partial differential equations or in implicit integral equations for the growth rate [35, 68, 92].

Moving to age-structured models in which the stochastic nature of the system is not neglected, the results developed do not allow for a solid and comprehensive stochastic theory (in contrast to the deterministic case). Recent years have seen a tremendous increase in age-structured stochastic models since they allow to capture both the heterogeneous and random nature of biology [92, 93]. Nevertheless, a comprehensive, coherent theory for age-structured models is still missing. The majority of the current works on the topic are only a generalisation of Bellman-Harris's framework where the stochastic dynamics is expressed in terms of renewal equations [97] for the generating functional of the probability. This leads to the essential limitations of Bellman's and Harris's formulation.

This topic will be extensively discussed in Ch. 2, but, essentially, Bellman and Harris proposed a way to model a specific class of reactions. Therefore, the current framework for *age-structured* populations has been developed mainly for specific types of dynamics, such as branching processes as studied by Bellman, Harris and Feller [35, 72]. Furthermore, a solid and general set of computational methods to simulate the evolution of age-structured population is still missing.

	Unstructured	Age-structured
Deterministic	ODE's	McKendrick-Von Foerster Euler-Lotka Leslie
Stochastic	Master Equation	Bellman-Harris

Figure 1.2: **State of the art of age-structured analysis.** The deterministic unstructured analysis is usually expressed in term of Ordinary Differential Equations (ODEs), while the standard stochastic approach is described in terms of Markov processes via Master Equation. Conversely, the age-structured dynamics can be deterministically described using Euler-Lotka integral formulation for the growth rate or McKendrick-von Foerster PDE's or Leslie-Matrix notation. The stochastic age-structured description substantially relies on Bellman's and Harris's work.

1.2.3 Conclusions

The core of this research project concentrates on the gap between the levels of stochastic description for *structured* and *unstructured* populations, as sketched in Fig. 1.2. The existence of this gap derives from the fact that there is still no reliable way to stochastically describe the evolution of age-structured populations.

To the reader, the efforts of coupling a stochastic description within the age-structured framework might seem unnecessary since a solid set of deterministic results is already available to model age-structured evolution. Therefore, the following paragraph provides a brief explanation of why the role of randomness is such a crucial and natural feature in biology.

Stochasticity is ubiquitous in natural phenomena. Randomness influences the evolution of populations or herds in ecology, genetics, cell biology and epidemiology [98, 99, 100]. For instance, in genetics, the DNA mutations occur randomly and affect the genetic diversity of herds and, in small-size populations,

Genetic Drifts push allele frequencies to change randomly from one generation to the next. [100]. In ecology, division or annihilation times exhibit strong fluctuations for each individual due to environmental factors, variability within the population and availability of resources [98]. The role of randomness can also be found in interacting models such as the Lotka-Volterra models [36], in which individuals exhibit stochastic behaviour due to randomness in encounters and environmental conditions.

A further example can be found in epidemic models. In fact, infectious diseases often follow stochastic patterns due to the random nature of contacts between individuals, variability in susceptibility, and environmental factors. In general, stochastic biological behaviour can be driven by external factors, environments, interactions or even adaptive strategies [98, 99].

In summary, there are extensive works addressing the role of noise in Biological models [101] and numerous results which provide insights on the effects induced age-variability [20, 93, 102]. However, a general stochastic theoretical framework to quantify the entanglement between the drifting process of ageing with the fluctuating behaviour of individuals is still missing. This research project is focused on developing a comprehensive theoretical framework to describe the stochastic nature of age-structured populations. The goal is to provide a set of analytical and computational methods to quantify the effects induced by the coexistence of noise and heterogeneity.

Instead of discretizing the dynamics as proposed by Leslie or in contrast with Bellman-Harris who derived their equation using standard probabilistic arguments, I suggest a different solution inspired by a few works scattered in the last decades. One of these works, maybe the most influential one, was proposed by Van Kampen in a paper *Master Equation treatment of ageing populations* in the 1977 [103]. In this work, Van Kampen presented a functional representation of age-structured stochastic processes. This result inspired the development of a more comprehensive theory on age-structured populations based on the theory of stochastic processes. Specifically, I propose to model the age-structure stochastic dynamics as a drifting and jumping stochastic process [3].

It will be demonstrated that Leslie's, Bellman's and Harris's results are the corner of a bigger picture where the age-structured density is described by stochastic functions. In this frame, any age-structured dynamics can be described with a set of NHPPs coupled with a deterministic drift. Therefore,

I propose a more general stochastic theory based the Chapman-Kolmogorov Equation (C.K.E.) [3] in which the probability functional of the density linearly drifts while adding or subtracting elements.

The theoretical derivation is mainly discussed in Ch. 2 in which several topics of stochastic process theory are adapted to describe the age-structured dynamics. Ch. 3 aims to present a potential set of methods to simulate the evolution of a stochastic age-structured population. The two subsequent Chs. 4 and 5 explores a paradigmatic age-structured model known as division-death model. The model is studied and simulated by means of the methods presented in Chs. 2 and 3. The model is presented as an application to study the survival frequency of cancer cell populations; the cell-cycle variability (age), combined with the fluctuations, depicts a novel landscape compared to the unstructured case. Ch. 6 aims to introduce a discussion on interacting age-structured scenarios and how to model their stochastic behaviour.

To the reader: each chapter begins with a short abstract where I outline which parts of the work are original and recognise the contributions of collaborators. I use the pronoun *I* when presenting my personal point of view, while *we* is used to discuss conclusions and results that are the outcome of collaborative efforts.

Chapter 2

A Stochastic Age-Dependent Theory

Abstract

A theoretical framework to quantify age-structured dynamics is presented in this chapter. The following work rises from fundamental concepts in Stochastic Processes and leads to a comprehensive framework to model age-structured populations. Along with a compact functional notation, I propose a formal derivation of the age-structured Chapman-Kolmogorov equation where the dynamics is induced by the overlap between ageing drift and stochastic reactions. Several analytical results are presented and applied to a trivial model as an example. In the final sections, I discuss the relationship between the framework developed and the theories provided by McKendrick, von Foerster, Bellman, and Harris [68, 72].

The age-structured dynamics can be represented as an overlapping of stochastic jumping processes with a deterministic shift (representing the ageing drift). In this dynamics, the state of a population can be encoded in stochastic functions and the probability in a functional. Starting from fundamental concepts, I derive and discuss the age-structure form of the Chapman-Kolmogorov Equation. (Sec. 2.1). Later, a functional generalisation of the standard stoichiometric reaction network is discussed (Sec. 2.2) and later encoded in the Master Equation (M.E.) to be expressed in terms of reaction rates, propensity and stoichiometric functions. Inspired by Bellman's and Harris's work, I also propose an integral representation of the Chapman-Kolmogorov Equation (Sec. 2.4). Such integral formulation allows to show that Bellman's and Harris's results are a direct application of a more general theory and can be generalised to a wide

class of branching processes. This Chapter goes on and narrows the attention down to age-structured branching processes (Sec. 2.5) and presenting a functional generalisation of the Galton-Watson theory [64]. Finally, Subsecs. 2.5.2 and 2.5.1 show how our theory directly recalls and generalises Bellman's and Harris integral results and the partial differential equation of McKendrick and von Foerster.

2.1 Differential Chapman-Kolmogorov Age-Structured Equations

The purpose of this section is to derive the Chapman-Kolmogorov age-structured Equations starting from the basic concepts of stochastic process theory. This derivation was inspired by the work proposed by Van Kampen in [103, 104].

The following theory is built around the assumption that the state (i.e. the abundance of individuals at time t) of an age-structured population can be encoded in random functions n^t such that $n^t(x)$ represents the number of individuals with age x at time t .

Therefore, let us define $n^t(x)$ as a stochastic process which is defined as a discrete or continuous sequence of random variables $(n^t(x))_{t \in I}$ each of which maps from the same sample space Ω to the same co-domain Y :

$$\forall t \in I : n^t(x) : \Omega \rightarrow Y. \quad (2.1)$$

The index set I represents the time $I = \mathbb{R}$ and is equipped with the distance function $|t_1 - t_2|$. The probability that the random variables $n^t(x)$ is equal to $n_x \in Y$ is denoted by $P(n^t(x) = n_x)$. Once the age spectrum is considered discrete (x_1, \dots, x_M) , the probability of finding the age-dependent population in a given state $(n(x_1) = n_{x_1}, \dots, n(x_M) = n_{x_M})$ at time t is defined as:

$$P((n^t(x_1) = n_{x_1}, t), (n^t(x_2) = n_{x_2}, t), \dots) = P(n_{x_1}, n_{x_2}, \dots, t). \quad (2.2)$$

Despite proposing the age-spectrum as discrete (as in Leslie's theory [57]), the age is a continuous property of the individuals. Therefore, the state of a population at time t can be encoded in a stochastic density function n^t such that

$n^t(x)$ labels the density of elements with age x :

$$P((n^t(x) = n_x)_{\forall x \in \mathbb{R}}, t) = \mathcal{P}[n^t = n, t], \quad (2.3)$$

where \mathcal{P} labels the probability density function of observing a given density n at a specific time t . Hence, the probability of observing the stochastic function $n^t = n$, under the condition that $n^s(x) = m$ at time $s < t$, is defined as:

$$\mathcal{P}[n^t = n, t | n^s = m, s] = \mathcal{P}[n, t | m, s]. \quad (2.4)$$

A *Markov process* is defined as a stochastic process $\{n^t\}$ whose conditional probabilities satisfy the Markov property:

$$\begin{aligned} & \mathcal{P}[(n_1, t_1), (n_2, t_2), \dots | (m_1, \tau_1), (m_2, \tau_2), \dots] \\ &= \mathcal{P}[(n_1, t_1), (n_2, t_2), \dots | (m_1, \tau_1)], \end{aligned} \quad (2.5)$$

where the set of times $\{t_i\}$ and $\{\tau_i\}$ are defined such that: $t_1 \geq t_2 \geq \dots$, $\tau_1 \geq \tau_2 \geq \dots$ and $t_j \geq \tau_i \forall j, i = 1, \dots$. The definition of Markov process is equivalent to considering a stochastic process $\{n^t\}$ such that:

$$\mathcal{P}[(n_i, t_i), (n_{i-1}, t_{i-1}), \dots] = \prod_{j=0}^{i-1} \mathcal{P}[(n_{j+1}, t_{j+1}) | (n_j, t_j)]. \quad (2.6)$$

The latter equation can be reduced to the Chapman-Kolmogorov Equation in its integral form where $t \geq t' \geq 0$:

$$\mathcal{P}[n, t | m, 0] = \int \mathcal{P}[n, t | q, t'] \mathcal{P}[q, t' | m, 0] \mathcal{D}q. \quad (2.7)$$

The Chapman-Kolmogorov Integral Equation encodes the memory-less property of Markov processes. In fact, Eq. (2.7) states that the probability of observing a stochastic process $(n, t | m, 0)$ can be decomposed into the probabilities of reaching and leaving an intermediate state q at time t' .

So far, the results presented do not exhibit any specific feature induced by the ageing process. In fact, the CKE (as presented in Eq. (2.7)) holds for any Markov processes whose state can be described by a random function n^t .

The age-dependent nature of the process arises as soon as the total time variation of \mathcal{P} is taken into account. In the absence of jumping processes, the

state of an age-structured population (n^t) is not static but undergoes a *drift* induced by the ageing process. This drifting process underlies the stochastic dynamics and can be interpreted as deterministic continuous motion $n^t(x) = n^{t+\Delta t}(x + \Delta t)$ (where $\Delta t > 0$ is a finite length of time).

To elucidate this point, consider the probability of observing the state n at time $t + \tau$ with initial condition $m^{t_0=0} = m$: $\mathcal{P}[n^{t+\tau} = n, t + \tau | m, 0]$. Then, the functional probability can be expanded as $\tau \rightarrow 0$:

$$\begin{aligned} \mathcal{P}[n^{t+\tau} = n, t + \tau | m, 0] &= \mathcal{P}[n^t = n, t | m, 0] \\ &\quad + \partial_t \mathcal{P}[n^t = n, t | m, 0] \tau \\ &\quad + \int \frac{\delta(\partial_x n(x) \mathcal{P}[n, t | m, 0])}{\delta n(x)} dx \tau + \mathcal{O}(\tau^2). \end{aligned} \quad (2.8)$$

The probability of finding a state at time $t + \tau$ is simply given by the probability of finding the state (n, t) ($\mathcal{P}[n, t | m, 0]$), added to the explicit time variation represented by the partial derivation with respect to time ($\partial_t \mathcal{P}[n, t | m, 0]$) and to the flux of the functional probability induced by the ageing process ($\frac{\delta(\partial_x n(x) \mathcal{P}[n, t | m, 0])}{\delta n(x)} dx$). This is one of the significant differences with unstructured processes.

In the following, the differential CKE is derived from Eq. (2.7) that is recalled here:

$$\mathcal{P}[n^{t+\tau} = n, t + \tau | m, 0] = \int \mathcal{P}[n^{t+\tau} = n, t + \tau | q, t] \mathcal{P}[q, t | m, 0] \mathcal{D}q, \quad (2.9)$$

where the time steps are $t + \tau \geq t \geq 0$. A first order Taylor expansion of the term $\mathcal{P}[n^{t+\tau} = n, t + \tau | q, t]$ gives:

$$\begin{aligned} \mathcal{P}[n, t + \tau | q, t] &= \mathcal{P}[n, t | q, t] + (\partial_{t'} \mathcal{P}[n, t' | q^t, t])_{t'=t} \tau \\ &\quad + \left(\int \frac{\delta(\partial_x n^t(x) \mathcal{P}[n, t | q, t])}{\delta n(x)} dx \right) \tau + \mathcal{O}(\tau^2). \end{aligned} \quad (2.10)$$

Note that $\mathcal{P}[n, t | q, t]$ is equal to $\delta_{n,q} = \delta[n - q]$ where the notation $\delta_{n,q}$ is a functional generalization of the delta function such that:

$$\delta_{n,q} = \begin{cases} \infty & \text{if } n(x) = q(x) \forall x \in \mathbb{R} \\ 0 & \text{otherwise} \end{cases} \quad (2.11)$$

and, as a consequence, the flux term vanishes in Eq.(2.10) coherently with the fact that we assumed infinitesimal time steps τ . Therefore, Eq. (2.10) can be reduced to :

$$\mathcal{P}[n, t + \tau | q, t] = \delta_{n,q} + (\partial_{t'} \mathcal{P}[n, t' | q, t])_{t'=t} + \mathcal{O}(\tau^2). \quad (2.12)$$

The term $(\partial_{t'} \mathcal{P}[n, t' | q, t])_{t'=t}$ can be decomposed in two parts. The first part (for $n \neq q$) represents the probability from a state q to a state n , usually named *transition probability* [3] and labelled as $\mathcal{W}[n|q]$. The second part ($q = n$), instead, can be expressed as:

$$1 - \int_{n' \neq q} \mathcal{W}[n'|q] \mathcal{D}n' \Delta t. \quad (2.13)$$

Hence, Eq. (2.10) becomes:

$$(\partial_{t'} \mathcal{P}[n, t' | q, t])_{t'=t} = (1 - \delta[n - q]) \mathcal{W}[n|q] + \delta[n - q] \left(1 - \int_{n' \neq q} \mathcal{W}[n'|q] \Delta t\right). \quad (2.14)$$

As final step, Eqs. (2.8) and (2.14) have to be plugged in Eq. (2.9) to obtain the age-structured forward differential Chapman-Kolmogorov Equation:

$$\left(\frac{\partial}{\partial t} + \int dx \partial_x n(x) \frac{\delta}{\delta n(x)} \right) \mathcal{P}[n, t | \cdot] = \int \mathcal{W}[n|q] \mathcal{P}[q, t | \cdot] - \mathcal{W}[q|n] \mathcal{P}[n, t | \cdot] \mathcal{D}q, \quad (2.15)$$

where for brevity the dependence of \mathcal{P} on the initial conditions was muted since they are not involved in the calculation. The left side operator $\frac{\partial}{\partial t} + \int dx \partial_x n(x) \frac{\delta}{\delta n(x)}$ is a hallmark feature of age-structured models and, in the following, is going to be called *Liouville's operator*. This operator allows for balancing the RHS of Eq. (2.15)(jumping stochastic processes) with the LHS made by two terms: the explicit time variations of the functional probability and the deterministic Liouville's term. The following notation is used for the *Liouville's operator*:

$$D_{n,t} = \partial_t + \int dx \partial_x n(x) \frac{\delta}{\delta n(x)}. \quad (2.16)$$

Therefore, the overlapping of the ageing drift with stochastic jumping processes

can be expressed via the forward age-structured Master Equation:

$$D_{n,t}\mathcal{P}[n, t|\cdot] = \int \mathcal{W}[n|q]\mathcal{P}[q, t|\cdot] - \mathcal{W}[q|n]\mathcal{P}[n, t|\cdot]\mathcal{D}q \quad (2.17)$$

or the backward age-structured Master Equation:

$$D_{m,t_0}\mathcal{P}[\cdot|m, t_0] = \int \mathcal{W}[q|m]\mathcal{P}[\cdot|m, t_0] - \mathcal{W}[q|m]\mathcal{P}[\cdot|q, t_0]\mathcal{D}q. \quad (2.18)$$

For the sake of brevity (in the latter equations and in the following ones), the dependence of \mathcal{P} on (n, t) ((m, t_0)) is muted when the state function n (m) is not involved in the Liouville's operator. The backward Master equation (Eq. (2.18)) is derived in a similar way to the Forward Master Equation. Nevertheless, in the backward equation, the main role is played by the initial conditions and how their variation affects the probability of observing a stochastic path $(n, t|m, t_0)$; for further details, see [3].

Eqs. (2.17) and (2.18) are equivalent to each other and both useful to characterise the *age-structured* dynamics. In standard *unstructured* applications, the forward CKE gives more directly the values of measurable quantities as function of the observed time t and tends to be used more. The backward equation finds most application in the study of first passage time or exit problems in which the objective is quantifying the probability for an agent to leave a region of space at a given time [63]. These alternated usages of backward and forward CKEs turn out to be true in the age-structured analysis. In addition, the backward Chapman-Kolmogorov Equation will have an additional role in an age-structured study. It allows encoding the age-structured dynamics in a similar way to the Bellman-Harris Equation (Sec. 2.4).

2.2 Age-Structured Reaction Networks

The evolution of an *age-structured* population is characterised by the overlapping of deterministic ageing with a set of stochastic changes in the number of individuals. The ageing process is deterministic and the whole stochasticity is encoded in the jumping processes, as it happens in *unstructured* jumping processes.

Such similarity pushed us to generalise some concepts rising in *unstructured* scenarios such as the use of a stoichiometric notation and the concepts of reaction

network, rates and propensity [63, 105].

In fact, the heterogeneity of an *age-structured* population can be fully described by a *species function*:

$$s_i(x) \quad \forall x \in \mathbb{R}, \quad (2.19)$$

which labels the class of agents belonging to the i -th species (out of M such that $i = 1, \dots, M$) with age x . Therefore, a multispecies age-structured population is described by a state $n = (n_1, \dots, n_M)$ where n_i is the density function of the i -th species and $n_i(x)dx$ is the number of individuals belonging to the i -th species with age $x \in [x, dx]$.

The Chapman-Kolmogorov Equations (Eqs. (2.15) and (2.18)) still hold, yet the Liouville's operator has to account for the drifts of different species:

$$D_{n,t} = \partial_t + \sum_{i=1}^M \int dx \partial_x n_i(x) \frac{\delta}{\delta n_i(x)}. \quad (2.20)$$

Let me now introduce a set of R reactions labelled by the index $r \in \{1, 2, \dots, R\}$. Using the stoichiometric representation, a set of *reactants*, a set of *products* and a rate can be associated to each reaction r :



I define the *reactants stoichiometric function* $\nu_r^-[\vec{x}] = \nu_{r,1}^-[\vec{x}], \dots, \nu_{r,M}^-[\vec{x}]$ as the vectors of densities required to perform the r -th reaction for each species. The elements of \vec{x} are the ages of reactants or of the products; in general, the ages are not fixed and might vary for each reaction.

On the other hand, the *products stoichiometric function* is labelled by $\nu_r^+[\vec{x}] = (\nu_{1,M}^+[\vec{x}], \dots, \nu_{1,M}^+[\vec{x}])$ and its i -th component represents the density of elements of species i -th with ages \vec{x} required to perform the r -th. Finally, the *change of state stoichiometric function* is defined as $\nu_r[\vec{x}] = \nu_r^+[\vec{x}] - \nu_r^-[\vec{x}]$ and Eq. (2.21) is expressed as:

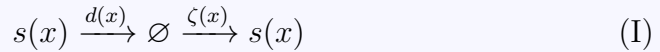
$$\sum_{i=1}^M \int_{\mathbb{R}^+} \nu_{r,i}^-[\vec{x}](u) s_i(u) du \rightarrow \sum_{i=1}^M \int_{\mathbb{R}^+} \nu_{r,i}^+[\vec{x}](u) s_i(u) du, \quad (2.22)$$

where $s_i(x)$ is one elements of the i -th species with age x . The latter equation allows me to describe the set of age-structure jumping processes in a formal

way. Eq. (2.22) generalises the concept of *stochastic reaction network* rising initially in Chemistry and which was then adopted in the *unstructured* model. I define the representation displayed in Eq. (2.22) as *age-structured stochastic reaction network*.

The functional representation of the stoichiometric properties (e.g. $\nu_{r,i}[\vec{x}]$) might appear "tricky" at first glance, especially the dependence on any ages \vec{x} of the reactants. Such notation may seem heavy and unnecessary, but it is required to ensure the theory's universality and allow its generalization to traits other than ages (see Ch. 7). Therefore, let me briefly consider an instance of interdependence between the products' and reactants' ages to support the exploitation of such notation. The reader considers a case of study where the age of the products depends on the age of the reactants as: $s_1(x) + s_2(y) \rightarrow s_3(\frac{x+y}{2})$. Two agents belonging to the first and second species can be replaced by an agent of the third species whose age is the average of the ones of the reactants. The age of the reactants $\vec{x} = (x_1 = x, x_2 = y, x_3 = 0)$ are required in the argument of the stoichiometric functions since $\nu^+[\vec{x}] = \delta_{x_1,x} + \delta_{x_2,y}$ and $\nu^+[\vec{x}] = \delta_{x_3,\frac{x+y}{2}}$. This short example only aims to justify the formalism chosen to account for any age-structured interdependence between reactants and products. An additional example is proposed in Example 1.

Example 1 Here, I consider a single species population $s_1(x) = s(x)$ evolving through migration and death. The migration process leads to the creation of a new agent $s(x)$ with rate function $\zeta(x)$, while the death process forces each agent $s(x)$ to die with age-dependent rate $d(x)$:



The stoichiometric death function depends on the age of the reactant and a can be expressed as $\nu_d[\vec{x}] = \nu_d[x] = -\delta_x$. Instead, the migration process is a zero-order process with a symmetric change of state function: $\nu_\zeta[\vec{x}] = \nu_\zeta[x] = \delta_x$.

Following the analogy with the standard notation, two other concepts can be introduced. The *propensity* $\Omega_r[n, \vec{x}]$ of the r -th reaction with ages \vec{x} represents the probability $(\Omega_r[n, \vec{x}] d\vec{x})$ that a r -th reaction will happen in the next infinitesimal range of time, given the system in a state n . Following from the Law of Mass-Action [3], the propensity (Ω) is usually expressed as the prod-

uct of the reaction rate functions (depending on age of the reactants $\vec{x} \in \mathbb{R}^{N_r}$ and labelled by γ_r), and the combinations of individuals able to perform such reactions $\Phi_r[n, \vec{x}]$:

$$\Omega_r[n, \vec{x}] = \gamma_r(\vec{x}) \Phi_r[n, \vec{x}]. \quad (2.23)$$

It is necessary to include a few comments about Eq. (2.23). First of all, the rate function $\gamma_r(\vec{x})$ is an identifying feature of age-structured populations. In the unstructured framework, the reaction rates are constant and the reaction times are exponentially distributed as a homogeneous Poisson process [3]. Instead, in an age-structured description, the event times do not necessarily follow an exponential distribution and are modelled as NHPPs [106]. For explanatory purposes, I consider a reaction (r^*) where the reactant stoichiometric function is $\nu_{r^*}^-[\vec{x}] = \delta_{\hat{x}}$ so that the reaction rate is described by a one-variable function $\gamma_{r^*}(x)$. Instead of following an exponential distribution, the reaction times (τ) are distributed accordingly with a probability density function $\phi_{r^*}(\tau)$:

$$\phi_{r^*}(\tau) = \gamma_{r^*}(\tau + x) \exp \left(- \int_0^\tau \gamma_{r^*}(u + x) du \right). \quad (2.24)$$

The relationship holding between reaction times distributions and rates is going to be crucial in this work both for developing sampling methods (Ch. 3) and investigating the dynamics in the applications (Secs. 4 and 5).

A second comment about Eq. (2.23) regards the propensity itself. Following the *law of mass-action* and taking into account a generic $r - th$ reaction, the transition probability \mathcal{W} can be expressed in terms of the propensity as $\mathcal{W}[n + \nu_r[\vec{x}]|n] = \Phi_r[n; \vec{x}] \gamma_r(\vec{x})$. Therefore the transition probability \mathcal{W} , so that:

$$\mathcal{W}[n + \nu_r[\vec{x}]|n] = \gamma(\vec{x}) \exp \left[\sum_{i=1}^M \int_0^\infty \binom{n_i(u)}{\nu_{r,i}^+[\vec{x}](u)} du \right], \quad (2.25)$$

where the big bracket notation refers to the binomial factor:

$$\binom{n_i(u)}{\nu_{r,i}^+[\vec{x}](u)} = \frac{n_i(u)!}{(n_i(u) - \nu_{r,i}^+[\vec{x}](u))! \nu_{r,i}^+[\vec{x}](u)!}. \quad (2.26)$$

To clarify the latter equation, let us consider an unstructured multi-species scenario. This scenario can be recalled by mapping $\mathcal{D}_{n,t}$ is to ∂_t in (2.15) and discretise the age variability spectrum (x_1, x_2, \dots) . The propensity would be

expressed as a product of all the combinations of elements able to perform a given reaction:

$$\prod_{j=1}^M \binom{n(x_j)}{\nu^+[\vec{x}](x_j)} du. \quad (2.27)$$

Therefore, the Chapman-Kolmogorov forward and backward Equations can be expressed as:

$$\begin{aligned} \mathcal{D}_{n,t}\mathcal{P}[n, t|m, t'] &= \sum_{r=1}^R \int_{\mathbb{R}^{N_r}} \mathcal{W}[n|n - \nu_r[\vec{x}], t]\mathcal{P}[n - \nu_r[\vec{x}], t|m, t']d\vec{x} \\ &\quad - \int_{\mathbb{R}^{N_r}} \mathcal{W}[n + \nu_r[\vec{x}]|n, t]\mathcal{P}[n, t|m, t']d\vec{x} \end{aligned} \quad (2.28)$$

and

$$\begin{aligned} \mathcal{D}_{m,t'}\mathcal{P}[n, t|m, t'] &= \sum_{r=1}^R \int_{\mathbb{R}^{N_r}} \mathcal{W}[m + \nu_r[\vec{x}]|m, t']\mathcal{P}[n, t|m, t']d\vec{x} \\ &\quad - \sum_{r=1}^R \int_{\mathbb{R}^{N_r}} \mathcal{W}[m + \nu_r[\vec{x}]|m, t']\mathcal{P}[n, t|m + \nu_r[\vec{x}], t']d\vec{x}. \end{aligned} \quad (2.29)$$

An interesting observation was also proposed during the defence of this thesis; it was pointed out that the \vec{x} is always encoded in the stoichiometric function ν_r in the latter equation. Therefore, Eqs.(2.28) and (2.29) could also be expressed in terms of a new measure $D\nu_r$ and the integral expressed in terms of the values of stoichiometric functions for each age set \vec{x} . Moreover, Eq. (2.23) allows to express Chapman-Kolmogorov (forward and backward) Equations in terms of the rate functions and the propensity as follows:

$$\begin{aligned} \mathcal{D}_{n,t}\mathcal{P}[n, t|m, t'] &= \sum_{r=1}^R \int_{\mathbb{R}^{N_r}} \gamma_r(\vec{x})\Phi_r[n - \nu_r, [\vec{x}]]\mathcal{P}[n - \nu_r[\vec{x}], t|m, t']d\vec{x} \\ &\quad - \sum_{r=1}^R \int_{\mathbb{R}^{N_r}} \Phi_r[n, \vec{x}]\gamma_r(\vec{x})\mathcal{P}[n, t|m, t']d\vec{x} \end{aligned} \quad (2.30)$$

and

$$\begin{aligned} \mathcal{D}_{m,t'}\mathcal{P}[n, t|m, t'] &= \sum_{r=1}^R \int_{\mathbb{R}^{N_r}} \gamma_r(\vec{x})\Phi_r[m, \vec{x}]\mathcal{P}[n, t|m, t']d\vec{x} \\ &\quad - \sum_{r=1}^R \int_{\mathbb{R}^{N_r}} \gamma_r(\vec{x})\Phi_r[m, \vec{x}]\mathcal{P}[n, t|m + \nu_r[\vec{x}], t']d\vec{x}. \end{aligned} \quad (2.31)$$

Now, two mathematical objects need to be introduced to make the notation compact. The first one is the operator Γ_w acting on a function f as $\Gamma_w[f] = \exp(\sum_{i=1}^M \int_0^\infty w_i(x) \ln(f(x)) dx)$. In the upcoming Example (Example 2), we discuss how this formulated can be applied to the example proposed in Example 1. The second is the step operator $\varepsilon_x^{\pm m}$ which shifts the argument of any functional \mathcal{F} : $\varepsilon_x^{\pm m} \mathcal{F}[n] = \mathcal{F}[n \pm m\delta_x]$, where δ_x denotes the Dirac- δ function centred in x . Employing the operators Γ_w and ε , the shifts induced by the reactions (in Eq. (2.15) ($n - \nu_r[\vec{x}]$) and in Eq. (2.18) ($m + \nu_r[\vec{x}]$)) can be encoded in a more compact way by combining the two operators as $\Gamma_{\pm\nu_r[\vec{x}]}[\varepsilon]$.

In fact, the forward Master Equation (2.15) can be expressed as:

$$D_{n,t} \mathcal{P}[n, t | \cdot] = \sum_{r=1}^R \int_{\vec{x}} \left(\Gamma_{-\nu_r[\vec{x}]}[\varepsilon] - 1 \right) \Phi_r[n; \vec{x}] \mathcal{P}[n, t | \cdot] d\vec{x} \quad (2.32)$$

and the backward Master Equation (2.18) becomes:

$$D_{m,t_0} \mathcal{P}[\cdot | m, t_0] = \sum_{r=1}^R \int_{\vec{x}} \Phi_r[m; \vec{x}] \left(1 - \Gamma_{\nu_r[\vec{x}]}[\varepsilon] \right) \mathcal{P}[\cdot | m, t_0] d\vec{x}. \quad (2.33)$$

The Chapman-Kolmogorov differential Equations were derived from basic concepts of stochastic process theory and combined with a functional generalisation of the stoichiometric notation. Eqs. (2.18) and (2.32) provide a relatively compact way to describe the evolution of age-structure multispecies population modelled as a jumping process with a deterministic drift. An application of the CKE equation to a death-migration model is presented in Example 2.

Example 2 This example aims only to show and discuss the application of a previous result to a concrete case. For an age-structured migration-death model, the Master Equation is given by:

$$\begin{aligned} D_{n,t} \mathcal{P}[n, t] &= \int_0^\infty d(x) (\varepsilon_x^{+1} - 1) n(x) \mathcal{P}[n, t] dx + \\ &\quad + \int_0^\infty \nu(x) (\varepsilon_x^{-1} - 1) dx \mathcal{P}[n, t] \end{aligned} \quad (\text{II})$$

The Liouville's operator still encodes the ageing drift (LHS) and the RHS accounts the stochastic jumps induced by two reactions (death and migration) with different propensities (Eq. (2.23)). Later, in Example 3, I show how this CKE can be manipulated to obtain a first-order PDE.

2.3 Generating Functionals

The generating function is a useful representation of the probability density, which often alleviates the burden of a long calculation. Here, the functional generalisation of the standard generating function is simply called generating functional. Recalling the definition of the generating function from [63], the moment-generating function Z for a random vector \vec{N}^t is defined as the expectation of the random variable $e^{\vec{H} \cdot \vec{N}}$:

$$Z(\vec{H}) = \sum_{\{\vec{N}\}} e^{\vec{H} \cdot \vec{N}} P(\vec{N}) \quad (2.34)$$

where P is the cumulative distribution function of \vec{N} , the symbol \cdot labels the standard scalar product and, for our goals, \vec{H} can be thought of as a dull variable, but, in general, it is defined as a frequency-domain vector or a real-valued conjugate vector to \vec{N} similar to Laplace's transformation. Providing further details would require an entire section on Fourier, Laplace, Melling and Z-transformations, which goes beyond the purposes of this thesis; a detailed dissertation on these topics can be found in [66, 107]. In the following, this concept is generalized in a functional context, and it will play a crucial role in the derivation of the results presented in this thesis; this generalization resembles the one usually exploited in Quantum and Classic Field Theory, where such functions are usually called *partition functions* and are defined in the path integral formalism [108, 109]. Two generating functionals are defined, the forward generating functional:

$$\begin{aligned} \mathcal{Z}[h, t|\cdot] &:= \int e^{\sum_{i=1}^M \int_0^\infty n_i(x) \ln(h_i(x)) dx} \mathcal{P}[n, t|m, 0] \mathcal{D}n \\ &= \int \mathcal{D}[n] \Gamma_n[h] \mathcal{P}[n, t|\cdot] \end{aligned} \quad (2.35)$$

and the backward generating functional:

$$\begin{aligned} \hat{\mathcal{Z}}[\cdot|\eta, t_0] &:= \int e^{\sum_{i=1}^M \int_0^\infty m_i(x) \ln(\eta_i(x)) dx} \mathcal{P}[n, t|m, 0] \mathcal{D}m \\ &= \int \mathcal{D}[m] \Gamma_m[\eta] \mathcal{P}[\cdot|m, t_0]. \end{aligned} \quad (2.36)$$

Note that the auxiliary variable is a general age-dependent vector of functions $h(x) = (h_1(x), \dots, h_M(x))$ ($\eta(x) = (\eta_1(x), \dots, \eta_M(x))$) and the integral is over

non-negative measures n (m) with positive support.

Similarly to the unstructured case, the generating functional allows expressing the forward and backward Master Equation (Eqs. (2.32) and (2.33)) as Functional Derivative Equations (F.D.E.) for \mathcal{Z} and $\hat{\mathcal{Z}}$. To do so, observe that the *ageing Liouville's operator* symmetrically is expressed after mapping $n(x) \rightarrow h(x)$ or $m(x) \rightarrow \eta(x)$:

$$\mathcal{D}_{n,t} \rightarrow \mathcal{D}_{h,t} \quad (2.37)$$

$$\mathcal{D}_{m,t_0} \rightarrow \mathcal{D}_{\eta,t_0}.$$

Then, the following two results do all the work:

$$\int e^{\int n_i(x) \ln(h_i(x)) dx} \varepsilon_x^{\pm m} \mathcal{P}[n, t] \mathcal{D}n = h_i^{\mp m}(x) \mathcal{Z}[h, t] \quad (2.38)$$

and:

$$\frac{\delta}{\delta h(y)} \mathcal{Z}[h, t] = \int n_1(y) e^{\int n_i(x) \ln(h_i(x)) dx} \mathcal{P}[n, t] \mathcal{D}n. \quad (2.39)$$

Finally, the forward and backward Chapman-Kolmogorov can be expressed as FDEs:

$$\mathcal{D}_{h,t} \mathcal{Z}[h, t] = \sum_{r=1}^R \int_{\vec{x}} \mathcal{H}_{\vec{x},r} \left[h, \frac{\delta}{\delta h} \right] \mathcal{Z}[h, t] d\vec{x} \quad (2.40)$$

and:

$$\mathcal{D}_{\eta,t_0} \hat{\mathcal{Z}}[\cdot | \eta, t_0] = \sum_{r=1}^R \int_{\vec{x}} \mathcal{Q}_{\vec{x},r} \left[\eta, \frac{\delta}{\delta \eta(x)} \right] \mathcal{Z}[\cdot | \eta, t_0] d\vec{x} \quad (2.41)$$

where the functional operator $\mathcal{H}_{\vec{x},r}$ ($\mathcal{Q}_{\vec{x},r}$) express a non-linear combination of the functional derivative operators associated with the i -th species $\frac{\delta}{\delta h_i(x)}$ ($\frac{\delta}{\delta \eta_i}$) and $h_i(x)$ ($\eta_i(x)$). This differential formulation (Eqs. (2.41) and (2.40)) works especially well for non-interacting populations. In such a case, Eqs. (2.41) and (2.40) become a FDE of order less than one and different methods to study this class of FDEs are available [110]. In Example 3, a similar case is discussed for a death-migration model.

Example 3 The CKE of an age-structured model can be expressed as a FDE of the generating function. From the forward CKE of the death-migration model (Example 2), a first-order FDE can be recalled:

$$\mathcal{D}_{h,t}\mathcal{Z}[h,t] = \int_0^\infty d(x)(1-h(x))\frac{\delta\mathcal{Z}[h,t]}{\delta h(x)}dx + \int_0^\infty \nu(x)(h(x)-1)dx\mathcal{Z}[h,t] \quad (\text{III})$$

Applying the Characteristic Curves Method (C.C.M.) [110], we obtain two ordinary differential equations: $\dot{t}(s) = 1$ and $\frac{d\mathcal{Z}[h(s),t(s)]}{ds} = \int_0^\infty \nu(x)(h(x,s)-1)dx\mathcal{Z}[h,t]$, and one PDE:

$$(\partial_s + \partial_x)h(x,s) = d(x)(h(x,s)-1) \quad (\text{IV})$$

The CCM can also be applied (a second time) to the last equation so that: $\dot{x}(s') = 1, \dot{t}(s') = 1$ and $\frac{d}{ds'}(h(x(s'),s(s')) = d(x(s'))(h(x(s'),s(s'))-1)$. Therefore, an exact solution of the generating functional \mathcal{Z} can be recalled:

$$\mathcal{Z}[h,t] = \exp\left(\int_0^\infty \nu(x)(h(x+t)-1) \int_0^t e^{-\int_s^t d(x+u)du} ds dx\right) \quad (\text{V})$$

This derivation path is not always available; for instance, in case the order of the FDE is higher than one or in case of a branching process where the age of the products is constant and does not depend on the age (see Ch. 4).

2.4 Integral Chapman-Kolmogorov Equations

The integral formulation proposed by Bellman and Harris allowed us to encode the age-structured dynamics in an integral Volterra's equation (Ch. 1). Its Non-Linear Volterra's representation [111] is a clever way to encode the age-structured dynamics and allows a quick derivation of several quantitative insights, such as the moments or the extinction probability [112]. Inspired by Bellman's and Harris's work [71], I showed that it is always possible to express a general age-structured stochastic process as a system of non-linear Volterra's equations. Here, I illustrated the main steps on the path to these results; a detailed proof can be found in App. A. The first step is noticing that equations (2.15) and (2.18) are FDEs. Therefore both equations can be studied via the method of characteristic curves so that the continuous variable s_1 (s_2) parametrises the characteristic curves rising from forward Master Equation Eq. (2.15) (backward Master equation Eq. (2.18)).

In the forward and backward CKEs, the times t and t_0 , along the characteristic, are described by the ODE's: $\dot{t}(s_1) = 1$ and $\dot{t}_0(s_2) = 1$. Instead, $2M$ transport equations can be recalled from terms with the functional derivatives in n_i and m_i (in Eqs. (2.18) and (2.15)): $(\partial_{s_1} + \partial_x)n_i(x, s_1) = 0$ and $(\partial_{s_2} + \partial_x)m_i(x, s_2) = 0$. Therefore, the following constraints follow from the continuity equations: $n_i(x, s_1) = n_i(x + t - s_1, t)$ and $m_i(x, s_2) = m_i(x - s_2, 0)$ for all the i -th species.

For brevity of notation, I use the following upper-index notation to label the translation $n_i(x, s_1) = n_i^{+t-s_1}(x, t)$ and $m_i(x, s_2) = m_i(x - s_2, 0) = m_i^{-s_2}(x, 0)$.

The functional probability \mathcal{P} is described along its tangent plane by :

$$\frac{d(\Pi(s_1)\mathcal{P}[s_1|\cdot])}{ds_1} = \int \Pi(s_1)\mathcal{W}[n(s_1)|q]\mathcal{P}[q, t(s_1)|\cdot]\mathcal{D}q, \quad (2.42)$$

where $\mathcal{P}[n(s_1), t(s_1)|\cdot] = \mathcal{P}[s_1|\cdot]$ and $\Pi_n(s_1)$ is defined as: $\Pi_n(s_1) = e^{\int \int_0^{s_1} \mathcal{W}[q|n^{+s'}(0)]\mathcal{D}q ds'}$. Instead, the functional probability of the other tangent plane (in respect of m) space is:

$$\frac{d(\Pi_m(s_2)\mathcal{P}[\cdot|s_2])}{ds_2} = - \int \Pi_m(s_2)\mathcal{W}[q|m(s_2)]\mathcal{P}[\cdot|q, t(s_2)]\mathcal{D}q, \quad (\text{eee})$$

where $\mathcal{P}[\cdot|m(s_2), t_0(s_2)] = \mathcal{P}[\cdot|s_2]$ and Π_m is defined as $\Pi_m(s_2) = e^{-\int \int_0^{s_2} \mathcal{W}[q|m^{-s'}(0)]\mathcal{D}q ds'}$.

At this point of the derivation, Eq. (eee) and Eq. (2.42) can be expressed in terms of the original variables $\{m, n, t, t_0\}$. The forward Master Equation becomes:

$$\begin{aligned} \mathcal{P}[\cdot|m, t_0] &= \Pi_m(t - t_0)\delta[n - m^{-(t-t_0)}] \\ &\quad + \int_0^{t-t_0} \int \Pi_m(y)\mathcal{W}[q|m^{-y}]\mathcal{P}[\cdot|q, t_0 + y]\mathcal{D}q dy, \end{aligned} \quad (2.43)$$

while the backward Master Equation becomes:

$$\begin{aligned} \mathcal{P}[n, t|\cdot] &= \Pi_n(t - t_0)\delta[n^{+(t-t_0)} - m] \\ &\quad + \int_0^{t-t_0} \int \Pi(y)\mathcal{W}[n^{t-y}|q]\mathcal{P}[q, y|\cdot]\mathcal{D}q dy, \end{aligned} \quad (2.44)$$

where $\mathcal{P}[n, t|m^{-(t-t_0)}, t]$ and $\mathcal{P}[n^{+t}, t_0|m, t_0]$ are respectively set equal to $\delta[n - m^{-(t-t_0)}]$ and $\delta[n^{+t} - m]$.

Eqs. (2.43) and (2.44) respectively describe a stochastic process $(n, t|m, t_0)$ in

terms of the last and the first events. Eq.(2.43) weights the probability of observing as last change in the process $\nu_r[\vec{x}]$ on the time distribution of this change times. Eq.(2.44) weights the probability of observing as first change in the process $\nu_r[\vec{x}]$ on the time distribution of this last change times.

As done for the differential CKE, the stoichiometric notation is used to express Eqs. (2.44) and (2.43) in terms of stoichiometric functions. The function q , in Eq. (2.43), can be expressed, for each i -th species, as $q_i = (q_{n,r}(\vec{x}, y))_i = n_i^{t-y} - \nu_{r,i}[\vec{x}]$. Therefore Eq. (2.43) becomes:

$$\begin{aligned}\mathcal{P}[n, t | \cdot] &= \Pi_n(t) \delta[n^{t-t_0} - m] \\ &+ \sum_{r=1}^R \int_{\vec{x}} \int_0^{t-t_0} \int \Pi_{n,\gamma_r}(y) \mathcal{P}[p_{n,r}(\vec{x}, y), t-y | \cdot] d\vec{x} dy,\end{aligned}\quad (2.45)$$

where $\Pi_n(t) = \frac{\Pi_{n,\gamma_r}(t)}{\gamma_r(\vec{x})} = e^{-\sum_{r=1}^R \int_0^t \int_{\vec{x}} \gamma_r(\vec{x}) \Phi_r[n^{t-s}; \vec{x}] d\vec{x} ds'}$ is the probability of not observing any reactions in the range of time $[0, t]$

In the backward CKE Eq.(2.44), the term $p_{m,r}$ can be expressed as $p_{m,r}(\vec{x}, y) = m^{-y} + \nu_r[\vec{x}]$, in order to obtain:

$$\begin{aligned}\mathcal{P}[\cdot | m, t_0] &= \Pi_m(t - t_0) \delta[m - m^{-(t-t_0)}] \\ &+ \sum_{r=1}^R \int_0^{t-t_0} \int_{\vec{x}} \Pi_{m,\gamma_r}(y, \vec{x}) \mathcal{P}[\cdot | q_{m,r}(\vec{x}, y), t_0 + y] d\vec{x} dy,\end{aligned}\quad (2.46)$$

where $\frac{\Pi_{m,\gamma_r}(t-t_0, \vec{x})}{\gamma_r(\vec{x})} = \Pi_m(t - t_0) = e^{-\sum_{r=1}^R \int_{\vec{x}} \int_0^{t-t_0} \gamma_r(\vec{x}) \Phi_r[m^{-s'}; \vec{x}] d\vec{x} ds'}$ and it still labels the probability of not having any reaction in the range of time $[t_0, t]$.

The same representation can be exploited for the forward and backward generating functional. Using the backward generating function in Eq. (2.45):

$$\begin{aligned}\hat{\mathcal{Z}}[\cdot | \eta, t_0] &= \Pi_n(t) \Gamma_{n^{t-t_0}}[h] \\ &+ \sum_{r=1}^R \int_{\vec{x}} \int_0^{t-t_0} \int \Pi_{n,\gamma_r}(y) \mathcal{Z}[p_{n,r}(\vec{x}, y), t-y | \eta, t_0] d\vec{x} dy,\end{aligned}\quad (2.47)$$

while using the forward generating function in Eq. (2.46):

$$\begin{aligned}\mathcal{Z}[h, t | \cdot] &= \Pi_m(t - t_0) \Gamma_{m^{-(t-t_0)}}[h] \\ &+ \sum_{r=1}^R \int_0^{t-t_0} \int_{\vec{x}} \Pi_{m,\gamma_r}(y, \vec{x}) \mathcal{Z}[h, t | q_{m,r}(\vec{x}, y), t_0 + y] d\vec{x} dy.\end{aligned}\quad (2.48)$$

Eqs. (2.49) and (2.46) are linear integral Volterra's equations and resemble the Bellman-Harris formula. To increase the similarity with it, observe that, for Time-homogeneous Markov chains [3], the time-integral on the RHS of the last two equations can be expressed as, i.e. Eq. (2.46):

$$\begin{aligned}\mathcal{Z}[h, t|\cdot] &= \Pi_m(t - t_0) \Gamma_{m-(t-t_0)}(h) \\ &+ \sum_{r=1}^R \int_0^{t-t_0} \int_{\vec{x}} \Pi_{m,\gamma_r}(y, \vec{x}) \mathcal{Z}[h, t-y|q_{m,r}(\vec{x}, y), t_0] d\vec{x} dy.\end{aligned}\quad (2.49)$$

Therefore, if the ages of the products do not depend on the reactants $q_{m,r}(\vec{x}, y) = q_{m,r}$, the age-structured dynamics is expressed in terms of renewal equations, as the Bellman's and Harris's formula. Secs. 2.5 and 2.5.2 are reserved to a detailed analysis of the difference and similarities between Eq. (2.46) and Bellman-Harris Equation ((1.26)).

In conclusion, I reserved Example 4 to show how the integral formulation can be applied to a death-migration scenario.

Example 4 *The integral CKEs allow us to express the dynamics with a system of Volterra's equations for the generating or the probability functional. In a death-migration model, the generating functional with initial condition $m = 0$ can be expressed as follows:*

$$\mathcal{Z}[h, t|0, 0] = \int_0^\infty \nu(y) \int_0^t \mathcal{Z}[h, t-u|\delta_{u+y}, 0] du dy \quad (\text{VI})$$

Instead, the initial condition $(\delta_x, 0)$ leads to the following integral equation:

$$\begin{aligned}\mathcal{Z}[h, t|\delta_x, 0]\Pi(x) &= \Pi(t+x)h(t+x) + \int_0^t \Pi_d(u)du + \\ &+ \int_0^\infty \nu(y) \int_0^t \mathcal{Z}[h, t-u|\delta_{u+y} + \delta_{x+u}, 0] du dy\end{aligned}\quad (\text{VII})$$

where Π is the survival probability of a newborn cell $\Pi(t) = \frac{\Pi_d(t)}{d(t)} = \exp(-\int_0^t d(u)du)$. Using Eq. (2.46), any initial condition can be described with an integral equation for the \mathcal{P} or \mathcal{Z} . Therefore, these expressions for different initial conditions can be nested one in the other to obtain a series of functions converging to the solution proposed in Example 2.

2.4.1 Moments

The evaluation of the expectation values of n -functionals is often an important part of the analysis of stochastic models. Here, possible methods to evaluate moments are presented. To begin, the expected value of a functional F of n is defined:

$$\langle F[n] \rangle = \int F[n] \mathcal{P}[n, t] \mathcal{D}n. \quad (2.50)$$

Then, Eq. (2.15) (and Eq. (2.18)) can be manipulated to derive Dynkin's formula for the expectation value of functional $F[n]$:

$$\begin{aligned} & \partial_t \langle F[n^t] \rangle + \sum_{i=1}^M \int \frac{\delta \langle F[n] \partial_x n_i(x) \rangle}{\delta n_i(x)} dx \\ &= \sum_{r=1}^R \int_{\vec{x}} \langle \Phi_r[n; \vec{x}] \left(\Gamma_{-\nu_r[\vec{x}]}[\varepsilon] - 1 \right) F[n] \rangle d\vec{x}. \end{aligned} \quad (2.51)$$

It is interesting to observe that the left side of the latter equation, i.e. $F[n] = n(x)$ is equal to $(\partial_x + \partial_t) \langle n \rangle(x, t)$ proposed in McKendrick's and von Foerster's deterministic work. On the other hand, the generating functional can also be exploited to determine the moments for the number of agents belonging to the $i-th$ species:

$$\left[\left(h_i(x) \frac{\delta}{\delta h_i(x)} \right)^l \mathcal{Z}[h, t | m, 0] \right]_{h(x)=1 \forall x \in \mathbb{R}} = \langle n_i(x)^l \rangle \quad (2.52)$$

and

$$\left[\frac{\delta^l}{\delta h_i^l(x)} \mathcal{Z}[h, t | m, 0] \right]_{h(x)=1 \forall x \in \mathbb{R}} = \left\langle \frac{\tilde{n}_{i,l}(x)}{l!} \right\rangle, \quad (2.53)$$

where $\tilde{n}_{i,l}(x)$ represents the factorial moments and is equal to $\frac{n_i(x)!}{l!}$. Applying a derivative with respect of $h(x)$ and setting $h(x) = 1 \forall x \in \mathbb{R}$, allows to write Eq. (2.47) as:

$$\begin{aligned} \left\langle \frac{\tilde{n}_{i,l}(x)}{l!} \right\rangle &= \theta(1-l) \Pi_m(t-t_0) \delta[m^{-(t-t_0)}](h) \\ &+ \sum_{r=1}^R \int_0^{t-t_0} \int_{\vec{x}} \Pi_{m,\gamma_r}(y, \vec{x}) \underbrace{\left\langle \frac{\tilde{n}_{i,l}(x)}{l!} | q_{m,r}(\vec{x}, y), t_0 + y \right\rangle}_{\mathcal{I}} d\vec{x} dy, \end{aligned} \quad (2.54)$$

in which the term \mathcal{I} represents the expectation value of the factorial moments conditioned on the different initial conditions. It is going to be clear in the

following that Eq. (2.54) allows the expression of statistical quantities as a system of integral linear equations.

In the following, I exploit Example 5 to show how the first moment can be recalled via Dynkin's formula or using Eq. 2.52 in a migration-death model.

Example 5 *An exact solution of the generating functional allows to exactly quantify any moment. Here, an example of*

$$(\partial_x + \partial_t)\langle n(x) \rangle = -d(x)\langle n(x) \rangle + \nu(x) \quad (\text{VIII})$$

The characteristic curves are described by three ODEs: $\frac{dx(s)}{ds} = 1$ $\frac{dt(s)}{ds} = 1$ and $\frac{d\langle n(s) \rangle}{ds} = -d(x(s))\langle n(s) \rangle$ and the solution can be exactly recalled. The same result can also be recalled by applying the functional derivative in respect of $h(x)$ and then setting $h(x) = 1 \forall x \in \mathbb{R}$ to the solution of the generating functional (Example 3):

$$\left(\frac{\delta \mathcal{Z}[h, t]}{\delta h(x)} \right)_{h(x)=1 \forall x} = \int_0^\infty \nu(y) \frac{\delta h(y+t)}{\delta h(x)} \int_0^t e^{-\int_s^t d(y+u)du} ds dy \quad (\text{IX})$$

The functional derivative is given by $\frac{\delta h(y+t)}{\delta h(x)} = \delta(y+t-x)$. After a few manipulations, for $x > t$, we obtain the average number of individuals with age x :

$$n(x, t) = \int_0^t \nu(x-t+u) e^{-\int_t^u d(x-t+z)dz} du \quad (\text{X})$$

The last equation can be plugged in the first equation (in this example) to show its coherence.

2.5 Age-Structured Branching Processes

The attention has to be now focused on age-structured dynamics driven by branching processes. Formally, an age-structured branching process is defined as a reaction r with a reactant stoichiometric function such that: $\int_{\mathbb{R}} \nu_{r,i}^-[\vec{x}](u)du = 1$; in other words, there is no interdependence between the reactants since the reaction rates depend only on the age of one reactant. The *stoichiometric reactant functions* do not allow more than one reactant so that:

$$s(x) \xrightarrow{\gamma_r(x)} \sum_{i=1}^M \int \nu_r^+[x](u) s_i(u) du. \quad (2.55)$$

Eq. (2.55) is equivalent to stating that the evolution of each individual is independent from the other. This can be expressed in terms of the functional probabilities with times $t' \leq t$:

$$\mathcal{P}[n, t|m, t'] = (\mathcal{P}[t|m - k, t'] * \mathcal{P}[t|k, t'])[n], \quad (2.56)$$

where the symbol $*$ labels the convolution product, or, equivalently, in terms of the generating functional as:

$$\mathcal{Z}[h, t|m, t'] = \mathcal{Z}[h, t|m - k] \mathcal{Z}[h, t|k, t']. \quad (2.57)$$

Eqs. (2.56) and (2.57) simply state that the evolution paths of each agent are independent. Therefore, given a stochastic process $(n, t|m, t_0)$, it is sufficient to study the process $(n, t|\delta_x, t_0)$ since:

$$\mathcal{Z}[h, t|m, t_0] = \exp \left(\sum_{i=1}^M \int_0^\infty m_i(x_0) \ln(\mathcal{Z}[h, t|_i \delta_{x_0} \delta_i, t_0]) dx_0 \right). \quad (2.58)$$

Setting an initial condition $m = \delta_x \delta_i$ (i.e. one agent with age x that belongs to the i -th species), Eq.(2.44) becomes:

$$\begin{aligned} \mathcal{Z}[h, t|\delta_{x_0}] &= \Pi(x_0, t) h(x_0 + t) \\ &+ \sum_{r=1}^R \int_0^t \Pi_{\gamma_r}(x_0, u) \Gamma_{\nu_r[x_0+y]} [\mathcal{Z}[h, t-u|\delta_\bullet]] du. \end{aligned} \quad (2.59)$$

From a physical point of view, Eq. (2.59) represents an integral equation for the offspring generating functional of a single individual with age x_0 .

Interestingly, an age-dependent formulation of the Galton-Watson framework can also be derived. This can be accomplished by noticing that the integral Chapman-Kolmogorov can be expressed in terms of the generating functional \mathcal{Z} as:

$$\mathcal{Z}[h, t|\delta_{x_0} \delta_i, 0] = \int \Gamma_q[\mathcal{Z}[h, t|\delta_\bullet, t']] \mathcal{P}[q, t'|\delta_{x_0} \delta_i, 0] \mathcal{D}q. \quad (2.60)$$

The latter expression shows that the generating functional has a propagator:

$$\mathcal{Z}[h, t|\delta_i \delta_{x_0}, 0] = \mathcal{Z}[\mathcal{Z}[h, t|\delta_\bullet, t'], t'|\delta_i \delta_{x_0}, 0]. \quad (2.61)$$

Moreover, given any periodic environment with period T (i.e. parameters con-

figurations of the system which periodically repeats themselves), the asymptotic value of the generating functional $\mathcal{Z}^*[h|\delta_{x_0}, 0]$ can be written as:

$$\mathcal{Z}^*[h|m, 0] = \mathcal{Z}[\mathcal{Z}^*[h|m, 0], T|\delta_{x_0}\delta_i, 0], \quad (2.62)$$

in which $\mathcal{Z}[\cdot, T|\delta_i\delta_{x_0}, 0]$ is the offspring generating function for a process $(n, T|\delta_{x_0}\delta_i, 0)$. Follows that the asymptotic generating functional can be expressed in a fixed point formula (2.62), as in Galton-Watson theory, and it can be expressed as a system of non-linear integral equations via Eq. (2.59). This framework can be adapted to describe any kind of age-structure branching process and can be considered as a functional representation of the Galton-Watson formulation. In the following chapters, the latter results are often applied (Secs. 4.3 and 5.3), especially for $h(x) = 0$. In such a case, the asymptotic extinction probability $p(x_0)$ for an initial particle with age x_0 is given by $p(x_0) = \lim_{t \rightarrow \infty} \mathcal{Z}[h = 0, t|\delta_{x_0}, 0]$

Leaving the Galton-Watson theory aside, a wide set of results is also available to compute the moments via Eq. (2.59). Here, the ones proposed by Feller, in [73], are taken into account:

Theorem 1 *Let G be a distribution function on $(0, \infty)$. We shall assume $G(0) = G(0^+) = 0$. Consider the equation:*

$$K(t) = f(t) + m \int_0^t K(t-u)dG(u), \quad (2.63)$$

where K is the unknown function, m is a positive constant, and f is a known Borel measurable function that is bounded on every finite interval. I adopt the convention that G is continuous to the right. The integral is interpreted as \int_0^{t+0} and is a Lebesgue-Stieltjes integral. The total variation of any function g on the interval $[t_1, t_2]$ is denoted by $\int_{t_1}^{t_2} |dg(t)|$. The convolutions of G are define by $G_1 = G$, $G_n(t) = \int_0^t G_{n-1}(t-u)dG(u)$. The function $H(m, t)$, which we shall see below is finite, is defined by:

$$H(m, t) = \sum_{n=1}^{\infty} m^{n-1} G_n(t). \quad (2.64)$$

Eq. (2.64) has one and only one solution that is bounded on every finite

interval. This solution has the form

$$K(t) = f(t) + m \int_0^t f(t-u)dH(m,u). \quad (2.65)$$

In particular, if $f(t) = G(t)$, then $K(t) = H(m,t) < \infty$.

Lemma 2.5.1 Suppose that G is not a lattice distribution and that α is defined by the following integral constraint:

$$m \int_0^\infty e^{-\alpha t} dG(t) = 1. \quad (2.66)$$

Suppose also that the following condition holds: $f(t)e^{-\alpha t}$ is the difference of two bounded non-increasing functions, each of which is integrable on $(0, \infty)$, and $\int_0^\infty t e^{-\alpha t} dG(t) < \infty$.

Then $K(t) \approx n_f e^{\alpha t}$ as $t \rightarrow \infty$ where:

$$n_f = \frac{\int_0^\infty f(t)e^{-\alpha t} dt}{m \int_0^\infty t e^{-\alpha t} dG(t)}. \quad (2.67)$$

Exploiting Feller's results (Theorem 1 and Lemma 2.5.1), the expectation value of N can always be expressed, in the asymptotic limit as:

$$\mathbb{E}\{N\}(t) = n_1 e^{\alpha t} \quad (2.68)$$

where α and n_1 are given by:

$$\begin{aligned} \int_0^\infty e^{-\alpha x} dG(x) &= \frac{1}{m} \\ n_1 &= \frac{\int_0^\infty e^{-\alpha y} (1 - G(y)) dy}{m \int_0^\infty y e^{-\alpha y} (1 - G(y)) dy}. \end{aligned} \quad (2.69)$$

Moreover, Eq. (1.26) allows to express the k -th moment as a function of the moments of orders $1, \dots, k-1$. It follows that each moment can be directly expressed as a function of α . For the sake of completeness, I remind the reader that Harris proposed also an analysis of the statistic properties of the variable N scaled by the asymptotic average $n_1 e^{\alpha t}$ [112].

2.5.1 Deterministic Limit

The closing part of this chapter aims to assess the coherence of this theory with previous well-known results. The first result is the McKendrick-von Foerster framework (Sec. 2.5.1) which can be derived from Dynkin's Eq. (2.51) with $F[n] = n(x)$. As in the McKendrick-von Foerster Equation, each individual $s(x)$ can divide (leading to the creation of two newborns $s(0)$) with rate $\gamma(x)$ or die with rate $d(x)$. Therefore, the Liouville's operator (LHS of Eq. (2.51)) applied to the expected number of agents with age $x \langle n^t \rangle$, is given by a transport PDE:

$$\begin{aligned} & \partial_t \langle n^t(x) \rangle + \int \frac{\delta \langle n(x) \partial_y n(y) \rangle}{\delta n(y)} dy \\ &= \partial_t \langle n^t(x) \rangle + \int \delta(x - y) \langle \partial_x n(x) \rangle = (\partial_t + \partial_x) \langle n^t(x) \rangle. \end{aligned} \quad (2.70)$$

while the RHS of Dinkyn's formula (Eq. (2.51)) can be split into two terms, one representing the division process:

$$\int_0^\infty \langle n(y) \left(\varepsilon_0^{+2} \varepsilon_x^{-1} - 1 \right) n(x) \rangle dy = -\gamma(x) n(x) + 2\delta(x) \int_0^\infty \gamma(y) \langle n(y) \rangle dy \quad (2.71)$$

and one the death rate:

$$\int_0^\infty \langle n(y) \left(\varepsilon_x^{-1} - 1 \right) n(x) \rangle dy = -d(x) n(x). \quad (2.72)$$

Setting Eq. (2.70) equal to the sum of Eqs. (2.71) and (2.72), Dinkyin's formula for the average abundances is given:

$$(\partial_t + \partial_x) \langle n^t(x) \rangle = -(\gamma(x) + d(x)) \langle n^t(x) \rangle + \delta(x) 2 \int \gamma(x) \langle n^t(x) \rangle dx. \quad (2.73)$$

The last equation is nothing else but the McKendrick-von Foerster Equation. In fact, for age $x = 0$, the initial conditions of McKendrick-von Foerster PDE are obtained:

$$\langle n(0, t) \rangle = 2 \int \gamma(x) \langle n^t(x) \rangle dx. \quad (2.74)$$

The deterministic evolution of a division-death age-structured process can be expressed as the average evolution of the stochastic trajectories; the validity of

the latter conclusion holds only for branching processes or, more in general, in any configuration ensuring the independence of the individual paths. This is a trivial result. However, the coherency with the deterministic results acts as a fundamental step in the development of this theory.

2.5.2 Comparison with Bellman-Harris Process

The Bellman-Harris process describes the stochastic trajectory of a newborn cell whose life-length τ is distributed an NHPP with rate λ : $\Pi_\lambda(\tau) = \lambda(\tau)e^{-\int_0^\tau \lambda(u)du}$ and, once the life of a cell ends, the cell turns into k -newborns with probability p_k (see Fig. 2.1 (a)). The original formulation of the Bellman-Harris Equation does not exploit a functional representation, instead, it quantifies the state of the system with the stochastic variable N counting the total number of cells. Formally, the Bellman-Harris Equation states that the probability generating function for an initial newborn evolves in accord with:

$$Z(H, t) = \Pi(t)H + \sum_{k=0}^M p_k(Z^k(H) * \Pi_\lambda)(t), \quad (2.75)$$

where Π is the surviving probability defined as $\Pi(\tau) = \frac{\Pi_\lambda(\tau)}{\lambda(\tau)}$, while the symbol $*$ labels the convolution product.

In the following, the same process is investigated using the results previously proposed in the chapter.

In contrast to Bellman's and Harris's formulation, each reaction is an independent NHPP such that:

$$s(x) \xrightarrow{\gamma_k(x)} ks(0) \quad k = 0, 1, \dots, M. \quad (2.76)$$

The process is a branching process ($\nu_k[\vec{x}] = k\delta_0 - \delta_x$) and can be studied with the functional methods proposed in Sec. 2.5. It follows an integral Volterra's equation for the generating forward functional \mathcal{Z} :

$$\mathcal{Z}[h, t|\delta_{x_0}]\Pi(x) = \Pi(t+x)h(t+x) \quad (2.77)$$

$$+ \sum_{k=0}^{\infty} \int_0^t \Pi_{\gamma_k}(u+x_0) \mathcal{Z}^k[h, t-u|\delta_0, 0] du, \quad (2.78)$$

where $\Pi(t) = \exp(-\int_0^t \sum_{k=0}^{\infty} \gamma_k(x+u) du)$ is the probability of observing

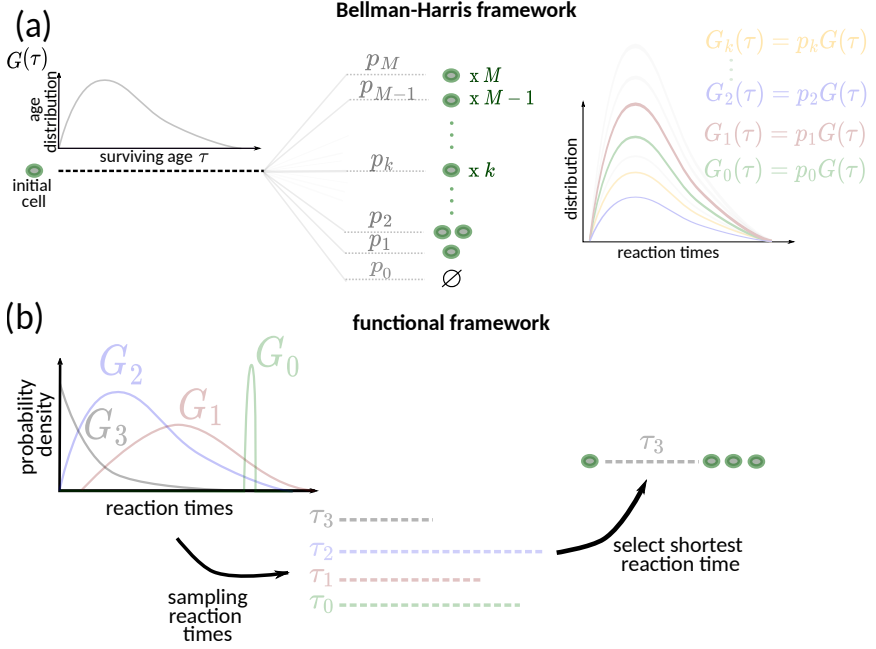


Figure 2.1: **Representation of the difference between Bellman-Harris process and the framework proposed in the thesis.** (a): cells lives are distributed accordingly with the same NHPP. The probability of dividing in k -newborn is given by $G(\tau_k)p_k$. (b): Each reaction time is distributed as an independent NHPP. The shortest sampled time from the different reaction time distributions coincides with the survival time.

no reactions until time t for an individuals with age x , while the quantity $\Pi_{\gamma_k}(t) = \gamma_k(t)\Pi(t)$ is the probability of surviving till time t for an initial cell with age 0 and then undergoing k -th reaction in the age range $[t, t + dt)$. If the initial condition is $x_0 = 0$, a functional generalisation of the Bellman-Harris Equation can be recalled:

$$\mathcal{Z}[h, t|0] = \Pi(t)h(t) + \sum_{k=0}^{\infty} \int_0^t \Pi_{\gamma_k}(u)\mathcal{Z}^k[h, t-u|\delta_0, 0]du. \quad (2.79)$$

A bridge with the unstructured case can be easily built by switching from the stochastic function $n^t(x)$ to the stochastic variable $N^t = \int_0^\infty n^t(x)dx$ which labels the total number of agents independently on the age. Fixing $h(x) = H \forall x \in \mathbb{R}$, Eq. (2.79) describes the evolution of generating function associated to the total number of cells $N = \int_{\mathbb{R}} n(x)dx$:

$$Z(H, t) = \Pi(t)h + \sum_{k=0}^M (Z^k(H) * \Pi_{\gamma_k})(t) \quad (2.80)$$

where $\Pi(t)e^{-\sum_{k=0}^M \int_0^t \gamma_k(u)du}$ still labels the surviving probability of survive until time t while $\Pi_{\gamma_k}(t)$ is the probability of observing the cell splitting into k -

newborns in the range of time $[t, t + dt]$.

Eq. (2.75) is a limit case of this novel formulation (Eq. (2.80)). De facto, the original Bellman-Harris Equation can be recalled from Eq. (2.80) under the constraint:

$$\gamma_k(u) = \frac{p_k}{\sum_{k=0}^M p_k} \lambda(u). \quad (2.81)$$

If constraint (2.81) holds, then $\Pi(t) = e^{-\int_0^t \lambda(u) du}$ and the Bellman-Harris Equation is exactly recalled. As shown in Fig. 2.1 (a,b), the constraint (2.81) imposes a proportionality between the probability density function of the reaction times which is absent in this work. The shapes of the reaction time distributions do not have any limitations in this theory and time-distributions with a peaked behaviour can be combined with one exhibiting wide fluctuations. This novelty is going to be crucial in the next chapters, especially in the analysis of time-dependent environment (Sects. 4.3 and 5.3). In fact, one of the major findings in this work, named *survival resonances*, rises as a direct consequence of the flexibility of this framework.

As last comment, the Bellman-Harris derivation was focused on the Generating function while the one proposed in Sec. (2.4) is both focused on the functional probability \mathcal{P} (Eqs. (2.45) and (2.46)) and on the generating functional \mathcal{Z} (Eqs. (2.18) and (2.49)). This allows to show that functional probability can be potentially calculated analytically. Further details are proposed in App. B.

2.6 Conclusions

The stochastic evolution of age-structured population can be described as a functional, drifting, jumping process. The Chapman-Kolmogorov Equations can be represented in a differential and an integral form using an implicit notation ((2.15),(2.18), (2.43) and (2.45)) or in the generalised age-structured stoichiometric framework ((2.32), (2.33), (2.44) and (2.46)). In my personal opinion, the last sections are of particular interest and they present several methods used in the following thesis (Chs. 4, 5 and 6). In Sec. 2.5, the Galton-Watson theory is discussed and, interestingly, its fundamentals are invariant to the continuous Liouville's drift (i.e. the ageing process). Sec. 2.5 also allows me to discuss the similarities and differences with the standard Bellman-Harris process which was derived from quite long and technical calculations [112]. The

integral formulation, instead, rises as the forward application of the Characteristic Curves methods to the Master Equation. The integral CKEs rely on the wide theory of stochastic processes, it does not imply any constraints on the time distributions, in addition to the many other differences discussed in Sec. 2.5.2.

In conclusion, this chapter contains a solid set of methods to quantify the evolution of an age-structured population. The coherency of these results is going to be tested in the following chapters comparing simulations and analytical results.

A few concepts in age-structured stochastic simulations are discussed in the following Ch. 3. Later, simulations and analytics are combined to study three different applications (Chs. 4, 5 and 6).

Chapter 3

Simulations

Abstract

Stochastic simulations represent a powerful approach to investigate a stochastic process and validate the analytical results. The standard simulation method for unstructured populations is Gillespie's algorithm in which the event times are sampled via the constant rate associated with each reaction. Here, no novel results are presented, instead I discuss a sampling method of reaction times from the rate function, in contrast to the standard Gillespie's algorithm where the rate is constant. The method is usually called thinning and, in its essence, is a rejection-sampling method.

The evolution of an *age-structured* population is driven by a set of reactions described through *age-structured reaction networks*. As shown in Ch. 2, each reaction can be described by a set of products, a set of reactants and the propensity of its occurrence. Following the notation introduced in Sec. 2.2, the stoichiometric functions (ν_r^-, ν_r^+) address the products and reactants while the function γ_r defines rate associated with r -th reaction times. In our framework, reactants and products are deterministic while reaction times encode the whole stochasticity of the process.

It has to be noted that each rate function is, in general, a hypersurface. Each r -th reaction can involve N different individuals with age x_1, x_2, \dots, x_N , so that the rate function can be defined as:

$$\begin{aligned} \gamma : \mathbb{R}^N &\rightarrow \mathbb{R} \\ \vec{x} &\rightarrow \gamma(\vec{x}), \end{aligned} \tag{3.1}$$

where each element of the vector \vec{x} increases linearly in time accordingly to the

ODE's:

$$\frac{dx_i(t)}{dt} = 1 \quad \forall i = 1, \dots, N_r. \quad (3.2)$$

Since each element is created after a reaction or initialised at the beginning of simulations, the initial conditions related to Eq. (3.2) are always known for each individual. It follows that each reaction can be characterised by a rate function depending on time:

$$\gamma_r(x_1(t), x_2(t), \dots, x_{N_r}(t)) = \gamma_r(t) \quad (3.3)$$

Stochastic processes characterised by a time-dependent rate function are known as a Non Homeogeneous Poisson Processes (NHPPs). Like Homogeneous Poisson Processes (HPP), a NHPP is a point process on the positive half line $[0, \infty)$ that can be described in three alternative ways: by *arrival times*, as *counting process* or using *inter-event times* [106, 113, 114].

The more suitable description for our purpose is given by the *arrival times* which are stochastic variables representing the events times of the NHPP. The event times probability density for a NHPP with rate $\gamma(t)$ is given by:

$$\phi(t) = \gamma(t)e^{-\int_0^t \gamma(x)dx}, \quad (3.4)$$

whose cumulative distribution is denoted by $\Pi(t)$. In addition to that, the rate function $\gamma(t)$ can be expressed in terms of probability density function $\phi(t)$ by the following equation:

$$\gamma(t) = \frac{\phi(t)}{1 - \int_0^t \phi(x)dx}. \quad (3.5)$$

I conclude this section by stressing the main results presented above: the arrival times of each reaction can be modelled as a NHPP. Therefore, the distribution of those times can be uniquely described either by the rate function or by the probability density function.

3.1 Rejection-Acceptance Sampling Method

To sample the events time distributed as ϕ (Eq. (3.4)), the intuitive idea is finding an alternative probability distribution G , with density function $g(x)$, for which an efficient sampling algorithm is available, but also such that the function $g(x)$ is “close” to $\phi(x)$ [115, 116]. In particular, the ratio $\frac{\phi(x)}{g(x)}$ has to

be bounded by a constant $c > 0$ such that:

$$\sup_x \left(\frac{\phi(x)}{g(x)} \right) \leq c. \quad (3.6)$$

. The framework of the rejection-acceptance algorithm can be outlined as:

1. Sample a variable y from the G distribution
2. Sample a variable u independent from y
3. If the condition $u \leq \frac{\phi(y)}{cg(y)}$ holds then accept the sampled value, reject it otherwise

In other words, the core idea is to thin the values sampled from G for the original distribution Π exploiting Eq. (3.6).

Before providing a formal analytic proof for the rejection-acceptance algorithm, a few points have to be outlined. First of all, the probability of rejection p is always equal to $\frac{1}{c}$. Moreover, the number of rejected samples N are a random variable themselves and are distributed as: $P(N = n) = (1 - p)^{n-1} p^n$, where $p = P(u \leq \frac{\phi(y)}{cg(y)})$. Thus, on average, the number of iterations required is given by $E\{N\} = \frac{1}{p}$.

This represents the reason why initially G had to be "close" to Π (in order to reduce the number of rejected values). To prove the consistency of the rejection-acceptance method, the following statement has to hold:

$$P \left(Y \leq y \middle| u \leq \frac{\phi(y)}{cg(Y)} \right) = \Pi(y). \quad (3.7)$$

In order to prove it, the following relationship has to be considered:

$$P(Y \leq y | U \leq \frac{\phi(y)}{cg(y)}) = P(u \leq \frac{\phi(y)}{cg(y)} | Y \leq y) \underbrace{\frac{P(Y \leq y)}{P(u \leq \frac{\phi(y)}{cg(y)})}}_{G(y)c}, \quad (3.8)$$

which follows from the Bayes theorem [3]. To prove the consistency of the

rejection-acceptance algorithm is sufficient to show that:

$$\begin{aligned}
P(Y \leq y | U \leq \frac{\phi(y)}{cg(y)}) &= \frac{P(Y \leq y, u \leq \frac{\phi(y)}{cg(y)})}{P(u \leq \frac{\phi(y)}{cg(y)})} \\
&= c \int_{-\infty}^y P\left(u \leq \frac{\phi(y)}{cg(y)} | Y = w\right) g(w) dw \\
&= \int_{-\infty}^y \phi(w) dw = \Pi(y).
\end{aligned} \tag{3.9}$$

Here, it was shown a method to sample event times (from a rate function) based on an alternative distribution and, with a couple of other adjustments (Sec. 3.2), will allow to simulate the evolution of age-structured populations.

3.2 Thinning and Extrande Algorithm

The *standard thinning method* is a type of rejection-acceptance method in which the density function (to sample from) is given by a NHPP $\phi(x) = \gamma(x)e^{-\int_0^x \gamma(u)du}$. In this case, a substitute distribution can be found in the HPP with rate equal to the maximum value of $\gamma(x)$: $\hat{g}(x) = \hat{\gamma}e^{-\hat{\gamma}x}$ where $\hat{\gamma} = \max_y \{\gamma(y)\}$, so that:

$$\frac{\phi(x)}{\hat{g}(x)} = \underbrace{\frac{\gamma(x)}{\hat{\gamma}}}_{\leq 1} \frac{e^{-\int_0^x \gamma(u)du}}{e^{-\hat{\gamma}x}} \leq \frac{e^{-\int_0^x \gamma(u)du}}{e^{-\hat{\gamma}x}} = c(x). \tag{3.10}$$

Furthermore, the *standard thinning methods* can be formulated in the steps:

1. Sample a random variable y distributed as a HPP with rate $\hat{\gamma}$
2. Sampled a random variable u independent from y
3. If the condition $u \leq \frac{\gamma(y)}{\hat{\gamma}}$ holds then accept the sampled values, reject it otherwise

The intuitive idea behind the *standard thinning* method is to first find a constant rate function $\hat{\gamma}$ which dominates the desired rate function $\gamma(t)$, generate a homogeneous Poisson time event with rate $\hat{\gamma}$ via *inverse-transform method* [106, 114, 117] and then reject an appropriate fraction of the generated events so that the desired frequency is achieved [113]. It follows that the *standard thinning algorithm* structure can be proposed as a sequence of simple

steps displayed in **Algorithm 1**, where $U(0, 1)$ labels the uniform distribution of random variables $u \in (0, 1)$:

Algorithm 1

Input: Homogeneous Poisson rate $\hat{\gamma}$, Non-Homogeneous Poisson rate $\gamma(t)$, Initial time t_0 . Evolution time t_{max}

Output: Array of sampled times **Times** distributed according to $\phi(t)$.

```

1. Initialize  $t \leftarrow t_0$ , Times  $\leftarrow [ ]$ 
2. while  $t \leq t_{max}$ :
3.   Generate  $u_1 \sim U(0, 1)$ 
4.   Set  $x \leftarrow t - \frac{1}{\hat{\gamma}} \log(u_1)$ 
5.   Generate  $u_2 \sim U(0, 1)$ 
6.   if  $u_2 \leq \frac{\gamma(x)}{\hat{\gamma}}$ :
7.      $t \leftarrow x$ 
8.   append(Times,  $t$ )
9. end
10. Return Times
```

The efficiency thus depends critically on how well $\hat{\gamma}$ approximates $\gamma(t)$. If the rate function $\gamma(t)$ exhibits heavy fluctuations in time, then the standard thinning algorithm will be inefficient. Ross et al. [113] provided a straightforward modification to the thinning method to mitigate excessive rejection which is usually called *piecewise thinning* method [113, 114]. The intuitive idea behind this extension is majorizing the desired rate function using an appropriately chosen piecewise constant function having k pieces, and then performing regular thinning within each piece. Specifically, first the horizon of interest $(0, t_0]$ is divided into k intervals $[t_{j1}, t_j)$ s.t. $j = 1, 2, \dots, k$ and then, the constants $\hat{\gamma}_j$ are chosen satisfying $\hat{\gamma}_j \geq \sup_{t \in [s_{j-1}, s_j]} \gamma(t)$.

The thinning methods are useful ways to sample reaction times, yet the goal is to simulate the whole age-structured dynamics. Multiple reaction times have to be sampled and the state n influences the propensities of each reaction. An extension to several reaction channels was proposed in the Exrande approach formulated by M. Voliotis, P. Thomas et al. [118]. The Exrande Algorithm (or Extra Reaction Algorithm for Networks in Dynamic Environments) allows exact stochastic simulation of any downstream reaction network, conditional upon a time course of the dynamic inputs which are simulated up-front [118]. The

Extrande approach can be understood as introducing a *virtual* reaction $r = R+1$ into the system (whose occurrence does not affect the state of the system $\nu_{R+1} = 0$). The propensity of such virtual reaction Φ_{R+1} is designed to fluctuate over the evolution so that (when added to the sum of all other reaction propensities) the total propensity $\sum_{j=1}^{R+1} \Phi_j[n, t]$ in the augmented system becomes constant between events and equal to an upper bound on the sum of the propensities in the original system:

$$\sum_{j=1}^R \Phi_j[n, t] \leq B \longrightarrow \sum_{j=1}^{R+1} \Phi_j[n, t] = B \quad 0 \leq t \leq L \quad (3.11)$$

where $\Phi_j[n, t]$ labels the propensities of the $j - th$ reaction at time $t \in [0, L]$, n labels the dependence of each reaction on the system state and t represents the explicit dependence of rate on time [118].

The method exploits the exogeneity of the dynamic inputs. In particular, their exogeneity means that Extrande is able to make use of the future trajectory of the inputs to find an upper bound, B , on the total propensity, which is valid over a certain time interval.

In **Algorithm 2.I** and **2.II**, the framework of the Extrande Algorithm is outlined. The focus is on simulating over a range of time $[0, T)$ of a reaction network with R - reactions ($r \in \{1, \dots, R\}$) with stoichiometric functions $\{\nu_1, \nu_2, \dots, \nu_R\}$. The state of the system is given by n and the *virtual* reaction is labelled with index $R + 1$. The first task of the algorithm is calculating the bound B for the effective (excluded the virtual reaction) reaction propensities (**Algorithm 2.I**, line 2). Then, sample a time τ is sampled from an exponential distribution $\exp(-B\tau)$, in other words, a HPP with rate B equal to the upper bound of a_0 (**Algorithm 2.I**, line 3). If the sampled reaction time τ exceeds the time horizon L , it is rejected; the system time advances by L (**Algorithm 2.I**, line 6), and the procedure restarts by determining a new bound.

Algorithm 2.I

```

1:Initialise time  $t \leftarrow 0$  and network state  $n \leftarrow n_0$ .
2:Choose  $L \leq T - t$  and  $B$  such that  $\Phi_0(t + u) \leq B$ 
   for  $0 \leq u \leq L$ , where  $\Phi_0(t + u) = \sum_{j=1}^M \Phi_j[n, t + u]$  is the sum
   of the propensities  $\Phi_j$  at time  $t + u$  provided that no
   reaction channel fires during  $(t, t + L)$ .
3:Draw exponentially distributed random number  $\tau \sim \text{Exp}(\frac{1}{B})$ .
4:if  $\tau > L$  :
5:  Reject sampled time
6:  Update time  $t \leftarrow t + L$ .
7:else:
8:  Algorithm 2.II
18:end If

```

On the other case, the reaction times at the sampled time $\Phi_0(t + \tau)$ is evaluated and the sum of the effective propensities is re-evaluated (**Algorithm 2.II**, lines 8-9). The next step regards the rejection or the acceptance of the time upfront sampling a uniform random variable u (**Algorithm 2.II**, lines 10). If the $\Phi_0(t) \geq Bu$, the sampled time is accepted and the reaction to perform as the r is chosen, such that. In addition to it, the state of the system is updated $n \leftarrow n + \nu_j$ (**Algorithm 2.II**, lines 11-13). In case the inequality $\Phi_0(t) \geq Bu$ does not hold, the state of the system remains unchanged and the virtual reaction $r = R + 1$ fires [118] (**Algorithm 2.II**, line 15).

3.3 Conclusions

I examined a set of methods to sample the events times of NHPP. These methods were integrated it in a wider framework to simulate the evolution of an age-structured population. In substance, the first event time of an individual is distributed as the first event time of NHPP. Different rejection-acceptance methods can be employed, in this context, here the thinning method was presented and its limitations were discussed.

An implementation of the algorithm was built to discuss the coherency of the results of Ch. 2 in the applications proposed in Chs. 4 and 5.

Algorithm 2.II

```
8:Update time  $t \leftarrow t + \tau$  and all propensities  $\Phi_j[n, t]$ 
9:Evaluate the sum: $\Phi_0(t) = \sum_{j=1}^R \Phi_j[n, t]$ 
10:Generate uniformly distributed random number  $u \sim U(0, 1)$ .
11:If  $\Phi_0(t) \geq Bu$  :
12:   'Accept' and choose reaction associated with the
       smallest positive integer  $j$  less than or equal
       to  $M$  satisfying:  $\sum_{i=1}^j \Phi_i[n, t] \geq Bu$ 
13:   Update state  $n \leftarrow n + \nu_j$ .
14: else:
15:   'Thin': The extra reaction channel fires and the state
       of the network remains unchanged
16: end if
17: until  $t \geq T$  (terminate when final time is exceeded)
```

Chapter 4

Birth and Death of Age-Structured Populations

Abstract

An age-structured division-death process is studied in constant and time-dependent environments. This model is used to quantify fractional killing which, in response to drugs, is a hallmark of non-genetic cellular heterogeneity. How individual lineages evade drug treatment, as observed in bacteria and cancer cells, is not quantitatively understood. We study a stochastic population model with age-dependent division and death rates, allowing for persistence. In periodic drug environments, we discover peaks in the survival probabilities at division or death times that are multiples of the environment duration. Survival resonances are unseen in unstructured populations and are amplified by persistence. This research project was developed in collaboration with P. Thomas, J. Pausch and P. Piho. The final results led to a publication in Physical Review Letter [119]. I was involved in all the analytics related to constant (Sec. 4.2) and time-dependent environments (Sec. 4.3). The simulations and numerical solutions were implemented by J. Pausch and P. Piho in Sec. 4.3. I personally simulated and implemented the numerical algorithm for the process depicted in Figs. 4.2, 4.4 and 4.6. Fig. 4.10 was provided by J. Pausch.

The stochastic age-structured theory (previously presented in Ch. 2) is now applied to study a paradigmatic example in population dynamics: the division-death process. In this model, each individual may divide into two newborns or die. In general, a division-death process is a simple, natural and formal framework for modelling various processes [35, 112, 120]. Here, I only remember its applications to demographic scenarios, as von Foerster did in its deterministic

framework [121], for Nuclear Chain Reactions (Feller [74], 1968) and to study the extinction of family names (Galton and Watson [64], 1875). This age-structured division-death model was developed to study cancer cells' evolution under therapeutic treatments.

The understanding of cancer and bacterial biology has dramatically increased during the last century, leading to important progress in cancer prevention and detection, and in medical treatment [122, 123]. Recent developments in microbiology, cancer imaging [124] and theoretical models [125] led to an enhanced comprehension of cancer evolution.

However, several queries still stand, especially in relation with the inefficiency of therapeutic treatments. In fact, under adverse conditions such as repeated drug treatments, most cells in a population die while few cells survive, a phenomenon called *fractional killing* [9, 10, 14]. The short timescale of drug exposure often excludes the evolution of drug resistance but requires non-genetic mechanisms underlying fractional killing, which are still not fully understood [126, 127, 128]. A well-accepted view is that heterogeneous survival arises from fluctuations in intracellular pathways influencing cell division, growth and apoptosis in coordination with the cell cycle [15, 16, 17]. Recent advances in single-cell imaging allow tracking heterogeneity in individual lineages that can drive insights into persistence against antimicrobial or anti-cancer treatments aided by quantitative stochastic models. Cellular heterogeneity in division times, as observed in experiments, can be described through age-structured branching processes [112, 129, 130, 131, 132, 133, 134]. Most of these models operate on a mean-field level as they often implicitly assume cell survival or large populations, and therefore cannot explain the fractional killing. Here, we provide a quantitative model of fractional killing for populations established from a single ancestor by analysing an age-structured branching process of cell division and death in time-dependent environments [135, 136, 137] (Fig. 5.1). As fractional killing is the survival of cells despite long or repeated exposure to adverse conditions, we focus on long-term, i.e. infinite-time, survival. We will refer to it simply as survival unless stated otherwise.

In the following sections, we present several results towards understanding fractional killing as a stochastic phenomenon that emerges due to heterogeneity and stochasticity. To achieve this, we consider the survival probability in constant environments and quantify fractional killing with persistence, where

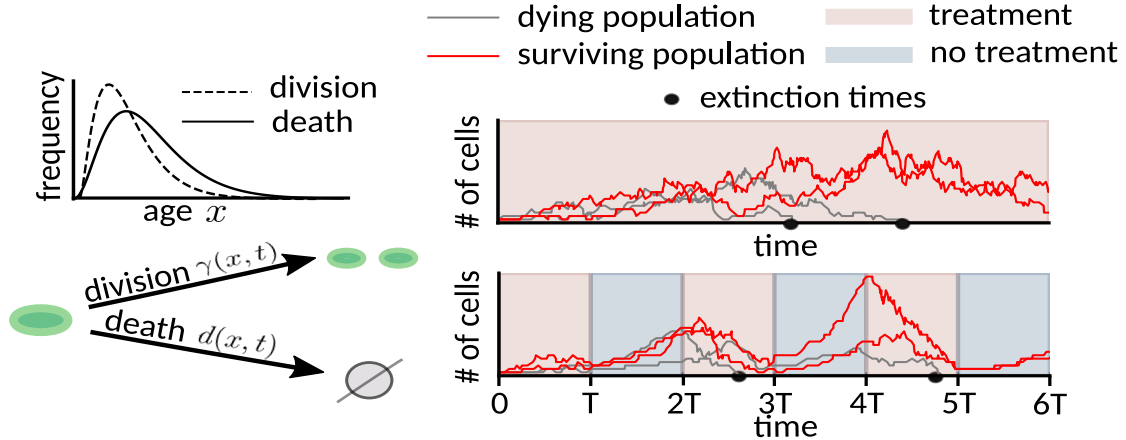


Figure 4.1: **Illustration of age-dependent population dynamics.** Top left panel: the distribution of division and death ages. Bottom left: cells divide and die depending on age and environment. Top right: constant environment. Bottom right: periodic on- and off-switching of a treatment. Some cells survive treatment and persist, and fractional killing occurs.

cells fail to die or divide. Next, we generalise the age-dependent branching model of Bellman and Harris [112], allowing arbitrary age-dependence of division and death rates in periodic environments. Here, we discover that periodic treatment settings can lead to resonance phenomena in the survival probability that are amplified by persistence. Our results reveal a complex dependence of resonances on division or death times and the environment that could be observed for cell-cycle dependent drugs such as chemotherapeutic drugs or antibiotics [138, 139, 140, 141].

4.1 Theoretical Framework

Division and death processes of cells drive the evolution of this age-structured model. The stoichiometric formalism proposed in Sec. 2.2 allows to introduce the reaction network of this model. In contrast to the unstructured division-death model, the division process requires some kind of relation holding between the ages of the reactant and products. In this work, we assume that individuals exhibiting age x divide into two newborns with ages $x = 0$.

Each cell with age x can divide with rate $\gamma(x)$ and die with rate $d(x)$, at time t . Therefore, in a single-species population, the reaction network for a

division and death process is:

$$\begin{aligned} s(x) &\xrightarrow{\gamma(x)} 2s(0), \\ s(x) &\xrightarrow{d(x)} \emptyset. \end{aligned} \tag{4.1}$$

The stoichiometric product and reactant functions follow directly from the latter equation; for the division process: $\nu_{r=1}^-[x] = \delta_x$, $\nu_{r=1}^+[x] = 2\delta_0$ and $\nu_{r=1}[x] = 2\delta_0 - \delta_x$ and for the death process: $\nu_{r=2}^-[x] = \delta_x$, $\nu_{r=2}^+[\hat{x}] = 0$ and $\nu_{r=2}[x] = -\delta_x$. The deterministic description of the process can be expressed via the McKendrick-von Foerster PDEs (see Sec. (2.5.1)) or via the integral Euler-Lotka's equation to determine the growth rate λ :

$$\frac{1}{2} = \int_0^\infty e^{-\lambda x} \gamma(x) e^{-\int_0^x (\gamma(u) + d(u)) du} dx. \tag{4.2}$$

In long-term regime, the density of individuals with age x can be expressed as $n(x, t) = N_0 \Phi(x) e^{\lambda t}$ where N_0 is the total initial number of individuals while $\Phi(x)$ labels the asymptotic age-distribution within the population and it is given by:

$$\Phi(x) = 2\lambda e^{-\lambda x} e^{-\int_0^x (\gamma(u) + d(u)) du}. \tag{4.3}$$

A sharp way to derive the last equation is plugging the ansatz $N_0 \Phi(x) e^{\lambda t}$ (with total number of initial cells N_0) into the McKendrick-von Foerster equation (Eq.(1.20)) to obtain:

$$\lambda \Phi(x) + \frac{d\Phi(x)}{dx} = -(\gamma(x) + d(x)) \Phi(x), \tag{4.4}$$

, so that $\Phi(x)$ can be recalled solving the ODE $\frac{d \ln(\Phi(x))}{dx} = -(\gamma(x) + d(x) - \lambda)$.

In addition, the normalization constant 2λ can be recalled from an extension to heritable inter-division times, which was elegantly displayed in [94].

McKendrick's and von Foerster's results allow us to recall the cell's density at a specific time t with age x : $n_1(x, t)$. Eq. (4.2), instead, can be exploited to calculate the growth rate of the population and the number of individuals with age x : $N_0 \Phi(x) e^{\lambda t}$.

The state of the population is encoded in a stochastic function n^t whose

probability is described by a functional \mathcal{P} . Based on the fact that the following process is a branching process, we discuss the evolution of a single particle with an initial age: $\mathcal{P}[n, t|\delta_{x_0}]$.

We now choose to consider also a possible explicit time dependency in the rate: $\gamma(x, t)$ and $d(x, t)$. This choice does not cause any loss of generality in the theoretical framework (Ch. 2) and anticipates the results presented in Sec. 4.3 for time-dependent environments: Eqs. (4.36) and (4.38). Therefore, the forward CKE can be expressed via Eq. (2.32):

$$\begin{aligned} \mathcal{D}_{n,t}\mathcal{P}[n, t|\delta_{x_0}] = & \int_0^\infty dx \left(\gamma(x, t)(\varepsilon_x^{+1}\varepsilon_0^{-2} - 1)n(x)dx + \right. \\ & \left. + d(x, t)(\varepsilon_x^{+1} - 1)n(x) \right) \mathcal{P}[n, t|\delta_{x_0}], \end{aligned} \quad (4.5)$$

whose mean-field is the McKendrick-von Foerster model [121]. Here, the step operator $\varepsilon_x^{\pm m}$ shifts the argument of any functional \mathcal{F} : $\varepsilon_x^{\pm m}\mathcal{F}[n] = \mathcal{F}[n \pm m\delta_x]$, where δ_x denotes the Dirac- δ function. For example, $\varepsilon_0^{-2}\varepsilon_x^{+1}$ stands for the division of a cell with age x into two cells of zero age.

The following step is deriving an integral functional equation for the generating functional \mathcal{Z} . This step can be done relying on the theoretical framework proposed in Ch. 2 in which the integral formulation of age-structured branching processes is discussed (Sec. 2.5). Here, we propose a slightly different derivation of the integral CKE for this system; we apply the Characteristic curves method to the FDE for the generating functional \mathcal{Z} rising from Eq. (4.5). The probability generating functional is given by $\mathcal{Z}[h, t|\delta_{x_0}, t_0] := \int \mathcal{D}[n] \exp(\int_0^\infty dx \ln(h(x))n(x)) \mathcal{P}[n, t|\delta_{x_0}, t_0]$ where the auxiliary variable is a general age-dependent function $h(x)$ and the integral is over all non-negative measures n with positive support. Using the definition of the generating functional in the Master Equation (4.5), we obtain a functional derivative equation for \mathcal{Z} :

$$\begin{aligned} \mathcal{D}_{h,t}\mathcal{Z}[h, t|\delta_{x_0}, t_0] = & \int_0^\infty \left[-(\gamma(x, t) + d(x, t))h(x) + \right. \\ & \left. + \gamma(x, t)h^2(0) + d(x, t) \right] \frac{\delta\mathcal{Z}[h, t|\delta_{x_0}, t_0]}{\delta h(x)} dx. \end{aligned} \quad (4.6)$$

Eq. (4.6) is a first-order FDE of the first order and can be manipulated via the method of characteristics [142]. Doing so, the characteristic curves are parameterised in terms of a continuous variable s and are described by two

ODEs:

$$\frac{dt(s)}{ds} = 1, \quad \frac{d\mathcal{Z}(s)}{ds} = 0 \quad (4.7)$$

and a PDE for $h(x, s)$:

$$(\partial_s + \partial_x)h(x, s) = (d(x, s) + \gamma(x, s))h(x, s) - \gamma(x, s)h(0, s)^2 - d(x, s). \quad (4.8)$$

We define $\Pi(s, x) = \exp\left(-\int_0^s \gamma(x+u, u) + d(x+u, u)du\right)$ and integrate Eq. (4.8) to obtain:

$$\begin{aligned} h(x, 0) &= \Pi(s, x)h(x+s, s) \\ &\quad + \int_0^s \Pi(y, x)(\gamma(y+x, y)h^2(0, y) + d(y+x, y))dy. \end{aligned} \quad (4.9)$$

Under the initial condition $t_0 = 0$ (so that $t(s=0) = 0$) and $\mathcal{Z}[h(\bullet, 0), t(0)|\delta_{x_0}, 0] = h(x_0, 0)$, we obtain $t(s) = s$ and $\mathcal{Z}[h(\bullet, s), t(s)|\delta_{x_0}, 0] = h(x_0, 0)$ from Eqs. (4.7). Therefore, Eq. (4.9) can be expressed as:

$$\begin{aligned} \mathcal{Z}[h(\bullet, s), s|\delta_{x_0}, 0] &= \Pi(s, x)h(x+s, s) \\ &\quad + \int_0^s \Pi(y, x)(\gamma(y+x, y)h^2(0, y) + d(y+x, y))dy. \end{aligned} \quad (4.10)$$

The final step is replacing $h^2(0, y)$ with a known function in Eq. (4.10). It follows from Eq. (4.8) that \mathcal{Z} is constant along any characteristic starting at $s = y$ and hence:

$$h(x_0, y) = \mathcal{Z}[h(\bullet, s), t(s)|\delta_{x_0}, y]. \quad (4.11)$$

Plugging Eq. (4.11) in Eq. (4.10), we obtain an integral equation for the offspring initial generating function in time-dependent environments:

$$\begin{aligned} \mathcal{Z}[h, t|\delta_{x_0}, 0] &= \Pi(t, x_0)h(x_0 + t) \\ &\quad + \int_0^t \Pi(y, x_0)\left(\gamma(x_0 + y, y)\mathcal{Z}^2[h, t|\delta_0, y] + d(y + x_0, y)\right)dy. \end{aligned} \quad (4.12)$$

Finally, we restrict our analysis to constant environments $\gamma(x, t) = \gamma(x)$ and $d(x, t) = d(x)$. Therefore, $\mathcal{Z}[h, t+T|m, T] = \mathcal{Z}[h, t|m, 0]$ for any range of time

T and Eq. (4.14) becomes:

$$\begin{aligned}\mathcal{Z}[h, t|\delta_{x_0}, 0]\Pi(x_0) = & \Pi(t + x_0)h(t + x_0) + \int_0^t \Pi(u + x_0)d(u + x_0)du + \\ & + \int_0^t \Pi(u + x_0)\gamma(u + x_0)\mathcal{Z}^2[h, t - u|\delta_0, 0]du.\end{aligned}\tag{4.13}$$

Note that Eq. (4.13) could also be recalled specialising the stoichiometric functions in Eq. (2.59) for a division-death process. Moreover, Eq. (4.13) can be expressed in terms of the functional probability:

$$\begin{aligned}\mathcal{P}[n, t|\delta_{x_0}, 0]\Pi(x_0) = & \Pi(t + x_0)\delta[\delta_{x_0+t} - n] \\ & + \int_0^t \left(\Pi_\gamma(x_0 + y)\mathcal{P}[n, t - y|2\delta_0, 0] + \Pi_d(y + x_0) \right) dy.\end{aligned}\tag{4.14}$$

The function $\Pi(x) = \exp(-\int_0^x \gamma(u) + d(u)du)$ is the probability of surviving (not dying or divide) until age x for a cell with age 0. The functions $\Pi_\gamma(x) = \gamma(x)\Pi(x)$ and $\Pi_d(x) = d(x)\Pi(x)$ are the probabilities for a newborn cell to divide or die at age x , respectively.

Eq. (4.13) is also the functional generalisation of the Bellman-Harris process. In fact, if the reactions are labelled with index $j = 1, 2$ and we assume $r_1(x) = \frac{p_2\lambda(u)}{p_0+p_2} = \gamma(x)$ and $r_2 = \frac{p_0\lambda(x)}{p_0+p_2}$ (see Sec. 2.5.2), Eq. (4.13) becomes:

$$\mathcal{Z}[h, t|\delta_0, 0] = \Pi(t)h(t) + \sum_{j=0,2} (\Pi_{r_j} * \mathcal{Z}^j[h|\delta_0, 0])(t).\tag{4.15}$$

In Sec. 2.5.2, I explained in a few paragraphs how Eq. (4.13) generalises the integral equation derived by Bellman and Harris [56]. Here, let us only observe that Eq. (4.13) accounts for possible variations of the initial ages. This is in contrast with Bellman's and Harris's derivation in which the dynamics was constrained to a newborn initial cell. In addition, the generating function with initial age δ_{x_0} (Eq. (4.13)) at each time t is a direct functional of $\mathcal{Z}[h, t|\delta_0]$, therefore, in the following, we study Eq. (4.13) for $x = 0$. Eq. (4.13) is a renewal equation for an initial newborn and can be manipulated with a broad set of methods available for renewal equations [97]. Actually, any initial configurations can be studied via Eq. (4.13) for $x_0 = 0$ (recalled here):

$$\mathcal{Z}[h, t|\delta_0, 0] = \Pi(t)h(t) + \int_0^t \Pi_d(u)du + \Pi_\gamma * \mathcal{Z}^2[h|\delta_0, 0](t)\tag{4.16}$$

because a generating functional \mathcal{Z} for branching processes can always be written as:

$$\mathcal{Z}[h, t|m, 0] = \Gamma_m[\mathcal{Z}[h, t|\delta_\bullet, 0]] \quad (4.17)$$

In the following, we focus our efforts on Eq. (4.16) but we urge the reader to consider that the following results can be obtained for any initial configurations.

4.2 Continuous Therapeutic Treatments

The terms *continuous treatment* or *constant environments* refer to the case where the evolution of the cancer is not affected by external factors or undergoes interruptions of any kind. Therefore, the division and death rates do not depend explicitly on time $d(x, t) = d(x)$ and $\gamma(x, t) = \gamma(x)$. It follows that the evolution of the Master Equation can be described by Eq. (4.15), recalled here in an explicit form:

$$\mathcal{Z}[h, t|\delta_{x_0, 0}]\Pi(x_0) = \int_{x_0}^{\infty} \Pi_d(u)du + \mathcal{Z}^2[h, t - u|\delta_{x_0, 0}] \int_{x_0}^{\infty} \Pi_{\gamma}(u)du. \quad (4.18)$$

To quantify fraction killing, the focus has to be on the extinction probability defined as: $\lim_{t \rightarrow \infty} \mathcal{Z}[h = 0, t|\delta_{x_0, 0}] = p^*(x_0) = 1 - p_{\text{surv}}(x_0)$, so that Eq. (4.18) becomes:

$$p^*(x_0)\Pi(x_0) = \int_{x_0}^{\infty} \Pi_d(u)du + (p^*(0))^2 \int_{x_0}^{\infty} \Pi_{\gamma}(u)du. \quad (4.19)$$

Setting $x_0 = 0$ and identifying $\nu_d = \int_0^{\infty} dx \Pi_d(x)$ and $\nu_{\gamma} = \int_0^{\infty} dx \Pi_{\gamma}(x)$ as the effective death and division probabilities, the solution for the survival probability follows:

$$p_{\text{surv}}(0) = 1 - \frac{\nu_d}{1 - \nu_d} \Theta\left(1 - \frac{\nu_d}{1 - \nu_d}\right). \quad (4.20)$$

where, due to the normalization of the division and death times distribution, $\nu_{\gamma} = 1 - \nu_d$, while the symbol Θ labels the theta of Heaviside. Together with Eq. (4.19), this provides an exact solution for the extinction probability of a population starting from a single ancestor with initial age x_0 .

To study the survival probability in an age-structure division-death process, we first observe that age-dependent rates imply division and death age distributions for which we label the means μ_{γ}, μ_d and coefficients of variation CV_{γ}^2 ,

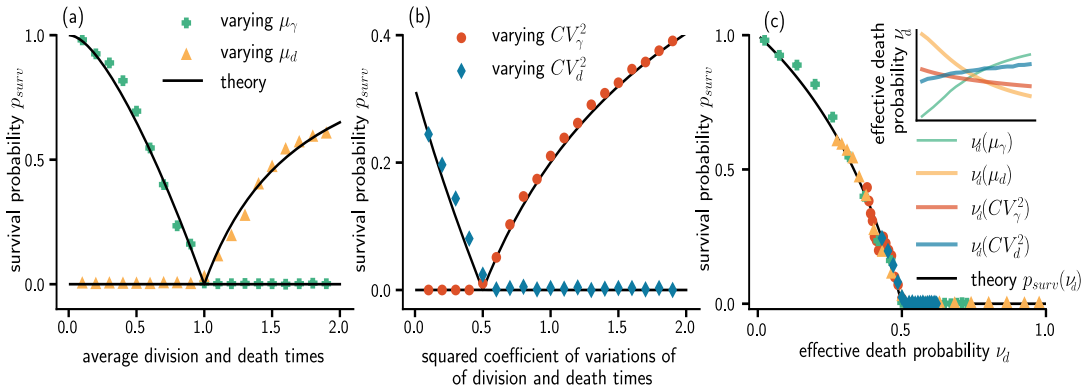


Figure 4.2: Survival probability p_{surv} of a newborn cell with division and death ages following Γ distributions. (a): Simulation (symbols) and theory (black line) of p_{surv} over average division and death ages, μ_γ and μ_d . (b) p_{surv} as a function of the coefficient of variation of division and death ages, CV_γ^2 and CV_d^2 . (c) p_{surv} as a function of the effective death probability ν . Inset: monotonic relation of ν to μ_d , μ_γ , CV_d^2 and CV_γ^2 . Death and division times follow Gamma distributions and, if not parametrized by the axes, are constrained to: $\mu_\gamma = \mu_d = 1$ and $CV_\gamma^2 = CV_d^2 = 0.5$.

CV_d^2 . This is in contrast with the age-independent (unstructured) case where $CV_\gamma^2 = CV_d^2 = 1$. A phenomenological understanding of age-dependent survival probability can be gained from Fig. 4.2 (a,b). Here, division and death ages follow $\Gamma(\alpha, \beta)$ -distributions $\Gamma(x; \alpha, \beta) = \frac{\beta^\alpha}{\Gamma(\alpha)} x^{\alpha-1} e^{-\beta x}$ with $\mu = \alpha/\beta$, $CV^2 = 1/\alpha$. The following results and conclusions were derived from a phenomenological analysis on distribution time given by Gamma distribution. To show the universality of this framework, later, the same phenomenological analysis is proposed for division and death times distributed as a Log-Normal random variables.

As in the age-independent case, p_{surv} becomes higher (lower) with μ_d (μ_γ) but it is also a monotonically increasing (decreasing) function of CV_d^2 (CV_γ^2). In particular, the survival chance of a population decreases with noise in death times but it increases with noise in division times (Fig. 4.2 (b)). This phenomenon is absent from the memory-less age-independent case, the noise in division and death is fixed. In Fig. 4.2, p_{surv} is plotted (black line) and compared to simulation results (symbols). Our result includes the well-known result for age-independent branching processes $\nu_\gamma = \mu_\gamma/\mu_d$ as a special case [143]. For Γ -distributed division and death times, the monotonic behaviour observed in Fig. 4.2 (a,b) is explained by the concatenation of monotonic relations between ν_d and the means and coefficients of variation, Fig. 4.2 (c) (inset) and between ν and p_{surv} , Fig. 4.2 (c).

Moreover, Eq. (4.20) demonstrates that the system exhibits a second-order phase transition between a sub-critical phase ($\nu_d > 1/2$) with almost sure ex-

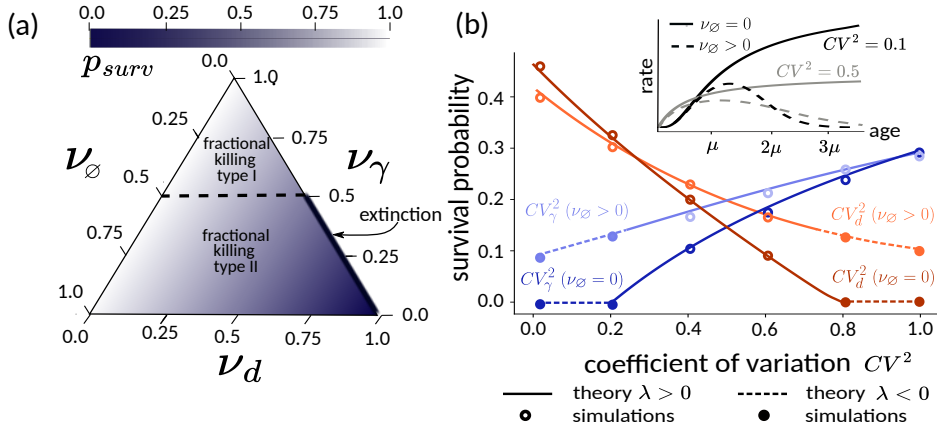


Figure 4.3: Noise-induced transitions in constant environments. (a) Phase diagram showing the regions of extinction (black line), fractional killing type I ($\lambda > 0$) and type II ($\lambda < 0$). (b) Survival probability shows transitions from extinction to fractional killing ($\nu_\phi = 0$), and type I to type II killing ($\nu_\phi > 0$) as the coefficient of variation in division or death times is varied, CV_γ^2 or CV_d^2 . Γ -distributed times assumed with $\mu_d = 1$, $\mu_\gamma = 0.9$, $w_\gamma = w_d = \{0.8, 1.0\}$, $CV_d^2 = CV_\gamma^2 = 0.5$ unless stated otherwise. Death and division times follow a Gamma distribution and, if not parametrized by the axes, the parameters are constrained to: $\mu_\gamma = \mu_d = 1$ and $CV^2 = CV_\gamma^2 = 0.5$.

tinction and a super-critical phase ($\nu_d < 1/2$) with positive survival probability. It thus confirms the presence of second-order phase transition, as for age-independent processes [144].

4.2.1 Persistence During Constant Treatments

Cancer growth is an extremely complex and articulated phenomenon and a division-death model is only able to partially reproduce its dynamics. For instance, a significant role is played by persistent cells in drug treatments which lead to fractional-killing and affect the simplistic division-death dynamics. In other words, persisting cancer cells (or bacterial) survive lethal antibiotic doses and promote residual cancer [18].

Due to these reasons, let us now consider a simple variation of the division-death model to incorporate persistence. Here, cells can either divide, die or persist, which occurs with different probabilities. We do not introduce a third reaction to include the role of persistence, instead, we introduce two normalisation constants w_γ, w_d such that the probability of division (in absence of death) at age $\in [x, x + dx]$ for an initial single cell with age 0 is:

$$\phi_\gamma(x) = w_\gamma \gamma(x) e^{-\int_0^x \gamma(u) du} \quad (4.21)$$

and the probability of death (in absence of division) is:

$$\phi_d(x) = w_d d(x) e^{-\int_0^x d(u) du}. \quad (4.22)$$

As a consequence, division and death rate functions are given by:

$$\gamma(x) = \frac{w_\gamma \phi_\gamma(x)}{w_\gamma \int_x^\infty \phi_\gamma(u) du + (1 - w_\gamma)} \quad (4.23)$$

and

$$d(x) = \frac{w_d \phi_d(x)}{w_d \int_x^\infty \phi_d(u) du + (1 - w_d)}. \quad (4.24)$$

If $w_{\gamma,d} = 1$, the division-death models is recalled, while if $w_\gamma < 1$ or (and) $w_d < 1$, a portion of cell randomly leave the system and survive with probability one. The rate functions (Eqs. (4.23) and (4.24)) allows to derive an interesting insight: the rates can be constant (as in unstructured models) only when $w_\gamma = w_d = 1$. It follows that persistence is an intrinsic property of our age-structured model and does not occur for constant rates.

The effective probabilities are defined ν_γ (division), ν_d (death) and $\nu_\emptyset = 1 - \nu_\gamma - \nu_d$ (persistence), and can be explicitly expressed as:

$$\nu_\emptyset = (1 - w_d)(1 - w_\gamma), \quad (4.25)$$

$$\nu_\gamma = \int_0^\infty du \gamma(u) e^{-\int_0^u dy (\gamma(y) + d(y))}, \quad (4.26)$$

$$\nu_d = \int_0^\infty du d(u) e^{-\int_0^u dy (\gamma(y) + d(y))}. \quad (4.27)$$

In absence of persistence, we calculated the survival probability via Eq. (4.19), considering its asymptotic limit and letting $h = 0$ and x_0 . Following a slightly different derivation, we observe that extinction probability is a fixed point of the generating function of offspring (over one generation) $z(h) = \nu_d + \nu_\gamma h^2$. Therefore, the survival probability is:

$$p_{\text{surv}}(0) = 1 - \frac{1 - \sqrt{1 - 4\nu_d(1 - \nu_\emptyset - \nu_d)}}{2(1 - \nu_\emptyset - \nu_d)}. \quad (4.28)$$

In Eq. (4.28) for $\nu_\emptyset = 0$, the survival probability demonstrates a second-order phase transition in the survival probability between a sub-critical phase ($\frac{\nu_d}{\nu_\gamma} > 1$) with almost sure extinction and a supercritical phase ($\frac{\nu_d}{\nu_\gamma} < 1$) with positive

survival probability, similar to the age-independent processes [143, 144]. When $\nu_\emptyset > 0$, cells survive also below the transition point. The second-order transition is replaced with a transition where the growth rate of the mean population size changes sign. The growth rate λ is the solution to the Euler-Lotka equation $1 = 2 \int_0^\infty du e^{-\lambda u} \gamma(u) e^{-\int_0^u dy(\gamma(y)+d(y))}$ [112]. While the transition in survival probability occurs only when $\nu_\gamma = \nu_d = \frac{1}{2}$, the transition of growth rate occurs when $\nu_\gamma = \frac{1}{2}$ (Fig. 4.3 (a)) regardless of ν_\emptyset . These lines separate the phases between extinction ($p_{\text{surv}} = 0, \lambda < 0$) and two fractional killing phases that we call type I ($p_{\text{surv}} > 0, \lambda > 0$) and type II ($p_{\text{surv}} > 0, \lambda < 0$).

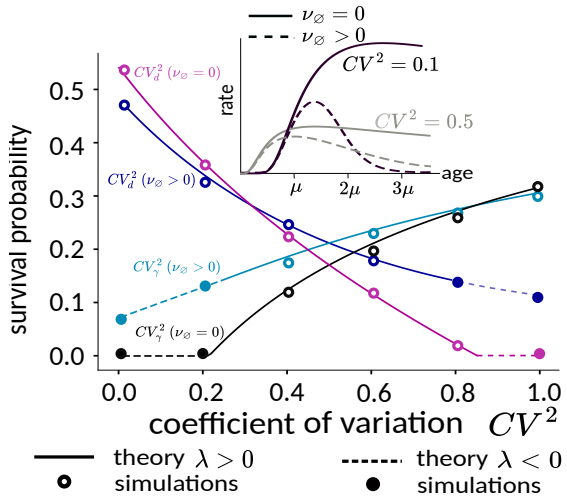


Figure 4.4: Survival probability in a constant environment with log-normal distributed division and death times. Survival probability shows transitions from extinction to fractional killing as a function of the coefficient of variations in division or death times, CV_γ^2 and CV_d^2 . The transitions from decaying ($\lambda < 0$, dashed) to growing dynamics ($\lambda > 0$, solid lines) are indicated through points. Log-normal-distributed division and death times with $\mu_d = 1$, $\mu_\gamma = 0.9$, $CV_d^2 = CV_\gamma^2 = 0.5$ and $w_\gamma = w_d = 0.8$ (corresponding to $\nu_\emptyset = 0.04$) are assumed.

To draw Figs. 4.3 and 4.4, the survival probability was computed for Γ -distributed division and death times, which allows us to vary the coefficients of variation of division and death times at constant mean times (μ_γ and μ_d). As shown in Fig. 4.3 (b), the survival probability increases with noise in division times (CV_γ^2) and decreases with noise in death times (CV_d^2). For $\nu_\emptyset = 0$, this dependence induces a transition from complete to fractional killing as division noise increases (Fig. 4.3 (b)), and the reverse transition is observed as death timing noise increases. The transition disappears for $\nu_\emptyset > 0$ and is replaced with a transition from type I to type II fractional killing as the survival probability crosses $\sqrt{2\nu_\emptyset}$. At this point, the dynamics changes from growing to decaying lin-

eages due to the effect of noise. A similar dependence is observed for log-normal distributed times (Fig. 4.4). Independently on the choice of times distributions, the survival process can be quantified via the phase diagram Fig. 4.3 (a).

4.3 Discontinuous Periodic Drug Treatments

The drugs used in cancer chemotherapy are toxic for normal tissues. As a result, the intensity of treatment is restricted by damage vital normal tissue [145]. Therefore, the majority of tumour treatments can not be administered for long, continuous range of time. To preserve the health of the patients, periodic treatments are administered in separate intervals of time (see Fig. 4.1, bottom right).

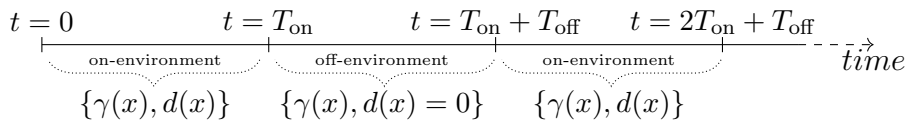


Figure 4.5: **Modelling alternated drug treatments.** The division rate functions $\gamma(x)$ is uninterrupted while the death rate function $d(x)$ is not zero only during the on-environments, i.e $t \in [n(T_{\text{on}} + T_{\text{off}}), (n+1)T_{\text{on}} + nT_{\text{off}}]$ with $n \in \mathbb{N}$

Motivated by periodic treatments, as used for cancer cells and microbial cells, we consider a repeated on-off-switching of the death process (Fig. 4.5). We consider on-environment of length T_{on} where the drug treatment is assumed to be active and off-environments of length T_{off} where the drug treatment is turned down. The death process is a time-dependent stochastic process and we define its rate function $d(x, t)$. The rate function is $d(x, t) = d(x)$ (i.e. time autonomous age-structured rate) in an on-environment and $d(x, t) = 0$ in an off-environment while cells keep dividing regardless $\gamma(x, t) = \gamma(x)$. Stochastic simulations display a complex landscape of survival probabilities with several peaks, -Fig. 4.6 (a,b). A few words are required to address the realism of this model setting. Data clearly shows that drug exposure is not constant or monotonic in time; its behaviour is instead shaped by the mean of subministration, the time spent from the administration of the drug and receptor properties [146, 147]. Indeed, this activation process usually fits a sigmoid function, which highlights the positive monotonic behaviour (activation) and asymptotes to a steady state (maximum activation). The model here considered, instead, shows a discontinuous transition from drug-free ($d(x, t) = 0$) to a steady drug

exposure ($d(x, t) = d(x)$). The following model acts as a basic representation of the age-structured division-death process in time-non-homogeneous environments. However, it can be extended to account for the drug exposure increment. A quick way to do that is to discretize the sigmoid-activation function and use the results reported here to approximate the sigmoid-activation in a step function. Other ways might involve other approximations of the sigmoid function, a trait-structured formulation of this theory (see Chapter 7) or the use of the unconstrained time dependence version of this model widely discussed directly in [119].

We consider the offspring distribution of the underlying branching process to calculate the survival probability. Here, the generating functionals of the offspring distributions originating from a cell with age x_0 after an on- or off-environment starting at time 0 and ending at $T_{\text{on/off}}$ are $\mathcal{Z}_{\text{on}}[h, T_{\text{on}}|\delta_{x_0}] := \int \mathcal{D}[n] \exp(\int_0^\infty dx \ln(h(x))n(x)) \mathcal{P}[n, T_{\text{on}}|\delta_{x_0}]$ and similarly $\mathcal{Z}_{\text{off}}[h, T_{\text{off}}|\delta_{x_0}]$. Here, we present a detailed derivation of the equations governing the survival probability during periodic on-off treatments. The equation is an application of the age-dependent Galton-Watson theory, Sec. 2.5.

For any branching processes, the evolution of each branch is independent and the generating functional for an initial density q can be expressed, for $t' < t$, as:

$$\mathcal{Z}[h, t|q, t'] = \exp \int_0^\infty q(x_0) \ln(\mathcal{Z}[h, t|\delta_{x_0}, t']) dx_0, \quad (4.29)$$

It follows that the Chapman-Kolmogorov integral equation (Eq. (2.7)) becomes:

$$\mathcal{Z}[h, t|m, 0] = \int e^{-\int_0^\infty q(x) \ln(\mathcal{Z}[h, t|\delta_x, t'] dx)} \mathcal{P}[q, t'|m, 0] \mathcal{D}q. \quad (4.30)$$

and it can be expressed by nesting generating functionals:

$$\mathcal{Z}[h, t|m, 0] = \mathcal{Z}[\mathcal{Z}[h, t|\delta_\bullet, t'], t'|m, 0], \quad (4.31)$$

where \bullet is a placeholder for the function argument, i.e., $\mathcal{Z}[h, t|\delta_\bullet, t'](x_0) = \mathcal{Z}[h, t|\delta_{x_0}, t']$.

The aim is to model periodic on-off treatment by nesting the generating functionals of on-environment $\mathcal{Z}_{\text{on}}[h, T_{\text{on}}|\delta_{x_0}, 0]$ and off-environments $\mathcal{Z}_{\text{off}}[h, T_{\text{off}}|\delta_{x_0}, 0]$. Since the on-off environment sequence is repeated with period $P = T_{\text{on}} + T_{\text{off}}$,

we define the offspring generating functional at time $t = P$ as:

$$\mathcal{W}[h, x_0] = \mathcal{W}[h, \bullet](x_0) = \mathcal{Z}_{\text{on}}[\mathcal{Z}_{\text{off}}[h, T_{\text{off}}|\delta_\bullet, 0], T_{\text{on}}|\delta_{x_0}, 0]. \quad (4.32)$$

Therefore, the offspring generating functional evaluated at time $t = kP$ (with $k \in \mathbb{N}$) can be expressed by nesting Eq. (4.32) k times:

$$\mathcal{Z}[h, t = kP|\delta_{x_0}, 0] = \mathcal{W}^k[h, x_0], \quad (4.33)$$

where we defined the k^{th} composition of functions as $\mathcal{W}^k[h; x_0] = (\mathcal{W} \circ \mathcal{W}^{k-1})[h, x_0] = \mathcal{W}[\mathcal{W}^{k-1}[h, \bullet]; x_0]$.

Following a similar argument to Harris [112], we set $h = 0$ to obtain the extinction probability and assumed the existence of an asymptotic steady state for $t > kP$:

$$\mathcal{W}[\mathcal{W}^k[0, \bullet], x_0] = \mathcal{W}[0, x_0]. \quad (4.34)$$

Finally, we obtain an expression (equal to Eq. (4.35)) for the asymptotic extinction probability $p^*(x_0) = 1 - p_{\text{surv}}(x_0)$ of a population starting from a single individual with age x_0 :

$$p^*(x_0) = \mathcal{W}[p^*, x_0] = \mathcal{Z}_{\text{on}}[\mathcal{Z}_{\text{off}}[p^*, T_{\text{off}}|\delta_\bullet, 0], T_{\text{on}}|\delta_{x_0}, 0]. \quad (4.35)$$

Manipulating Eq. (4.35) via Eq. (4.18), we obtain a system of integral equations:

$$\mathcal{G}[x_0, t; p^*]\Pi^{\text{on}}(x_0) = \Pi^{\text{on}}(x_0 + t)\mathcal{H}[x_0 + t, t; p^*] \quad (4.36)$$

$$\begin{aligned} &+ \int_0^t \Pi_\gamma^{\text{on}}(u + x_0) (\mathcal{G}[0, t - u; p^*])^2 du \\ &+ \int_0^t \Pi_d^{\text{on}}(u + x_0) du, \end{aligned} \quad (4.37)$$

$$\mathcal{H}[x_0, t; p^*]\Pi^{\text{off}}(x_0) = \Pi^{\text{off}}(x_0 + t)\mathcal{G}[x_0 + t, T_{\text{off}}; p^*] + \quad (4.38)$$

$$+ \int_0^t \Pi_\gamma^{\text{off}}(x_0 + u) (\mathcal{H}[0, t - u; p^*])^2 du, \quad (4.39)$$

where we defined $\mathcal{G}[x, t; p^*] = \mathcal{Z}_{\text{on}}[\mathcal{Z}_{\text{off}}[p^*, t|\delta_\bullet, 0], T_{\text{on}}|\delta_x, 0]$ and $\mathcal{H}[x, t; p^*] = \mathcal{Z}_{\text{off}}[p^*, t|\delta_{x_0}]$. Eqs. (4.36) and (4.38) represent a system of coupled integral

equations that can be numerically solved for $p^*(x_0) = \mathcal{G}[x_0, T_{\text{off}}; p^*]$. The probabilities with superscript ^{on} and ^{off} are defined as shown in Fig. 4.5 with rate functions, respectively, $\{\gamma(x), d(x)\}$ and $\{\gamma(x), 0\}$.

The same procedure can be implemented for any values of $h(x)$ if the generating functional has a steady solution in the asymptotic regime. In general, the generating functional in on environments is described by:

$$\begin{aligned}\mathcal{Z}_{\text{on}}[h, t | \delta_{x_0}] \Pi(x_0) &= \Pi(t + x_0) h(t + x_0) + \int_0^t du \Pi_d(u + x_0) \\ &\quad + \int_0^t du \Pi_\gamma(u + x_0) \mathcal{Z}_{\text{on}}^2[h, t - u | \delta_0],\end{aligned}\quad (4.40)$$

while, during the off-environment, is described by:

$$\begin{aligned}\mathcal{Z}_{\text{off}}[h, t | \delta_{x_0}] &= e^{-\int_0^t \gamma(u+x_0) du} h(t + x_0) \\ &\quad + \int_0^t du e^{-\int_0^u \gamma(y+x_0) dy} \gamma(u + x_0) \mathcal{Z}_{\text{off}}^2[h, t - u | \delta_0].\end{aligned}\quad (4.41)$$

In conclusion, it is also possible to observe that Eqs. (4.36) and (4.38) (and potentially Eqs. (4.40) and (4.41)) can be solved numerically by 1) discretising functions and integrals and 2) iteratively inserting them into each other until the fixed point is reached.

4.4 Survival Resonances

The following step was extracting the numerical solution of Volterra's Eqs. (4.40) and (4.41) and simulating the dynamics to validate the results. In agreement with simulations (Fig. 4.6 (a,b)), the survival probability displays narrow peaks which emerge when the environment period $P = T_{\text{on}} + T_{\text{off}}$ is tuned precisely to the mean division μ_γ or average death time μ_d . These peaks are absent in unstructured models with constant division and death rates (App. C).

Reminiscent of overtones, the peaks repeat for higher integer multiples of P , so we called this phenomenon *survival resonances*. We found two types of resonances: *deterministic* and *noise induced survival resonances*.

4.4.1 Deterministic Resonances of Survival Probability

Deterministic resonances occur when division and death times fluctuate little, i.e. small fluctuation $CV_d^2, CV_\gamma^2 \ll 1$, Fig. 4.6 (a). In this limit, division and

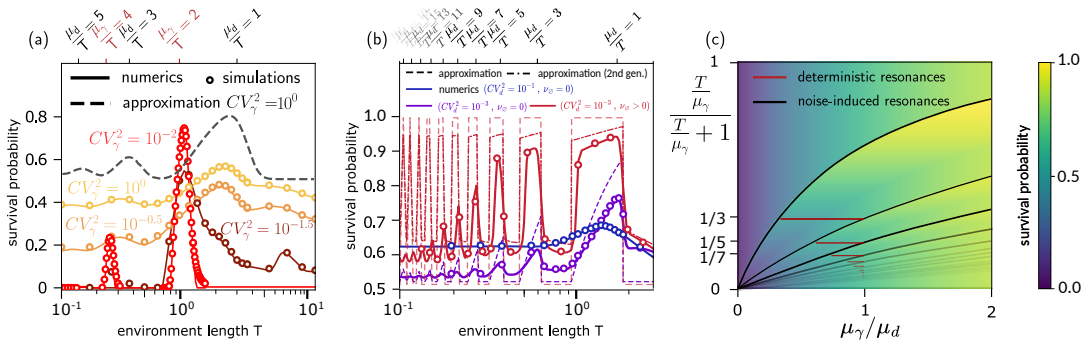


Figure 4.6: Survival resonances under periodic on-off treatments of length $T = T_{\text{on}} = T_{\text{off}}$ (x-axis (a) and (b) and y-axis in (c) on log-scale). (a): Survival probability ($p_{\text{surv}}(0)$) shows a crossover from deterministic (red) to noise-induced resonances (yellow and orange) as division noise (CV_γ^2) increases. (b): Noise-induced survival resonances increase with decreasing noise in death time (blue and violet) and are amplified by persistence ($\nu_\emptyset > 0$, red) in agreement with the approximations (Eq. (5.26) with (5.48) and 2nd generation, Eq. (4.48), $CV_d^2 = 0$). Theoretical locations of deterministic (red, Eq. (4.42)) and noise-induced resonances (black ticks, Eq. (5.49)) are shown as top ticks. (c): Phase diagram of survival probability peaks in scaled $T\mu_d/\mu_\gamma$ space with heat-map of the approximation (Eq. (5.26) with (5.48)) for $\nu_\emptyset = 0$. Division and death times are Γ distributed with parameters $\mu_\gamma = 2$, $\mu_d = 1.8$, $CV_d^2 = 10^{-2}$, $w_\gamma = w_d = 1$ in (a) and $\mu_\gamma = 1.8$, $\mu_d = 2$, $CV_\gamma^2 = 1$, $w_\gamma = w_d = 1$ in (b,c) or 0.99 in (red, b). The figure was depicted using data provided by J.Pausch (numerics) and P.Piho (simulations).

death occur at fixed ages μ_γ and μ_d . If $\mu_\gamma < \mu_d$, death never occurs because no cell ever reaches the age of death μ_d , and $p_{\text{surv}}(0) = 1$, see Fig. 4.6 (c). If $\mu_\gamma > \mu_d$, cells die if they reach the age of death μ_d in any of the on-environments $A_m := mP + [0, T_{\text{on}}]$. Descendants synchronously exceed the deadly age μ_d in time intervals $B_n = n\mu_\gamma + (\mu_d, \mu_\gamma]$, $n \in \mathbb{N}_0$. Moreover, all of them die simultaneously if this occurs in any on-environment A_m , leading to the survival condition that $\forall m, n : A_m \cap B_n = \emptyset$ implies $p_{\text{surv}}(0) = 1$. Consequently, only singular, fine-tuned combinations of $T_{\text{on},\text{off}}$ and μ_γ allow deterministic resonance:

$$\{T_{\text{on},\text{off}} : \mu_\gamma = nP, n \in \mathbb{N}, 0 < \mu_\gamma - \mu_d < T_{\text{off}}\}. \quad (4.42)$$

Physically, Eq. (4.42) is a renewal condition: all the generations are approximately born at the beginning of an on-environment, as sketched in Fig. 4.7.

We made the following observations on the effect of noise seen in Fig. 4.6 (a). Firstly, higher overtones of survival probabilities are progressively attenuated because they have a higher absolute variance of division ages and, therefore, are less tuned to P . Secondly, the asymmetry and shift of peaks are due to noise since division times longer than nP lead to death, while cells with shorter

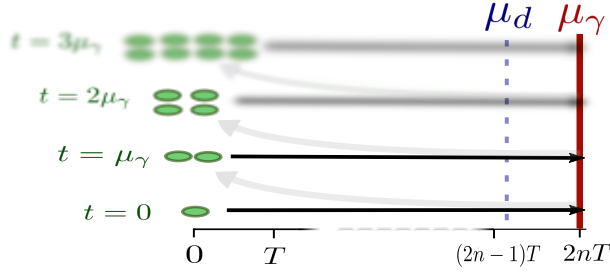


Figure 4.7: **Graphical sketch of the renewal condition in deterministic resonances.** Cells reach age μ_γ when Eq. (4.42) holds. Due to the small noise, cells divide at age μ_γ , creating a new set of newborns. These newborns undergo the same process as their ancestor, reaching age μ_γ and dividing into larger set of newborns. In the figure, we assumed $CV_\gamma^2 \rightarrow 0$ and $CV_d^2 \rightarrow 0$

division times avoid it. Persistence does not introduce any significant variation to the *deterministic resonances*. De facto, *deterministic resonances* represent parameter spots in which the cell fits the escape conditions, and persistence simply reduces the portion of dead cells.

4.4.2 Noise-induced Resonances of Survival Probability

As more and more noise in division timing is introduced (Fig. 4.6 (b)), *deterministic resonances* disappear and give way to the second type of resonance, which we call *noise-induced resonances*. Here, peaks in p_{surv} appear for specific combinations of μ_d and $T_{\text{on},\text{off}}$ with only small fluctuations in death times. These resonances also appear for $\mu_\gamma < \mu_d$, and their emergence is qualitatively explained by considering the death probability of the first cell. Assuming that death is deterministic ($CV_d^2 \rightarrow 0$) with putative death time $\tau_d \approx \mu_d$ and that the cell was born at time $t = 0$ at the start of the first on-environment, we identified two regimes. If τ_d falls in an on-environment, the death probability is the product of the probability w_d that death would occur at time τ_d times the probability that the cell does not divide before τ_d , $\phi_\gamma(\tau_d) = e^{-\int_0^{\tau_d} du \gamma(u)}$. If τ_d falls in an off-environment, the cell either dies at the next on-environment ($w_d = 1$) or never ($w_d < 1$) due to the zero death rate at old ages, see Fig. 4.2 (b). This consideration leads to the effective death and persistence probability of the first cell:

$$\begin{aligned} \nu_d &\approx \mathbb{E} \left[1_{\text{on}}(\tau_d) w_d \phi_\gamma(\tau_d) + 1_{\text{off}}(\tau_d) \delta_{w_d,1} \phi_\gamma \left(\left\lfloor \frac{\tau_d}{P} + 1 \right\rfloor P \right) \right] \\ \nu_\emptyset &\approx (1 - w_\gamma) \mathbb{E} [1_{\text{on}}(\tau_d)(1 - w_d) + 1_{\text{off}}(\tau_d)(1 - \delta_{w_d,1})], \end{aligned} \quad (4.43)$$

where $\delta_{w_d,1}$ is the Kronecker- δ , $\mathbf{1}_{\text{off/on}}(\tau_d)$ is 1 if τ_d falls into an off/on environment.

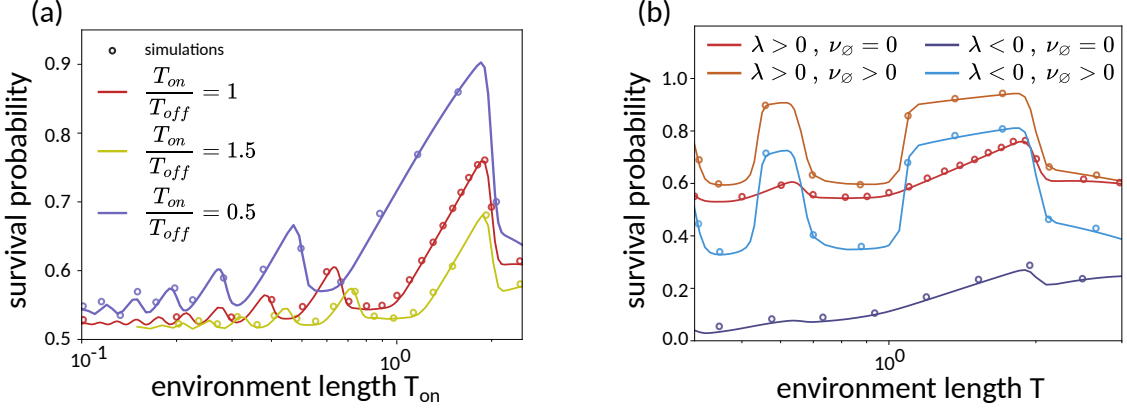


Figure 4.8: Dependence of noise-induced resonances on environment shape, growth regimes and persistence probability. (a) Survival resonances as a function of the on-environment length (T_{on}) for pulsed ($\frac{T_{\text{on}}}{T_{\text{off}}} = 0.5$, purple line), even ($\frac{T_{\text{on}}}{T_{\text{off}}} = 1$, red line), and anti-pulsed ($\frac{T_{\text{on}}}{T_{\text{off}}} = 1.5$, yellow line) modulations of the on-environment. The survival probability is peaked around $T_{\text{on}} = \mu_d - nP$ with period $P = T_{\text{on}} + T_{\text{off}}$, in agreement with Eq. (4.44). (b) Noise-induced resonances exist both in sub-($\lambda < 0$ during the on-environment, blue line) and supercritical ($\lambda > 0$ during the on-environment, red line) growth regimes. The amplification induced by persistence exists both in sub-($\lambda < 0$ during the on-environment, light blue line) and supercritical ($\lambda > 0$ during the on-environment, orange line) growth regimes. Division and death times are Γ distributed with parameters $\mu_d = 2, CV_d^2 = 10^{-3}, \mu_\gamma = 1.8, CV_\gamma^2 = 1, w_\gamma = w_d = 1$ in (a); $\mu_d = 2, CV_d^2 = 10^{-3}, \mu_\gamma = 1.8, CV_\gamma^2 = 1$ (red line $w_\gamma = w_d = 1$, orange line $w_\gamma = w_d = 0.99$) and $\mu_\gamma = 2.94$ (blue line $w_\gamma = w_d = 1$, light blue line $w_\gamma = w_d = 0.99$) in (b). The figure was depicted using data provided by J.Pausch (numerics) and P.Piho (simulations).

ment and zero otherwise and the average is over the distribution of death.

As a rough approximation, we assumed that the cells of later generations have the same death probability as the first cell and then use Eq. (4.43) in the solution of the survival probability in constant environments Eq. (4.28). These approximations, strictly valid only for constant environments, predict resonances at the following environment lengths:

$$\{T_{\text{on/off}} : \mu_d = T_{\text{on}} + nP, n \in \mathbb{N}\}, \quad (4.44)$$

which reproduce all the noise-induced resonances seen in the simulations and numerics (dashed lines, Fig. 4.6 (a,b)).

Intuitively, resonances occur when a cell's putative death time falls shortly after the end of an on-environment because this maximises its time to divide. The approximation produces ramps followed by sudden drops and thus provides qualitative agreement with the exact results (Fig. 4.9).

We were also able to calculate the transient survival probabilities, which show that the first generation determines the locations of all noise-induced resonances in the following generations, Fig. 4.6 (b). In detail, the extinction probability for the first generation (i.e. the first cell born at $t = 0$) was given in Eq. (4.43) by:

$$p_{\text{ext}}^I(\mu_d) = 1_{\text{on}}(\mu_d)w_d\phi_\gamma(\mu_d) + 1_{\text{off}}(\mu_d)\delta_{w_d,1}\phi_\gamma\left(\left\lfloor \frac{\mu_d}{P} + 1 \right\rfloor P\right). \quad (4.45)$$

In the second generation, the two newborns have a synchronised age and thus their extinction probability $p_{\text{ext}}^{II}(\mu_d, \tau_d)$ for a putative death time τ_d equals:

$$\begin{aligned} p_{\text{ext}}^{II}(\mu_d, \tau_d) &= \int_0^{\tau_d} p(\tau_\gamma = x | \tau_\gamma < \tau_d)(p_{\text{ext}}^I(\mu_d + x))^2 dx \\ &= \int_0^{\tau_d} \frac{f_\gamma(x)}{\int_0^{\tau_d} f_\gamma(u)du} (p_{\text{ext}}^I(\mu_d + x))^2 dx. \end{aligned} \quad (4.46)$$

If $w_d = 1$, then $\tau_d = 1_{\text{on}}(\mu_d)\mu_d + 1_{\text{off}}(\mu_d)\lfloor \frac{\mu_d}{P} + 1 \rfloor P$. If $w_d < 1$, then $\tau_d = 1_{\text{on}}(\mu_d)\mu_d + 1_{\text{off}}(\mu_d)a$ with $a \rightarrow \infty$. This allows reducing $p_{\text{ext}}^{II}(\mu_d, \tau_d)$ to $p_{\text{ext}}^{II}(\mu_d)$.

The probability that the first cell divided equals $p_{\text{div}}^I = 1 - p_{\text{ext}}^I$ in the case without persistence, and in the case with persistence

$$p_{\text{div}}^I(\mu_d) = 1_{\text{on}}(\mu_d)w_\gamma \left(w_d \int_0^{\mu_d} f_\gamma(u)du + (1 - w_d) \right) + 1_{\text{off}}(\mu_d)w_\gamma, \quad (4.47)$$

$$p_{\text{ext} \leq 2}(\mu_d) = p_{\text{ext}}^I(\mu_d) + p_{\text{div}}^I(\mu_d) \cdot p_{\text{ext}}^{II}(\mu_d). \quad (4.48)$$

The above equation derives from Eq. (4.13). In Fig. 4.9 (c, d), we compared the survival probability of the first and second generations and how they approach the asymptotic survival probability. The effect of persistence is shown in Fig. 4.6 (b).

Leaving the generational approximation aside, we observed that neither changes in $\frac{T_{\text{on}}}{T_{\text{off}}}$ nor the sign of the growth rate λ in the on-environment affect the existence and locations of noise-induced resonances. Such changes only affect their amplitudes (Fig. 4.8). Resonances were significantly boosted in cases with persistence ($\nu_\varnothing > 0$, Fig. 4.6 (b) and Fig. 4.8 (b)). This is explained by resonant filtering through a decreasing death rate for old cells (Fig. 4.2 (b) inset, Eq. (4.43)). Predictions of the resonance profile, including the ramp shape and finite survival probability, improved when transients beyond the approximation in Eq. (4.43) were taken into account (red dotted-dashed line, 4.6). We sum-

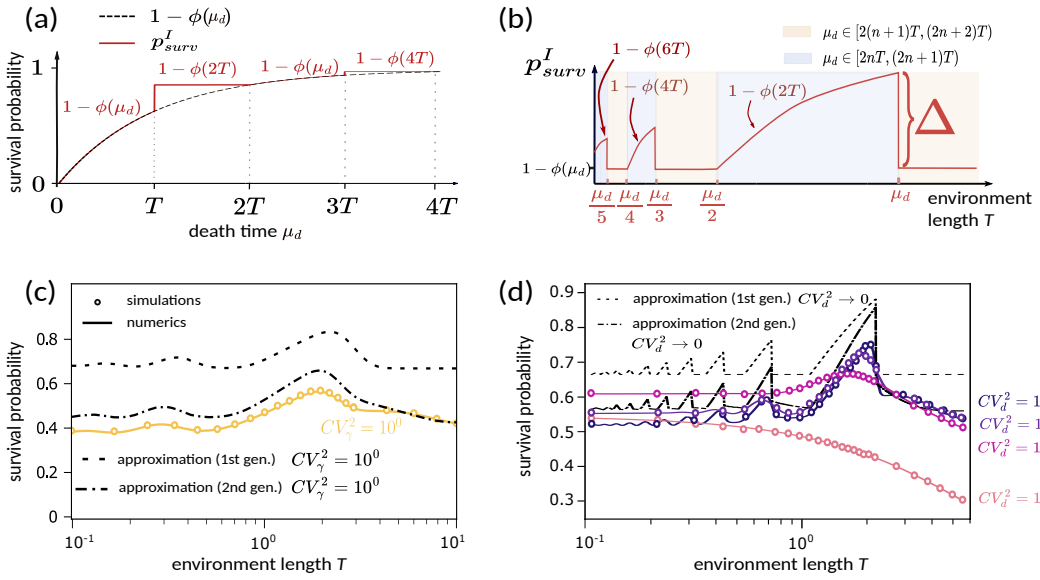


Figure 4.9: Transient behaviour of the survival probability in periodic on-off environments. $w_d = w_\gamma = 1 \Rightarrow \nu_\emptyset = 0$. (a) Survival probability of the initial cell (p_{surv}^I , first-generation approximation) as a function of μ_d (red line) is discontinuous at multiples of the environment length $T = T_{\text{on}} = T_{\text{off}}$. $1 - \phi(\mu_d) = 1 - e^{-\int_0^{\mu_d} du \gamma(u)}$ is the corresponding survival probability in a constant environment, assuming $CV_d^2 \rightarrow 0$. (b) Noise-induced jumps of the survival probability in the first generation (p_{surv}^I) as function of the environment length T . The height Δ of the first resonance peak is analytically approximated via Eq. (4.49), see also Fig. 4.10. (c) The survival probabilities of the first and second generations (Eqs. (4.45) and (4.46)) approximate the asymptotic behaviour (yellow line). (d) First- and second-generation approximations (Eqs. (4.45) and (4.46)) of noise-induced resonances, as shown in Fig. 4.6 with $\mu_d = 2.0$, $\mu_\gamma = 1.8$ and $CV_\gamma^2 = 1$. Non-monotonic behaviour is also observed for finite noise in death time ($CV_d^2 \in \{10^{-1}, 10^{-2}, 10^{-3}\}$) except for the age-independent case ($CV_d^2 = 1$, rose line). Parameters are $\mu_d = 1.8$, $CV_d^2 = 10^{-2}$, $\mu_\gamma = 2.0$ and $CV_\gamma^2 = 1$ as in Fig. 4.6 (b).

marised the locations of deterministic and noise-induced survival resonances in a phase diagram (Fig. 4.6 (c)), which is independent of persistence.

This section ends with a brief overview of the relation between noise-induced survival resonances and stochastic resonances [148]. To this end, we considered the relationship between noise-induced jumps in p_{surv} and the noise affecting division times. The magnitude Δ of the first resonance peak of the survival probability can be approximated by the corresponding magnitude in the survival probability of the first generation. Based on Eq. (4.45), we found:

$$\Delta \approx w_d \phi_\gamma(T_{\text{on}}) - \delta_{w_d, 1} \phi_\gamma \left(\left\lfloor \frac{T_{\text{on}}}{P} + 1 \right\rfloor P \right). \quad (4.49)$$

In Fig. 4.10, we used this equation to quantify the output-performance (Δ) versus the input noise magnitude (CV_γ^2) for Γ -distributed division times. We ob-

served that, for specific values of μ_d , the jump height displays a non-monotonic dependence on CV_γ^2 . The peaks indicate an increase in the signal-to-noise ratio with the noise intensity, which is the signature of stochastic resonance.

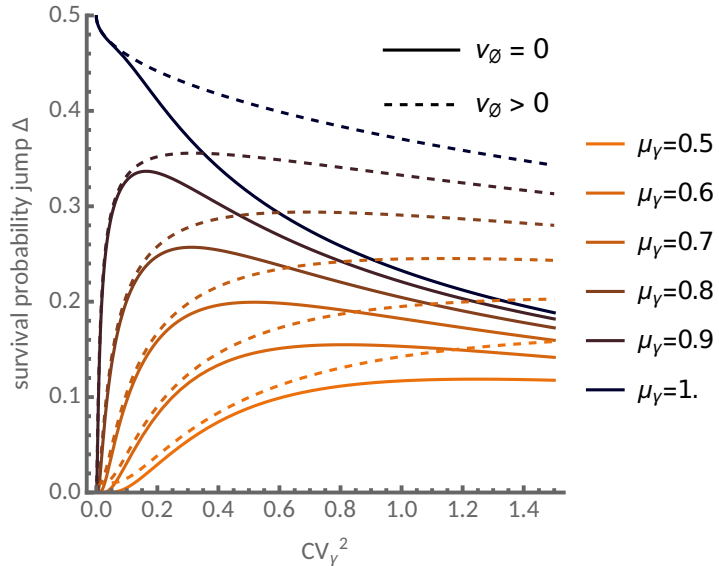


Figure 4.10: **Stochastic resonance-like behaviour of the survival probability peaks.** Dominant jump (of the survival probability in the first generation) versus the noise in division times at $\frac{\mu_d}{T_{on}} = 1$. For some values of μ_γ , the survival jumps display a non-monotonic behaviour following Eq. (4.49) (solid lines, $w_d = w_\gamma = 1$). For the case with persistence (dashed lines, $w_d = w_\gamma = 0.99$), the peaks broaden displaying an amplification of the survival probability over a wide range of noise levels in division times.

4.5 Conclusions

We examined a stochastic population model with cell cycle-dependent division and death rates to understand how fractional killing may emerge from the interplay of cellular heterogeneity with fluctuations.

We found that survival chances increase with noise in division timing but decrease with noise in death timing. This suggests that division heterogeneity combined with controlled cell death could represent a strategic advantage for cells to persist in continuous drug treatment.

Then, we analysed survival probabilities under periodic treatments and discovered deterministic and noise-induced resonances, observed under a tuning of division and death rates to the environment duration. Doubling times of cancer cell lines vary from one to several days but lengthen significantly in tumours [149] and after drug exposure [150]. In comparison, treatment lengths are

experimentally (one to several days in cell lines) and clinically set parameters (months), and how to tune these optimally is subject to ongoing research [151]. Survival resonances should thus be observable within experimental and clinical parameter ranges.

In populations with pre-existing genetic variability, such as in genetic screens or cancer, these resonances could be difficult to avoid as division and death rates are heterogeneous and can be selected by adjusting the environmental duration. The survivors of this selection process will be located predominantly along peaks of the survival probability, shown as lines in the phase diagram, Fig 4.6 (c). Under this hypothesis, deterministic resonances select low-noise phenotypes within a narrow band of division times that are even integer multiples of the environmental duration, Eq. (4.42). Noise-induced resonances select on cells with death times being odd multiples of the environmental duration. Interestingly, for $\mu_d > \mu_\gamma$, the resonance increases with division time noise and, in some cases, reaches a maximum (Fig. 4.10), which is a hallmark of stochastic resonance [148]. The intuition is that cells are killed when they stochastically exceed an age-dependent death threshold and these events are resonantly filtered by periodic forcing. Threshold fluctuations attenuate resonances but enhance the survival probability away from them (Fig. 4.6 (b)) in contrast to constant environments. Complex intracellular pathways implement such thresholds [15,135,152] and our findings could link their noise properties with evolvable survival strategies that can be exploited for decision-making or synthetic biology. A future research path might focus on the relation between diversity (age heterogeneity) and selection [153]. Specific initial age distributions may evolve following synchronized behaviour with periodic treatment, leading to enhanced survival probability for specific age ranges (selection). The analytics framework for time-dependent environments can be easily extended to account for different initial age distributions, and the environment's length can be tuned to observe possible favourable survival probability for specific age conditions.

A limitation of our approach is that we ignored generational inheritance [132,154], for example, through cell size control in bacteria. This can be included by averaging Eq. (4.43) over the size distribution, which would deviate from the ramp-like behaviour of survival resonances but not their location. Another limitation is that we neglected effects that are dependent on drug exposure time [155], which could be incorporated using Eqs. 4.14.

In summary, we have identified a possible non-genetic mechanism for fractional killing emerging in response to periodic drug treatments. These stochastic mechanisms could be one of many contributing factors to drug persistence, among other active mechanisms such as phenotypic switching [156]. Since periodically forced age-structured branching processes are ubiquitous, such as in epidemics and ecology, we anticipate survival resonances to be widespread in stochastic population dynamics.

Chapter 5

Survival Strategies of Cancer Cells

Abstract

Fractional killing, i.e. residual cancer, often leads to a relapse of the tumour. This suggests that persistent states may be transitory. Here, we studied a stochastic population model where cells can divide, die or escape the system for a random time. Modelling periodic treatments, we recovered the survival resonance and we observed extinction peaks. This research project was initially developed by P. Thomas and myself, and strongly improved by J. Pausch in the last months (Sec. 5.3). Also, L. Magnani and H. Dewhurst have to be acknowledged for providing meaningful insights into the biological nature of the application. My contribution to this project consisted of conducting and being involved with all analytics of the following Chapter. I urge the reader to note that the numerical solutions presented in Sec. 5.3 are exclusively a result of J. Pausch's efforts. Instead, numeric algorithms and simulations presented in Figs. 5.2, 5.3 and 5.4 were implemented by myself.

The division-death model, with the introduction of persistence, allows a schematic representation of cells under treatment. In reality, it is still not clear how cells persist and how their metabolic paths are tuned during persistence. Another issue stands in not knowing the time spent by cells in a persistent state since several experimental works [122, 123] show a significant degree of fluctuations in the awakening times.

In general, the words *persistence* and *dormancy* are often used as synonyms in the literature to classify specific survival strategies adopted by cells to escape the treatment. Here, the terms persistence and dormancy define two different survival strategies. Cells can leave the system and persist the treatment, we

called this phenomenon *persistence*. Cells can temporarily interrupt dividing or dying by hiding in a dormant state, we called this phenomenon *dormancy* (Fig. 5.1).

Dormancy can be defined as a survival strategy where cells can avoid the treatment by hiding in a dormant state for limited (random) times. Cells may divide, and die but in a non-dormant state. In contrast to persistence, they are able to awake from the dormant state to continue dividing and dying.

A known real scenario is the one related to hormone dependent breast cancer (HDBC) which is the most commonly diagnosed tumour in women. A vast proportion of HDBC patients incur long periods of clinical dormancy after the treatment. De facto, HDBC cells go into an inherently unstable dormant state where the role of stochastic non genetic events has clinical implications [157].

Until the cancer is detected and treated, the majority of cancer cell populations grow steadily; after administering the drug, the majority of cancer cells die while a residual part of them lays down in a dormancy state. During the dormancy state, the cancer cells "escape" the treatment and are not detectable by the current diagnostic instruments. After a given time, the dormant cells "awake" and start growing back [157]. The "awakening" represents the main issue in HDBC treatment since the dormant time is not yet predictable as well as the reasons behind it.

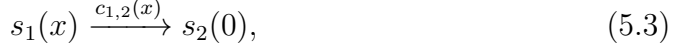
Here, we propose a way to quantify the dynamics of a division-death process where cells are able to hide in a persistent or dormant state. The whole analysis still revolves around the stochastic age-structured theory proposed in Ch. 2 and can be considered as a generalisation of the model proposed in Ch. 4.

5.1 Theoretical Framework

The distinction between dormant and non-dormant cells can be modelled via a multispecies model and the theory (Ch. 2) was implemented to account for any number of species.

Hence, we considered a two species population to include the dormancy dynamics in the division-death process. The first species s_1 represents the non-dormant cells, while s_2 represents the dormant cells. Specifically, the species function $s_1(x)$ labels the cells with age x which can divide, die or escape in a dormant state, i.e. transforming in species s_2 . The cells of the dormant species

$s_2(x)$ exhibit an age x and are only allowed to wake up from the dormant state and switch back to the first species. The stoichiometric reaction network (Fig. 5.1, bottom left, for a general time-dependent case) can be expressed as follows:



The reaction network above replicates the dormancy and awakening processes as renewal processes (age is set equal to zero) from one species to another. The theory will be developed for the renewal case and later generalized to non renewal cases in Subsection 5.2.3.

The functions γ , d , $c_{1,2}$ and $c_{2,1}$ respectively encode the rates of division, death, dormancy and awakening from dormancy. In age-structured analysis, the event times related to division, death or to the dormant-awaken cycle are not constrained to be exponentially distributed, as in the unstructured case (Fig. 5.1, top left). The reaction network can also be described by stoichiometric functions:

$$\nu_\gamma[\vec{x}] = 2\delta_0\delta_{i,1} - \delta_x\delta_{i,1} \quad (5.5)$$

$$\nu_d[\vec{x}] = -\delta_{i,1}\delta_x \quad (5.6)$$

$$\nu_{c_{1,2}}[\vec{x}] = -\delta_x\delta_{i,1} + \delta_0\delta_{i,2} \quad (5.7)$$

$$\nu_{c_{2,1}}[\vec{x}] = -\delta_x\delta_{i,2} + \delta_0\delta_{i,1}. \quad (5.8)$$

The deterministic dynamics of the system can be encoded in a generalised McKendrick-von Foerster PDE (Eq. 1.22) where the number of non-dormant (dormant) cells with age x at time t is defined as $n_1(x, t)$ ($n_2(x, t)$). One PDE for the density of non-dormant agents:

$$(\partial_t + \partial_x)n_1(x, t) = -(\gamma(x) + d(x) + c_{1,2}(x))n_1(x, t) + c_{2,1}(x)n_2(x, t) \quad (5.9)$$

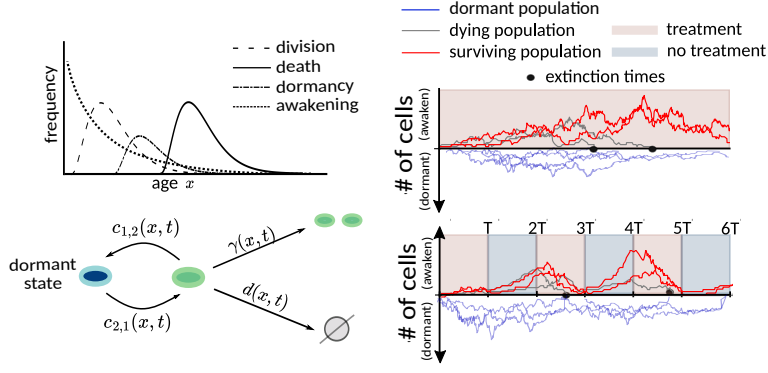


Figure 5.1: **Illustration of age-dependent population dynamics.** Top left panel: the distribution of division, death, dormancy and awakening times depend on the ages of cells. Bottom left: cells divide, die, go dormant or awake depending on age and environment. Top right: constant environment, no interruption of the death process is accounted. Bottom right: periodic on-and off-switching of a treatment. Some cells survive treatment and persist, and fractional killing occurs. Cells can go dormant or awake from it, regardless of the environment.

with boundary condition:

$$n_1(0, t) = 2 \int_0^\infty \gamma(u) e^{-\int_0^u \gamma(x) + d(x) + c_{1,2}(x)} n_1(u, t) du + \int_0^\infty c_{2,1}(u) e^{-\int_0^u c_{1,2}(x)} n_2(u, t) du, \quad (5.10)$$

and one for the second species:

$$(\partial_t + \partial_x) n_2(x, t) = c_{1,2}(x) n_1(x, t) \quad (5.11)$$

with boundary condition:

$$n_2(0, t) = \int_0^\infty n_1(u, t) c_{1,2}(u) e^{-\int_0^u (\gamma(y) + d(y) + c_{2,1}(y)) dy} du. \quad (5.12)$$

In addition, the growth rate of the non-dormant population λ can be expressed via the Euler-Lotka integral Equation :

$$1 = \int_0^\infty e^{-\lambda x} (c_{1,2}(x) + 2\gamma(x)) e^{-\int_0^x (\gamma(u) + d(u) + c_{1,2}(u)) du}. \quad (5.13)$$

This equation can be justified by following the definition of the Euler-Lotka Equation: $c_{1,2}(x) + 2\gamma(x)$ is the average number of offspring born from an individual of age x during the time step and $e^{-\int_0^x (\gamma(u) + d(u) + c_{1,2}(u)) du}$ is the survival probability for a single newborn. In fact, the awakening process happens with

probability one in the asymptotic regime $t \rightarrow \infty$.

The same process can also be described as stochastic process $(n, m) = (n_1, n_2, t|m_1, m_2, 0)$ with initial distributions m_1 (non-dormant cells) and m_2 (dormant cells) and leading to a state (n_1, n_2) at time t . For brevity, Eq. (2.32) can be specialized for this case of study:

$$\begin{aligned} \mathcal{D}_{n_1, n_2, t} \mathcal{P}[n, t|m, 0] &= \int_0^\infty \gamma(x)(\varepsilon_1^{+1}(x)\varepsilon_1^{-2}(0) - 1)n_1(x)\mathcal{P}[n, t|m, 0]dx \quad (5.14) \\ &\quad + \int_0^\infty d(x)(\varepsilon_1^{+1}(x) - 1)n_1(x)\mathcal{P}[n, t|m, 0]dx \\ &\quad + \int_0^\infty c_{1,2}(x)(\varepsilon_1^{+1}(x)\varepsilon_2^{-1}(0) - 1)n_1(x)\mathcal{P}[n, t|m, 0]dx \\ &\quad + \int_0^\infty c_{2,1}(x)(\varepsilon_2^{+1}(x)\varepsilon_1^{-1}(0) - 1)n_2(x)\mathcal{P}[n, t|m, 0]dx. \end{aligned}$$

The process is intrinsically a branching process. Therefore, the integral representation of the Chapman-Kolmogorov Equation can be exploited to obtain a system of non-linear Volterra's equations for the generating functional (Sec. 2.5). It follows that the generating functional for an initial non-dormant cell ($m_1 = \delta_x, m_2 = 0, 0$) is given by:

$$\begin{aligned} \mathcal{Z}[h, t|\delta_x\delta_{i,1}, 0]\Pi(x) &= \Pi(t+x)h_1(t+x) \quad (5.15) \\ &\quad + \int_0^t \Pi_\gamma(u+x)\mathcal{Z}^2[h, t-u|\delta_0\delta_{i,1}, 0]du \\ &\quad + \int_0^t \Pi_{c_{1,2}}(u+x)\mathcal{Z}[h, t-u|\delta_0\delta_{i,2}, 0]du \\ &\quad + \int_0^t \Pi_d(u+x)du. \end{aligned}$$

The quantity $\Pi(x) = \exp(-\int_0^x (\gamma(u) + d(u) + c_{1,2}(u))du)$ represents the probability for a newborn non-dormant cell to survive, i.e. not dividing, not dying or not going dormant. Therefore, the probabilities of dividing, dying or going dormant in an age range $[x, x+dx]$ are respectively given by: $\Pi_\gamma(x) = \gamma(x)\Pi(x)$, $\Pi_d(x) = d(x)\Pi(x)$ and $\Pi_{c_{1,2}}(x) = c_{1,2}(x)\Pi(x)$.

On the dormant side, the generating functional for an initial dormant cell with age x , i.e. $(m_1 = 0, m_2 = \delta_x)$, evolves accordingly with:

$$\begin{aligned} \mathcal{Z}[h, t|\delta_x\delta_{i,2}, 0]\pi(x) &= \pi(t+x)h_2(t+x) + \quad (5.16) \\ &\quad + \int_0^t \pi_{c_{1,2}}(u+x)\mathcal{Z}[h, t-u|\delta_0\delta_{i,1}, 0]du. \end{aligned}$$

The quantity $\pi(x) = \exp(-\int_0^x c_{2,1}(u)du)$ is the probability of remaining dormant for a dormant cell with age $x = 0$, while $\pi_{c_{2,1}}(x) = c_{2,1}(x)\pi(x)$ is the probability awake at age $x \in [x, x + dx]$.

The goal is to quantify the extinction frequency for an initial cell that is not in a dormant state. Eqs. (5.15) and (5.16) can be combined to obtain a recursive function the generating functional associate with the initial condition $m = (m_1 = \delta_x, m_2 = 0, t = 0)$:

$$\begin{aligned} \mathcal{Z}[h_1, h_2, t | \delta_x, 0, 0] \Pi(x) = & \Pi(t + x) h_1(x + t) + \\ & + \int_0^t \Pi_{c_{1,2}}(u + x) \pi_{c_{1,2}}(t - u) h_2(t - u) du \\ & + \int_0^t (\Pi_\gamma(u + x) \mathcal{Z}^2[h_1, h_2, t - u | \delta_0, 0, 0])(t) \\ & + \int_0^t \Pi_c(u + x) \int_0^{t-u} \pi_{c_{2,1}} \mathcal{Z}[h_1, h_2, t - y | \delta_0, 0, 0] dy du \\ & + \int_0^t \Pi_\gamma(u + x) du. \end{aligned} \quad (5.17)$$

Similarly to the division-death process, the functional formalism allows to account different initial conditions (ages) and, as shown in Chapter 4, it is crucial to model periodic treatment. Finally, the notation can be made more compact if the initial cell has age $x = 0$:

$$\begin{aligned} \mathcal{Z}[h_1, h_2, t | \delta_0, 0, 0] = & \Pi(t) h_1(t) + (\Pi_{c_{1,2}} * h_2 \pi)(t) \\ & + (\Pi_\gamma * \mathcal{Z}^2[h_1, h_2 | \delta_0, 0, 0])(t) + (\Pi_d * 1)(t) \\ & + (\Pi_{c_{1,2}} * \Pi_{c_{2,1}} * \mathcal{Z}[h_1, h_2 | \delta_0, 0, 0])(t), \end{aligned} \quad (5.18)$$

where we muted the time dependence notation of the generating functional to account the convolution product labelled with $*$, e.g:

$$(\Pi_\gamma * \mathcal{Z}^2[h_1, h_2 | \delta_0, 0, 0])(t) = \int_0^t \Pi_\gamma(u) \mathcal{Z}^2[h_1, h_2, t - u | \delta_0, 0, 0]. \quad (5.19)$$

On the RHS Eq. (5.18), from top to bottom: the probability that no division or death events happen for non-dormant ($\Pi(t)h_1(t)$) and dormant cells ($(\Pi_{c_{1,2}} * \pi h_2)(t)$). Division ($\Pi_\gamma * \mathcal{Z}^2[h_1, h_2 | \delta_0, 0, 0]$) and death ($\Pi_d * 1$) are the only reactions leading to a change of the abundances. The dormancy-awakening term ($\Pi_{c_{1,2}} * \Pi_{c_{2,1}} * \mathcal{Z}[h_1, h_2 | \delta_0, 0, 0]$) represents the possibility that a cell goes dormant and awakes before dividing or dying in the dormant time-interval. The

components of Eq. (5.18) can be better understood if Eq. (5.18) is expressed in terms of the functional probability \mathcal{P} :

$$\begin{aligned}\mathcal{P}[n_1, n_2, t | \delta_0, 0, 0] = & \Pi(t) \delta_{n_1, \delta_0} \delta_{n_2, 0} + \int_0^t \Pi_{c_{1,2}}(t-u) \delta_{n_2(u), 1} \pi(u) du \\ & + (\Pi_\gamma * \mathcal{P}^2[n_1, n_2 | \delta_0, 0, 0])(t) + (\Pi_d * 1)(t) \\ & + (\Pi_{c_{1,2}} * \Pi_{c_{2,1}} * \mathcal{P}[n_1, n_2 | \delta_0, 0, 0])(t),\end{aligned}\quad (5.20)$$

Eq. (5.18) is a multi type generalisation of the Bellman-Harris process. The following analysis is mainly focused on quantifying the survival probability of cells, however, the methods proposed in Sec. 2.5 allow to quantify the moments exactly and in its asymptotic regimes.

5.2 Continuous Treatments of Cancer Cells

Navigating a path similar to Ch. 4, the effects of dormancy on the division-death dynamics is first studied in constant environments (constant drug treatments). Then, the dynamics of a birth-death-dormancy process is discussed for time-dependent environments, where the effects of drugs is alternated and periodically interrupted.

5.2.1 Theoretical Framework of a Division-Death-Dormancy Model in Absence of Persistence

The aim is to quantify the survival probability in a division-death process where cells can escape to (and awake from) a dormant state. The analysis begins by considering a constant drug treatment where the rate functions do not explicitly depend on time but only on the age of cells. Similarly to Ch. 4, Eq. (5.18) can be exploited to obtain an expression of the survival probability, $p_{surv} = 1 - p(0) = 1 - \lim_{t \rightarrow \infty} \mathcal{Z}[0, t | \delta_0]$:

$$p(0) = \nu_\gamma p^2(0) + \nu_d + \nu_{c_{1,2}} p(0). \quad (5.21)$$

Alternatively, the p_{surv} can be expressed in a standard division-death frame as:

$$p(0) = \frac{\nu_\gamma}{1 - \nu_{c_{1,2}}} p^2(0) + \frac{\nu_d}{1 - \nu_{c_{1,2}}}. \quad (5.22)$$

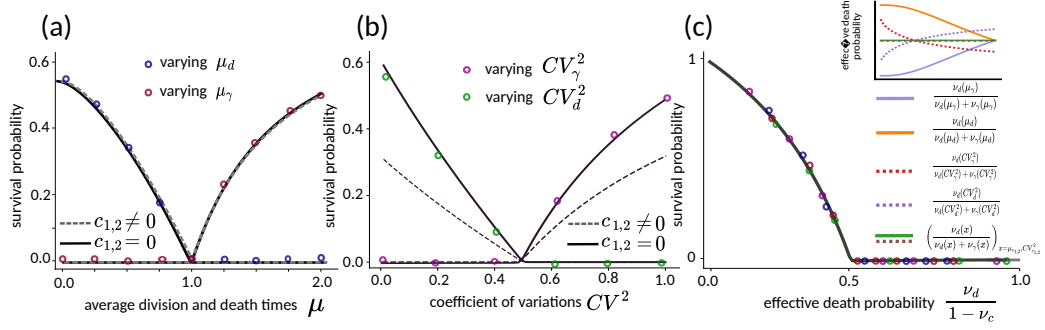


Figure 5.2: **Survival probability** p_{surv} of a newborn cell with division, death, dormancy and awakening ages following Γ distributions. (a): Simulation (symbols) and theory (black line) of p_{surv} over average division and death ages, μ_γ and μ_d . (b) p_{surv} as function of the coefficient of variation of division and death ages, CV_γ^2 and CV_d^2 . (c) p_{surv} as a function of the effective death probability $\frac{\nu_d}{1 - \nu_{c_{1,2}}}$. Inset: monotonic relation of $\frac{\nu_d}{\nu_d + \nu_\gamma}$ to μ_d , μ_γ , $\mu_{c_{1,2}}$, CV_d^2 , CV_γ^2 and $CV_{c_{1,2}}^2$. Γ -distributed times assumed with $\mu_d = 1$, $\mu_\gamma = 1$, $\mu_{c_{1,2}} = 1$, $CV_d^2 = CV_\gamma^2 = CV_{c_{1,2}}^2 = 0.5$ unless stated otherwise

The quantities $\nu_d = \int_0^\infty dx \Pi_d(x)$, $\nu_\gamma = \int_0^\infty dx \Pi_\gamma(x)$ and $\nu_{c_{1,2}} = \int_0^\infty dx \Pi_{c_{1,2}}(x)$ are defined as the effective death, division and dormancy probabilities. We urge the reader to note that the survival probability does not depend on the awakening rate since it is a renewal process ($s_2(x) \xrightarrow{c_{2,1}(x)} s_1(0)$). Moreover, $p_{\text{surv}}(x)$ with initial age x can still be expressed as a function of $p_{\text{surv}}(0)$:

$$(1 - p_{\text{surv}})(x)\Pi(x) = (1 - p_{\text{surv}})^2(0) \int_0^\infty \Pi_\gamma(u + x) \\ + (1 - p_{\text{surv}}(0)) \int_0^\infty \Pi_{c_{1,2}}(u + x)du \\ + \int_0^t \Pi_d(u + x)du, \quad (5.23)$$

while the survival probability is still given by $p_{\text{surv}}(0)$ for an initial dormant cell ($m_1 = 0, m_2 = \delta_x$). Since the persistence effects are absent, the constraint $\nu_\gamma + \nu_d + \nu_{c_{1,2}} = 1$ holds and the probability of survival or extinction is uniquely encoded in the couple of factors ν_d and ν_γ (or $(\nu_d, \nu_{c_{1,2}})$ or $(\nu_{c_{1,2}}, \nu_\gamma)$).

To provide an intuitive explanation of the effects induced by dormancy, we relied on Fig. 5.2 where we studied a *critical* scenario (average division and death times are equal) where the fluctuations can push the system toward a *super-critical* or *sub-critical* phase. Here, division, death and going dormant ages follow $\Gamma(\alpha, \beta)$ -distributions with $\mu = \alpha/\beta$ and $CV^2 = 1/\alpha$. The variations in the average division and death times (μ_d and μ_γ) do not present any detectable fluctuations in the growth rate induced by dormancy (Fig. 5.2 (a)),

due to the same symmetric fluctuation ($CV_\gamma^2 = CV_d^2$). Instead, the effects of dormancy become evident while increasing fluctuations in division or death times (Fig. 5.2 (b)) where dormancy promotes the escape from the sub-critical regions, compared to the case $c_{1,2} = 0$ (Fig. 5.2 (b)).

Figs. 5.2 (a,b) provide just a sketch of the effects of dormancy in a specific configuration where the fluctuations (and the mean times) are symmetric for division and death: Fig. 5.2 (b) (Fig. 5.2 (a)). To better understand the interplay between dormancy, division and death, the exact solution of the survival probability can be recalled from Eqs. (5.21) and (5.22):

$$p_{\text{surv}} = 1 - \frac{\nu_d}{1 - \nu_{c_{1,2}} - \nu_d} \Theta \left(1 - \frac{\nu_d}{1 - \nu_d - \nu_{c_{1,2}}} \right). \quad (5.24)$$

We observe that the transition between fractional killing ($p_{\text{surv}} > 0$) and total extinction ($p_{\text{surv}} = 0$) is located at $\nu_d = \nu_\gamma = \frac{1}{2}(1 - \nu_{c_{1,2}})$. In other terms, death and division probabilities have to be equal, regardless of the value of $\nu_{c_{1,2}}$ but under the constraint: $\nu_{c_{1,2}} + \nu_\gamma + \nu_d = 1$.

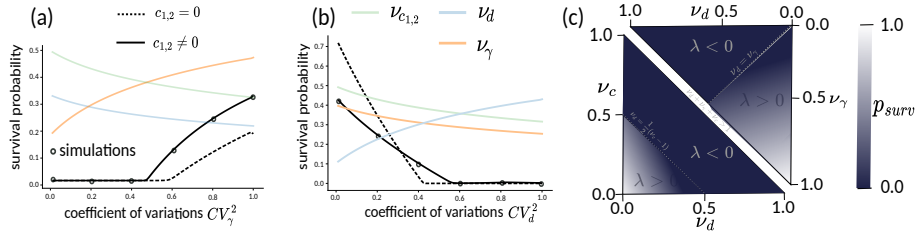


Figure 5.3: Dormancy induces a shift of the transition point between fractional killing and total extinction. (a) The effects induced by dormancy ($c_{1,2} \neq 0$, black line) promotes the escape from extinction: $\mu_d = 0.9, \mu_\gamma = 1, \mu_{c_{1,2}} = 1.1, CV_d^2 = CV_{c_{1,2}}^2 = 0.5$. (b) Pockets where the dormancy is not favourable to cells. Dormancy induce a later transition $\mu_d = 1.1, \mu_\gamma = 1, \mu_{c_{1,2}} = 0.9, CV_d^2 = CV_{c_{1,2}}^2 = 0.5$. (c) Two Phase diagrams: upright survival probability in terms of (ν_γ, ν_d) and, down left, in term of $(\nu_{c_{1,2}}, \nu_d)$

The effects induced by dormancy become easier to understand by noticing that the system is a division-death process where the probability to die is a conditional probability ($\frac{\nu_d}{\nu_d + \nu_\gamma}$) (Eq. (5.22)). This is evident in Fig. 5.2 (c), where the behaviour of the conditional death probability is compared to the survival probability itself. Fig. 5.2 (c) displays in detail (top right) how fluctuations in the division, death and dormancy times (Γ -distributed) promote or not the survival of the cells.

Fig. 5.2 helped us to introduce the effects induced by dormancy (Fig. 5.2 (a,b)) and suggested a way to encapsulate the dynamics in effective reaction variable (ν_s) (Figs. 5.2 (c) and Eq. 5.22). Let us now consider Fig. 5.3 to validate our

conclusions. We note that dormancy does not necessarily promote the chances of survival (Fig. 5.3 (a,b)). Indeed, there are configurations where dormancy tunes the survival probability down (Fig. 5.3 (b)).

Moreover, Eq. (5.13) is equal to $2\nu_\gamma + \nu_{c_{1,2}} = 1$ on the transition line between negative and position growth rate ($\lambda = 0$). This coincides with the transition between total and fractional killing since $\frac{\nu_{c_{1,2}}+2}{2} = \nu_d$. Therefore, the phase transition from growth rate positive ($\lambda > 0$) to negative ($\lambda < 0$) is still expressed with the constraint $\nu_\gamma = \nu_d$, as shown from the intersection of orange and green lines in Fig. 5.3 (a,b).

This is a clear difference from the dynamics proposed for persistence introduced in Sec. 4.2 in which we observed different critical points for the survival probability and growth rate. Substantially, increasing $CV_{\gamma(d)}^2$ and decreasing $\mu_{\gamma(d)}$ usually lead to an increment of the survival probability. The variations in $CV_{c_{1,2}}^2$ and $\mu_{c_{1,2}}$, instead, are always influenced by the configurations of division and death times distributions. Dormancy, in substance, introduces a probability that the system will not divide or die but it is just renewed with an age-dependent frequency. This new event may promote extinction or survival depending on the infinite possible configurations of division and death times distribution.

In conclusion, I would like to highlight that, since dormancy can also lead to a decrement in the growth rate, there are points where the effects of dormancy do not influence the division-death process (Fig. 5.3 (b), intersection grey and black lines):

$$\int_0^\infty \gamma(y) e^{-\int_0^y (\gamma(u)+d(u)) du} dy = \frac{\nu_\gamma}{1 - \nu_{c_{1,2}}}. \quad (5.25)$$

It follows that the division probability conditioned (to not being previously dormant) is equal to the probability with $c_{1,2} = 0$. A comprehensive representation of the dynamics is proposed in Fig 5.3 (c) where the behaviour of the survival probability is uniquely expressed in terms of (ν_c, ν_d) and (ν_γ, ν_d) . The picture displayed by simulations and analytics implies that dormancy does not have a positive or a negative role on the result of the treatment. Instead, it simply changes the statistical properties of division and death times. The extinction probability is encoded in the efficient probabilities $\nu_{d,\gamma,c_{1,2}}$. Therefore, we have three quantities, all depending on the fluctuation and the mean of each reaction

time. Dormancy simply introduces a second degree of freedom. An intuitive picture on the role of dormancy can be drawn simply considering the deterministic limit $e^{-\int_0^t \gamma(x)dx} = \delta(t - \tau_\gamma)$, $e^{-\int_0^t d(x)dx} = \delta(t - \tau_d)$ and $e^{-\int_0^t c(x)dx} = \delta(t - \tau_c)$ where τ_d , τ_γ and τ_c are dummy deterministic death, division and dormancy times. If $\tau_d < \tau_\gamma, \tau_c$ ($\tau_\gamma < \tau_d, \tau_c$) we observe total extinction (survival). The interesting case arises when $\tau_c < \tau_\gamma$ and $\tau_c < \tau_d$ where, in a totally deterministic framework, we observe the survival of a single initial cell. As soon as small fluctuations are introduced, the asymptotic survival probability will lead to zero survival probability if $\tau_\gamma > \tau_d$ or to a growing cell population $\tau_\gamma > \tau_d$. Dormancy simply restarts the process so that the reaction with the shorter meantime is enhanced.

5.2.2 Division, Death, Dormancy and Persistence

Persistence and dormancy are often used as synonyms in the literature [122, 123]; they are usually used to refer to the fractional killing of cells after drug treatments. The factors leading to fractional killing can be various, but the core idea is that cells are able to interrupt specific metabolic paths in order to escape the treatments. Here, we proposed two different ways for cells to hide: dormancy (a temporary state in which the cell can go to and awake from), and persistence, in which cells escape the reaction network till the end of the process. This difference in the terms "dormancy" and "persistence" only relates to this work and does not find any counterparts in scientific literature. Here, this terminology is adopted in order to distinguish between a temporary process (dormancy) and a conclusive process (persistence). Once persistence is introduced, the cell either divides, dies, goes dormant or persists with probabilities ν_γ (division), ν_d (death), $\nu_{c_{1,2}}$ (go dormant), or $\nu_\emptyset = 1 - \nu_{c_{1,2}} - \nu_\gamma - \nu_d$ (persist). As in the absence of persistence ($\nu_\emptyset = 0$), the awakening rate does not influence the dynamics since it is a renewal process (later I propose a case where this statement does not hold anymore (Subsec. 5.2.3)).

To include persistence in the model, three weights $\{w_\gamma, w_d, w_c, \}$ are defined so that the times distributions (i.e. for death ϕ_d) are not normalised ($\phi_d(x) = w_d d(x) e^{-\int_0^x d(u)du}$) with rate $d(x) = \frac{w_d \phi_d(x)}{w_d \int_x^\infty \phi_d(u)du + (1-w_d)}$). The persistence probability can be expressed in terms of the weights $\nu_\emptyset = (1 - w_\gamma)(1 - w_d)(1 - w_c)$

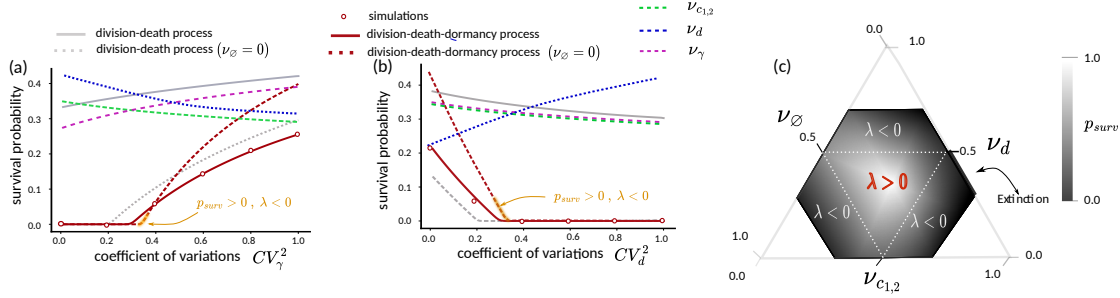


Figure 5.4: Comparative analysis of models with and without persistence: (a,b) show the behaviour of a division death process (dotted grey line), with persistence effects (continuous grey line), affected by dormancy (dotted red line) or perturbed by both persistence and dormancy (red continuous lines). (a)-parameters: $\mu_d = 1, \mu_\gamma = 0.9$ and $\mu_{c_{1,2}} = 1$ and $CV_d^2 = CV_{c_{1,2}}^2 = 0.5$. (b)-parameters: $\mu_d = 0.9, \mu_\gamma = 1$ and $\mu_{c_{1,2}} = 1$ and $CV_\gamma^2 = CV_{c_{1,2}}^2 = 0.5$. Weights: $w_\gamma = w_d = w_{c_{1,2}} = 0.8$ in Figs (a,b). (c): Trigonometric plot with heat-map refers to the survival probability with $\nu_\gamma = 0.2$. We identified three different survival areas where $\lambda < 0$, surrounding the supercritical case $\lambda > 0$

so that the survival probability for a cell with age $x = 0$ is:

$$p_{\text{surv}}(0) = 1 - \frac{1 - \sqrt{1 - (\nu_d + \nu_\gamma) \frac{4}{\nu_d + \nu_\gamma} \nu_d (1 - \nu_{c_{1,2}} - \nu_d - \nu_\phi)}}{2(1 - \nu_\phi - \nu_{c_{1,2}} - \nu_d)}. \quad (5.26)$$

As in the absence of persistence, the probability of surviving is still encoded in the effective probabilities ν_γ , ν_d , ν_ϕ and $\nu_{c_{1,2}}$. The cell population goes completely extinct only when $(\nu_\gamma < \nu_d, \nu_\phi = 0)$ (Fig. 5.4 (a,b)). On the other hand, the growth rate is encoded in Eq. (5.13) so that the transition of the growth rate happens when $2\nu_\gamma + \nu_{c_{1,2}} = 1$. The existence of configurations in which dormancy has a neutral effect is still present (see intersection of red continuous and dotted lines in Fig. (5.4) (a,b)). As a consequence of persistence, some areas can be observed where the survival probability is not zero and yet the growth rate can be negative (Fig. (5.4) (a,b)). A general interpretation can be provided by the effective probabilities ν and Eq. (5.26).

Fig. 5.4 (c) provides the relation between death, dormancy and persistence in the case where ν_γ is constant (i.e. $\mu_\gamma \rightarrow \infty$). Three different regimes can be observed for the growth rates λ : total extinction with $\lambda < 0$ and $p_{\text{surv}} = 0$ ($\nu_\phi = 0, \nu_\gamma < \nu_d$), fractional killing Type II with $\lambda < 0$ and $p_{\text{surv}} > 0$ ($\nu_\phi > 0, \nu_\gamma < \nu_d$) and fractional killing Type I with $\lambda > 0$ and $p_{\text{surv}} > 0$ ($\nu_\phi > 0, \nu_\gamma > \nu_d$). In conclusion, the system can always be studied once the rate functions or the distribution of the reaction times are known. This allowed us to recall the effective event probabilities and forecast the survival probability of the process

(Fig. 5.4 (c)).

5.2.3 The Renewal Condition and the Inheritance Problem

The concept of dormancy was introduced, alluding to a temporary state where cells are not able to divide or die. Despite being a realistic representation, other processes may take place during the dormancy-awakening cycle. One of the most debated points is the cycle-arrest undergone by cells during the dormancy period [19, 158]. It is still not clear how the cell-cycle state (age) varies during the transitions from and to a dormant state.

Here, let us consider a model able to account for the possible inheritance process of the property *age* x when a cell switches between dormant and awakened state. For simplicity, if a cell transitions to a dormant state, then its age is scaled by a factor α , while if a cell transitions back to the non-dormant state, its age is scaled by a factor β :

$$s_1(x) \xrightarrow{c_{1,2}(x)} s_2(\alpha x), \quad (5.27)$$

$$s_2(x) \xrightarrow{c_{1,2}(x)} s_1(\beta x). \quad (5.28)$$

Following the detailed derivation proposed in App. D, the following integral equation can be obtained for an initial non-dormant cell with age x :

$$\begin{aligned} \mathcal{Z}[h, t | \delta_x \delta_{i,1}] \Pi(x) = & \Pi(x + t) h_1(x + t) + \quad (5.29) \\ & + \int_x^{t+x} \Pi_{c_{1,2}}(u) \frac{\pi(t - u + x + \alpha u)}{\pi(\alpha u)} h_2(t - u + x + \alpha u) dx \\ & + \int_0^t \Pi_\gamma(u + x) \mathcal{Z}^2[h, t - u | \delta_0 \delta_{i,1}] du + \int_0^t \Pi_d(u + x) du \\ & + \int_0^t \frac{\Pi_{c_{1,2}}(u + x)}{\Pi(x)} \left[\int_0^\infty \frac{\pi_{c_{2,1}}(y + \alpha(u + x))}{\pi(\alpha(u + x))} \mathcal{Z}[h, \hat{t} | \delta_w \delta_{i,1}] dy \right] du, \end{aligned}$$

where, to be compact, the quantities w and \hat{t} are defined as: $w = \beta(y + \alpha(u + x))$ and $\hat{t} = t - x - y - u$. Moreover, imposing $\alpha = \beta = 0$, Eq. (5.17) is recalled.

It is possible to show that the extinction probability can be expressed as:

$$p(0) = p^2(0)(1 - \mathcal{L}_{\alpha, \beta})^{-1}[\nu_\gamma](0) + (1 - \mathcal{L}_{\alpha, \beta})^{-1}[\nu_d](0), \quad (5.30)$$

where the operator $\mathcal{L}_{\alpha,\beta}$ is given by the integral functional:

$$\mathcal{L}_{\alpha,\beta}[f](x) = \frac{1}{\Pi(x)} \int_x^\infty \frac{\Pi_{c1,2}(u)}{\pi(\alpha u)} \left[\int_{\beta \alpha u}^\infty \pi_{c2,1}\left(\frac{y}{\beta}\right) f(y) dy \right] du. \quad (5.31)$$

The system can still be represented as a division death process where the effective death and division probabilities can be calculated via Eq. (5.31). The same conclusions proposed in Sec. 5.2 can be adapted under the mapping: $\nu_d \rightarrow (1 - \mathcal{L}_{\alpha,\beta})^{-1}[\nu_d](0)$ and $\nu_\gamma \rightarrow (1 - \mathcal{L}_{\alpha,\beta})^{-1}[\nu_\gamma](0)$ and different initial age conditions can be accounted.

The operator $\mathcal{L}_{\alpha,\beta}$ is defined such that $\mathcal{L}_{\alpha,\beta}[\nu_\gamma](x)$ ($\mathcal{L}_{\alpha,\beta}[\nu_d](x)$) is the probability, for a non-dormant cell with age x , to go dormant, awake and then divide (die). The physical meaning of functional $\mathcal{L}_{\alpha,\beta}$ allows to better understand what the effective death and division probabilities are. The coefficient of Eq. (5.30) a_2 and a_0 such that: $p(0) = a_2 p^2(0) + a_0$, can be expressed as:

$$a_0 = \sum_{k=0}^{\infty} \mathcal{L}_{\alpha,\beta}^k[\nu_d](0), \quad (5.32)$$

$$a_2 = \sum_{k=0}^{\infty} \mathcal{L}_{\alpha,\beta}^k[\nu_\gamma](0). \quad (5.33)$$

where each term $\mathcal{L}_{\alpha,\beta}^k(\nu_d)(0)$ (and $\mathcal{L}_{\alpha,\beta}^k(\nu_\gamma)(0)$) is the probability for a cell with age $x = 0$ to going and dormant and awake for k -times straits and then die (divide). It must be noted that the awakening rate is a crucial quantity in the analysis of inheritance.

5.3 Interrupted Drug Treatments

The majority of tumour treatments can not be administered for long times, therefore periodic treatments were developed to administer drug doses at different interval times. For periodic treatment, a significant query regards the underlying reasons triggering the phenotypic switching (dormancy). The standard view is that the dormant state is a survival strategy adopted by cells when the drug is active. However, it is still not clear how cells decide to go dormant, therefore, in this study, we explored three different cases of activation of the awakening-dormancy cycle.

Before this exploration, I would like to thank J. Pausch for implementing the algorithm to obtain numerical solutions depicted in Figs. 5.6, 5.7 and 5.8

and elaborating the rate choice.

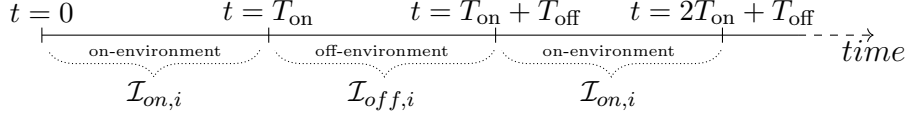


Figure 5.5: Schematic representation of alternated drug treatments. The division rate functions $\gamma(x)$ is uninterrupted during the whole process. The death rate function $d(x)$ is not zero only for $t \in [n(T_{\text{on}} + T_{\text{off}}), (n+1)T_{\text{on}} + nT_{\text{off}}]$ with $n \in \mathbb{N}$. The dormancy and awakening processes have rates function: $c_{1,2}^{\text{on}}$ and $c_{2,1}^{\text{on}}$ in the on-environments and $c_{1,2}^{\text{off}}$ and $c_{2,1}^{\text{off}}$ in off-environments

The framework is based on the age-structured generalisation of the Galton-Watson process (Sec. 2.5, similarly to Sec. 2.59). Let us consider the generating functionals (offspring distributions) of a cell with age x_0 after an on- or off-environment (starting at time 0 and ending at $T_{\text{on/off}}$): $\mathcal{Z}_{\text{on}}[h, T_{\text{on}} | \delta_{x_0}] := \int \mathcal{D}[n] \exp(\int_0^\infty dx \ln(h(x))n(x)) \mathcal{P}[n, T_{\text{on}} | \delta_{x_0}]$ and similarly $\mathcal{Z}_{\text{off}}[h, T_{\text{off}} | \delta_{x_0}]$. It follows that the generating functional of offspring after each period $t = T_{\text{off}} + T_{\text{on}}$ can be written as:

$$\mathcal{Z}_{\text{on}}[\mathcal{Z}_{\text{off}}[h, T_{\text{off}} | \delta_\bullet], T_{\text{on}} | \delta_{x_0}], \quad (5.34)$$

where \bullet is a placeholder for the function argument. Since the environments are periodic, offspring distributions are invariant across environments after one period. This means that the survival probability $p_{\text{surv}}(x_0)$, starting from a single cell with age x_0 , satisfy the embedded Galton-Watson chain fixed point:

$$1 - p_{\text{surv}}(x_0) = \mathcal{Z}_{\text{on}}[\mathcal{Z}_{\text{off}}[1 - p_{\text{surv}}, T_{\text{on}} | \delta_\bullet], T_{\text{off}} | \delta_{x_0}]. \quad (5.35)$$

. This last equation with Eq. (5.17) can be expressed a system of two integral equations. Another way recall Eq. (5.35) begins considering the time-dependent version of Eq. (5.18). In this case, the rates are age x and time t dependent ($\gamma(x, t)$, $d(x, t)$, $c_{1,2}(x, t)$ and $c_{2,1}(x, t)$), so that the generating function can be

expressed as:

$$\begin{aligned}
\mathcal{Z}[h_1, h_2, t | \delta_x, 0, 0] \hat{\Pi}(x) = & \hat{\Pi}(t+x) \hat{h}_1(x+t) \\
& + \int_0^t \hat{\Pi}_{c_{1,2}}(u+x) \hat{\pi}_{c_{1,2}}(t-u) h_2(t-u) du \\
& + \int_0^t \hat{\Pi}_\gamma(u+x) \mathcal{Z}^2[h_1, h_2, t-u | \delta_0, 0, 0] du \\
& + \int_0^t \hat{\Pi}_c(u+x) \int_0^{t-u} \hat{\pi}_{c_{2,1}} \mathcal{Z}[h_1, h_2, t-y | \delta_0, 0, 0] dy du \\
& + \int_0^t \hat{\Pi}_\gamma(u+x) du,
\end{aligned} \tag{5.36}$$

where the survival probability for a non-dormant cell is defined as:

$$\hat{\Pi}(x, t) = e^{-\int_0^t (\gamma(u+x, u) + d(u+x, u) + c_{1,2}(u+x, u)) du} \tag{5.37}$$

and the reaction times probabilities are defined as: $\hat{\Pi}_\gamma(x, t) \gamma(t+x, t) = \hat{\Pi}_d(x, t) d(t+x, t) = \Pi(t, x)$. In this framework, we considered the following rate functions: $\gamma(x, t) = \gamma(x)$, $d(x, t) = \delta_{on}(t) d(x)$, $c_{1,2}(x, t) = \delta_{off}(t) c_{1,2}^{off}(x) + \delta_{on}(t) c_{1,2}^{on}(x)$ and $c_{2,1}(x, t) = \delta_{off}(t) c_{2,1}^{off}(x) + \delta_{on}(t) c_{2,1}^{on}(x)$ where the notation is intuitive. Plugging these rates in Eq. (5.36), we obtained a system of two integral Volterra's equations, the same encoded in Eq. (5.35).

In the following, three different types of time-dependence for the rates are considered: three different configurations of the death, dormancy and awakening rates for the on-environment ($\{\mathcal{I}_{on,i} = (\gamma(x), 0, c_{1,2}^{on,i}, c_{2,1}^{on,i})\}$) and for the off-environment $\{\mathcal{I}_{off,i} = (\gamma(x), d(x), c_{1,2}^{off,i}, c_{2,1}^{off,i})\}$. Let us first consider the case where each cell can go dormant or awake regardless of the environment (S1 .i.e. strategy 1):

$$\mathcal{I}_{on,1} = \{\gamma(x), d(x), c_{1,2}(x), c_{2,1} = 0\}, \tag{5.38}$$

$$\mathcal{I}_{off,1} = \{\gamma(x), d(x) = 0, c_{1,2}(x), c_{2,1}(x)\}. \tag{5.39}$$

For this configuration, the dynamics is encoded in a coupled system of Volterra's

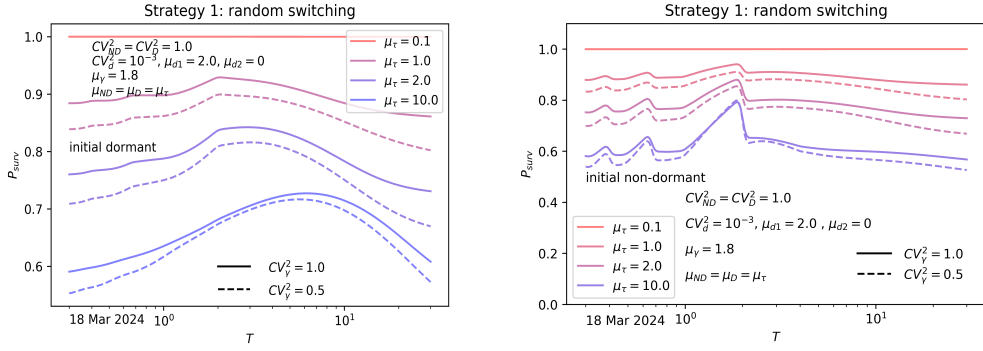


Figure 5.6: **Strategy 1: switching irrespective of environment.** (a) The survival probability is non-monotonic even for an initial dormant cell. ($\mu_\gamma = 1.8, \mu_d = 2, \mu_{c_{1,2}} = \mu_{c_{2,1}}, CV_d^2 = 10^{-3}$ and $CV_{c_{1,2}}^2 = CV_{c_{2,1}}^2 = 1$) (b) Survival resonances are present and smoothed out by the effects of dormancy. Here, the initial cell was assumed to be non-dormant.

equations, one for the on-environment:

$$\begin{aligned} \mathcal{Z}_{\text{on}}[h, t | \delta_{x_0}] \Pi(x_0) &= \int_0^t du \Pi_d(u + x_0) \\ &\quad + \int_0^t du \Pi_\gamma(u + x_0) \mathcal{Z}_{\text{on}}^2[h, t - u | \delta_0] \\ &\quad + \int_0^t \Pi_c(u + x_0) \int_0^{t-u} \pi_{c_{2,1}} \mathcal{Z}_{\text{on}}[h_1, h_2, t - y | \delta_0, 0, 0] dy du, \end{aligned} \quad (5.40)$$

and one for the off-environment:

$$\begin{aligned} \mathcal{Z}_{\text{off}}[h, t | \delta_{x_0}] &= \int_0^t du \Pi_\gamma(u + x) \mathcal{Z}_{\text{on}}^2[h, t - u | \delta_0] + \\ &\quad + \int_0^t \Pi_c(u + x) \int_0^{t-u} \pi_{c_{2,1}} \mathcal{Z}_{\text{on}}[h_1, h_2, t - y | \delta_0, 0, 0] dy du. \end{aligned} \quad (5.41)$$

Far from critical configurations, S1 enhances the survival probability (Fig. 5.6), as in the homogeneous case. We acknowledged the presence of a non-monotonic behaviour of p_{surv} in presence of dormancy (Fig. 5.6 (a)) and the enhancement of p_{surv} caused by the fluctuations in division times. It must be noted that the survival resonances are still present for certain values of $\mu_{c_{1,2}}$ but they can also be annihilated by the presence of dormancy (see Fig. 5.6 (b), for $(\mu_{c_{1,2}} \ll \mu_d, \mu_\gamma)$, no resonances is detectable).

The attention is now switched to a second strategy (S2) where the awakening and dormancy rates are not age-dependent ($CV_{c_{1,2}}^2 = CV_{c_{2,1}}^2 = 1$). S2 allows dormant cells to go dormant (awake) with rates $c_{1,2}$ ($\frac{1}{c_{2,1}}$) in on-environments and $\frac{1}{c_{1,2}}$ ($c_{2,1}$) in off-environments. This choice was made to reproduce a possible process where the drug effects trigger the dormant state and reduce the

awakening, while the inverse behaviour characterises the off-environments that push cells towards dormancy:

$$\mathcal{I}_{on,2} = \{\gamma(x), d(x), c_{1,2}, 1/c_{2,1}\}, \quad (5.42)$$

$$\mathcal{I}_{off,2} = \{\gamma(x), d(x) = 0, 1/c_{1,2}, c_{2,1}\}. \quad (5.43)$$

The dynamics are still encoded in a system of Volterra's equations:

$$\begin{aligned} \mathcal{Z}_{on}[h, t|\delta_{x_0}] \Pi(x_0) &= \int_0^t du \Pi_d(u + x_0) \\ &\quad + \int_0^t du \Pi_\gamma(u + x_0) \mathcal{Z}_{on}^2[h, t - u|\delta_0] \\ &\quad + \frac{c_{1,2}}{c_{2,1}} \int_0^t \Pi(u + x_0) \int_0^{t-u} \pi \mathcal{Z}_{on}[h_1, h_2, t - y|\delta_0, 0, 0] dy du \end{aligned} \quad (5.44)$$

and:

$$\begin{aligned} \mathcal{Z}_{off}[h, t|\delta_{x_0}] &= \int_0^t du \Pi_\gamma(u + x) \mathcal{Z}_{on}^2[h, t - u|\delta_0] + \\ &\quad + \frac{c_{2,1}}{c_{1,2}} \int_0^t \Pi(u + x) \int_0^{t-u} \pi(y) \mathcal{Z}_{on}[h_1, h_2, t - y|\delta_0, 0, 0] dy du. \end{aligned} \quad (5.45)$$

Survival resonances are still present with strategy two, however, I would like to focus the attention on a different phenomenon observed in this case. S2 allows to observe a new phenomenon where the survival probability drops down in a limited range of the environment length, Fig. 5.7. From an inverted standpoint, this phenomenon is an *extinction resonance* inducing a peaked behaviour of the survival probability. Extinction resonances are still to be characterised and studied, we do not provide any conclusive observations of this phenomenon. However, it may be observed that death is deterministic so the reasons behind it is a different dynamics for the first generation of cells.

In conclusion, a third strategy (S3) is considered: non-dormant cells switch more frequently during treatment to dormancy and dormant cells switch back more frequently when the treatment is absent:

$$\mathcal{I}_{on,3} = \{\gamma(x), d(x), c_{1,2}(x), 1/c_{2,1}\}, \quad (5.46)$$

$$\mathcal{I}_{off,3} = \{\gamma(x), d(x) = 0, 1/c_{1,2}(x), c_{2,1}\}. \quad (5.47)$$

Fig. 5.8 displays noise-induced resonances for different initial conditions: dor-

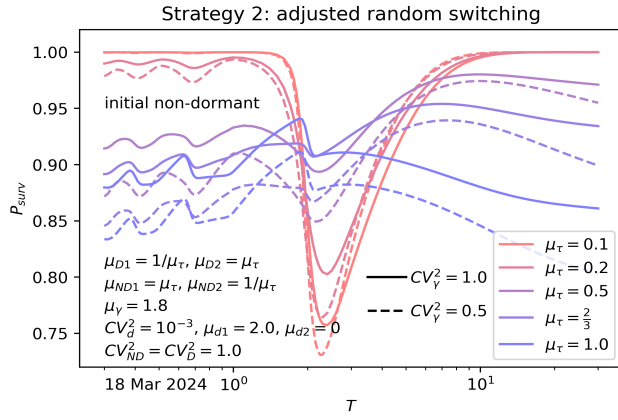


Figure 5.7: **Strategy 2: the inverse tendency for awakening and dormancy** Survival resonances vanish for small dormancy mean times, leading to a drop in the survival probability. $\mu_\gamma = 1.8, \mu_d = 2, \mu_{c_{1,2}} = \mu_{c_{2,1}}, CV_d^2 = 10^{-3}$ and $CV_{c_{1,2}}^2 = CV_{c_{2,1}}^2 = 1$.

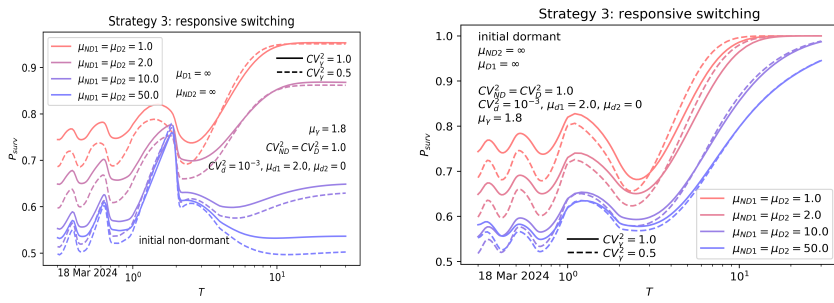


Figure 5.8: **Strategy 3: inverted dormancy and awakening** Noise-induced resonances are still displayed despite the introduction of S2 (Left and Right). S2 reduce the survival probability for almost all the environments lengths ($T_1 = T_2 = T$). The survival resonance for initial condition $\delta_0\delta_2$ (Left) are smoothed out (compared to initial condition $\delta_0\delta_1$, (Right) due to the delay induced by the awakening process. The distributions for the events times are the same in Fig. 4.6.

mant or non-dormant newborn cells. The resonances are still present and, in contrast to continuous treatment, a different initial species influences the survival probability. This is induced by the stochastic time delay for a cell before going non-dormant and being able to divide or die (if the drug is on).

A further and broader analysis of these (and others) configurations is required. The dormancy seems to have a potentially negative and positive effect on the survival probability. Noise induced resonances can be detected for any configuration and can be influenced by the delay in the awakening process.

5.3.1 Survival Resonances and Dormancy

Survival resonance still appears despite dormancy, both deterministic and noise-induced for all of three strategies (S1, S2 and S3). Due to limited time, we proposed just an initial approach to quantify resonances in the dormancy-division-death process. Let us focus on noise-induced resonances since it allows to exploit the first-cell property (see Subsec. 4.4.2): the final survival probability can be approximated as the survival probability of the first cell. As in absence of dormancy, the peaks in p_{surv} appear for specific combinations of μ_d and $T_{\text{on},\text{off}}$ with only small fluctuations in death times. The resonances still emerge as a consequence of the death, dormancy division probability of the first cell. Assuming that death is deterministic ($CV_d^2 \rightarrow 0$) with putative death time $\tau_d \approx \mu_d$ and that the cell was born at time $t = 0$ at the start of the first on-environment, two regimes can be identified. If τ_d falls in an on-environment, the death probability is the product of the probability w_d that death would occur at time τ_d times the probability that the cell does not divide or goes dormant before τ_d , $\phi_{c_{1,2},\gamma}(\tau_d) = e^{-\int_0^{\tau_d} du(c_{1,2} + \gamma(u))}$. If τ_d falls in an off-environment, the cell either dies at the next on-environment ($w_d = 1$) or never ($w_d < 1$) due the zero death rate at old ages. The same argument can be also proposed for the dormancy effective probability. In fact, if μ_d falls in an on environment, the dormancy probability is the product $w_{c_{1,2}}$ that the cell will go dormant, times the probability that cell go dormant in the interval $[0, \tau_d]$: $\Lambda(\tau) = e^{-\int_0^{\tau_d} \gamma(u)du} P(\tau_{c_{1,2}} < \tau_d)$. This considerations lead to the effective death, dormancy and persistence probability

of the first cell:

$$\begin{aligned}\nu_d &\approx \mathbb{E} \left[1_{\text{on}}(\tau_d) w_d \phi_{c_{1,2},\gamma}(\tau_d) + 1_{\text{off}}(\tau_d) \delta_{w_d,1} \phi_{c_{1,2},\gamma} \left(\left\lfloor \frac{\tau_d}{P} + 1 \right\rfloor P \right) \right], \\ \nu_{c_{1,2}} &\approx \mathbb{E} \left[1_{\text{on}}(\tau_d) w_{c_{1,2}} \Lambda(\tau_d) + 1_{\text{off}}(\tau_d) \delta_{w_{c_{1,2}},1} \Lambda \left(\left\lfloor \frac{\tau_d}{P} + 1 \right\rfloor P \right) \right], \\ \nu_\emptyset &\approx (1 - w_\gamma) \mathbb{E} [1_{\text{on}}(\tau_d)(1 - w_d) + 1_{\text{off}}(\tau_d)(1 - \delta_{w_d,1})].\end{aligned}\quad (5.48)$$

where $\delta_{w_d,1}$ is the Kronecker- δ , $\mathbf{1}_{\text{off/on}}(\tau_d)$ is 1 if τ_d falls into an off/on environment and zero otherwise and the average is over the distribution of death. Similarly to Sec. 4.3, the cells of later generations approximately have the same death probability as the first cell. Therefore, we used Eq. (5.48) in the solution of the survival probability in constant environments Eq. (5.26). These approximations, strictly valid only for constant environments, predict resonances at the following environment lengths:

$$\{T_{\text{on/off}} : \mu_d = T_{\text{on}} + nP, n \in \mathbb{N}\}, \quad (5.49)$$

which reproduce all the noise-induced resonances seen in the simulations and numeric solutions. The extinction probability for the first generation (i.e. the first cell born at $t = 0$) can also be directly calculated:

$$p_{\text{ext}}^I(\mu_d) = 1_{\text{on}}(\mu_d) w_d \phi_{c_{1,2},\gamma}(\mu_d) + 1_{\text{off}}(\mu_d) \delta_{w_d,1} \phi_{c_{1,2},\gamma} \left(\left\lfloor \frac{\mu_d}{P} + 1 \right\rfloor P \right). \quad (5.50)$$

Other quantities can be extracted following this path as shown in Sec. 4.3 and similar conclusions regarding the approximated analytics of the survival probability can be recalled.

5.4 Conclusions

A set of methods is presented in this chapter to model possible survival strategies adopted by cells to promote fractional killing. These methods are used to study an age-structured population where divisions, death and phenotype switching rates depend on the cell-cycle (age).

We observed fractional killing ($p_{\text{surv}} > 0$) in constant environments and quantified the effects induced by dormancy. Phenotype switching can promote either super-critical or sub-critical behaviour. To predict it, we proposed a theoretical model based on the effective event probability ν , with or without

persistence.

A further analysis should be pursued on the inheritance model (Sec. 5.2.3). The non-resetting of the age opens a completely different landscape where the survival probability can also be non-monotonic in the absence of time variations of the environment. In such a model, the awakening rate plays a crucial role due to the variations on the age when going dormant (α) and awakening (β). Further observations are presented in App. 5.2.3.

The study of time-dependent treatments leads, once again, to survival resonances. The dormancy effects do not crack the main conclusions drawn in Sec. 4.3 about deterministic and noise-induced resonances. Moreover, it is also possible to show that the heights of noise-induced jumps with dormancy, might behave as stochastic resonance, with a specific noise value at which the height is maximised.

This work is an intermediate stage and further work is required. Further details on the topic are presented in Sec. 7.

Chapter 6

Preliminary Study of an Age-Structured SIS Model

Abstract

The dynamics of epidemics are usually studied via a class of models called compartmental models. Here, we consider the compartmental Susceptible-Infected-Susceptible (S.I.S.) model, where each compartment is age-structured. I urge the reader to consider that this work is still in a primordial phase and that few applications of the theoretical framework have been proposed. This chapter aims to showcase the flexibility of the age-structured theory (Ch. 2) for a model not belonging to the class of branching processes. Apart from Sec. 6.1, each section displays results developed by P. Thomas and myself.

Epidemic models aim to forecast the spread of infectious diseases. The development of these models started in the 18th Century (Sec. 1.1.2) and accelerated during the 20th century. Two milestones should be remembered: at the beginning of the last century, William Hamer [159] and Ronald Ross [160] proposed a founding work in which they exploited the law of mass action to model epidemic behaviour. Later, the first compartmental models with susceptible, infected and recovered species were implemented by Kermack, McKendrick [161, 162], Reed and Frost [163].

In general, the interaction between individuals required by the spread of disease does not belong to the class of branching processes since the trajectory of each individual is not independent of the other [35, 75, 120, 164]. Nevertheless, the theory presented in Ch. 2 can still be exploited to study the evolution of interacting processes.

In the following sections, I recall the main deterministic results regarding

Susceptible-Infected-Susceptible Models (S.I.S.) and propose a few possible research directions to study their stochastic dynamics. The framework of the SIS compartmental model accounts for two species: the agents who have been *infected* and the ones who are *susceptible* to the disease. Specifically, each infected agent can recover from the disease and convert to susceptible (recovery process), and each infected-susceptible couple can convert to two infected (infection process). Despite their simple structure, SIS models have turned out to be a simple but effective way to understand the spread of epidemics in different scenarios, for instance as HIV [165], Malaria [166] and COVID19 [167].

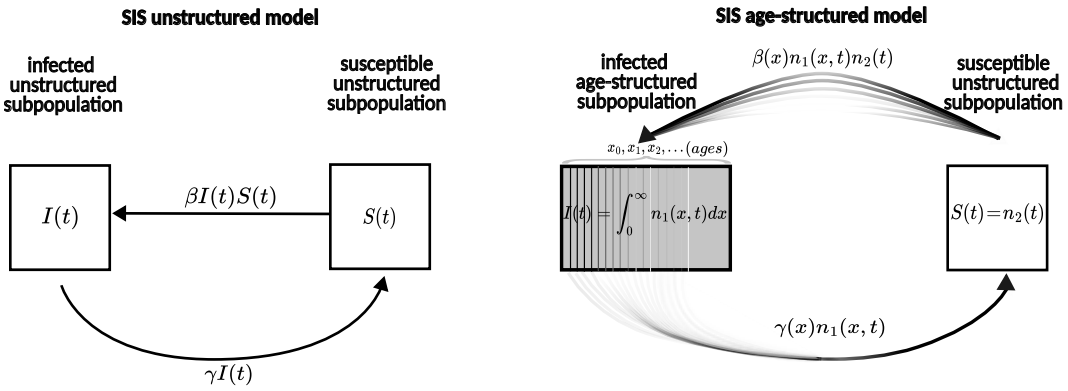


Figure 6.1: **Comparison between unstructured and age-structured Susceptible-Infected-Susceptible models.** Standard representation of the SIS unstructured dynamics [20] (left). Interpretation of the age-structured SIS dynamics where the susceptible species remains unstructured and the age-spectrum is introduced for the infected agents (right). The rate functions are paradigmatic features of age-structure, as if an infinite multi-species was accounted.

6.1 Deterministic SIS Model

The original deterministic formulation of the SIS was unstructured, and it is due to Ross in 1916 [168]. Ross's work displays the spread of an epidemic in a population of N individuals in the absence of age heterogeneity. The population can be divided into two subpopulations: infected (abundance labelled with $I(t)$) and susceptible (abundance labelled with $S(t)$). Each infected agent can recover with a constant rate γ , and each coupled infected-susceptible may turn into two infected with the constant rate β (see Fig.6.1, left), so that:

$$\frac{dI(t)}{dt} = -\gamma I(t) + \beta I(t)S(t) \quad (6.1)$$

$$S(t) = N - I(t)$$

The latter equation can be manipulated to obtain a first-order ODE for the total number of infected whose asymptotic solution ($I^* = I(t)_{t \rightarrow \infty}$) is given by:

$$I^* = \begin{cases} 0 & \text{if } R_0 = \frac{N\beta}{\gamma} \leq 1 \\ N\left(1 - \frac{1}{R_0}\right) & \text{if } R_0 = \frac{N\beta}{\gamma} > 1 \end{cases} \quad (6.2)$$

where R_0 labels the basic reproduction number [20] and, due to the close nature of the system ($S(t) = N - I(t)$), the number of susceptible agents also follows. An exact (not asymptotic) analytical solution can also be found via the map $I(t) = \frac{1}{Y(t)}$ in Eq.(6.1). For $R_0 \leq 1$, we still observe the system escaping the infection as a whole, while if $R_0 > 1$, the number of infected grows as:

$$I(t) = \frac{I^*}{1 + Ae^{-(N\beta - \gamma)t}} \quad (6.3)$$

where $A = \frac{I^*}{I_{t=0}} - 1$. Eq. (6.3) is a logistic function which reflects the asymptotizing value of $I(t)$ to I^* (due to the close nature of the system) and shows the non-exponential behaviour due to second order propensity of the infection process. Further properties of the SIS model can also be recalled from the age-structured generalization assuming constant rates, which is introduced in the upcoming paragraphs.

The first appearance of a deterministic age-structured SIS model was proposed by A. G. McKendrick and W. O. Kermack in 1927 [161, 162]. This model formally describes the deterministic evolution of an SIS model where the ages of the infected agents influence the recovery and infection process (see Fig.6.1, right). The framework consists of an *age-structured* population made by two species: *age-structured* infected (labelled with the index ₁) and *unstructured* susceptible (labelled with the index ₂, see Fig.6.1). The infected species exhibits an age x while the variability of susceptible elements is neglected. In this context, x does not represent exactly the *age* but it usually defines the *incubation time* which is the time past since the infection happened; therefore, the second species does not exhibit any age variability.

The whole evolution is driven by two reactions: the infected individuals might recover and return susceptible with a rate function γ_1 , and each couple of susceptible-infected elements might convert to a new infected element with age $x = 0$ coupled with the original infected.

The abundances of infected x -aged agents $n_1(x, t)$ and the number of susceptible

individuals $n_2(t)$ evolve as described by the following differential equations:

$$(\partial_t + \partial_x)n_1(x, t) = -\gamma_1(x)n_1(x, t), \quad (6.4)$$

$$\frac{dn_2(t)}{dt} = \int_0^\infty \gamma_1(x)n_1(x, t)dx - n_2(t) \int_0^\infty \gamma_2(x)n_1(x, t)dx, \quad (6.5)$$

respectively coupled with the initial conditions:

$$\begin{aligned} n_1(x, 0) &= \Psi(x), \\ n_1(0, t) &= \int_0^\infty \gamma_2(x)n_2n_1(x, t)dx, \\ n_2(0) &= n_{2,0}, \end{aligned} \quad (6.6)$$

The function Ψ labels the initial age distribution of the infected individuals, and $n_{2,0}$ is the initial number of agents of the second species. The total number of individuals (infected and susceptible) remains constant during the evolution. In fact, the evolution of the total number of infected can be derived from (6.4) integrating over the age:

$$\underbrace{\frac{d}{dt} \left(\int_0^\infty n_1(x, t)dx \right)}_{\text{total number of infected}} = n_1(0, t) - \int_0^\infty \gamma_1(x)n_1(x, t)dx \quad (6.7)$$

and it can be shown that Eq.(6.7) is exactly equal to $-\frac{dn_2(t)}{dt}$ (Eq.(6.5)) so that:

$$\frac{d(\int_0^\infty n_1(x, t)dx + n_2(t))}{dt} = 0.$$

The PDEs expressed in Eqs. (6.4) and (6.5) do not allow an exact solution, but they can be manipulated to derive significant insights on the system. In the following, I derive some well-known results for the age-structured SIS models, which will turn out to be useful in the next sections. The derivation is based on Chapter V of *Population Dynamics in Demography and Epidemiology* [35]. The derivation begins by introducing a function $\nu(x, t)$ such that $\nu(x, t)N\Gamma(x) = n_1(x, t)$ where $\Gamma(x) = e^{-\int_0^x \gamma_2(u)du}$ is the probability for a newly infected individual not to recover. Mapping Eqs. (6.4) and (6.6) in terms of the function ν , we obtain:

$$(\partial_t + \partial_x)\nu(x, t) = 0, \quad (6.8)$$

$$\nu(0, t) = R_0 \left(1 - \int_0^\infty \Gamma(u)\nu(u, t)du \right) \int_0^\infty \phi(u)\nu(t, u)du, \quad (6.9)$$

where R_0 is the basic reproduction number and $\phi(x)$ labels the probability distribution of the occurrence of secondary infections:

$$R_0 = N \int_0^\infty \gamma_1(u) \Gamma(u) du, \quad (6.10)$$

$$\phi(x) = \frac{\gamma_1(x) \Gamma(x)}{\int_0^\infty \gamma_1(u) \Gamma(u) du}. \quad (6.11)$$

Now, an equilibrium solution $\nu(x) = \nu^*$ is assumed to be reached by the system in the asymptotic limit. In the equilibrium state, Eq. (6.12) becomes:

$$\nu^* = \nu(0, t) = R_0 \left(1 - \nu^* \int_0^\infty \Gamma(u) du\right) \nu^* \int_0^\infty \phi(u) du, \quad (6.12)$$

$$1 = R_0 \left(1 - \nu^* \int_0^\infty \Gamma(u) du\right) \quad (6.13)$$

Therefore, the steady state can be explicitly quantified as $\nu^* = \frac{1}{\int_0^\infty \Gamma(u) du} \left(1 - \frac{1}{R_0}\right)$.

Considering small perturbation around the steady state, Eq. (6.12) can be linearized around $\nu^* = 0$:

$$(\partial_t + \partial_z) \nu(t, x) = 0, \quad (6.14)$$

$$\nu(0, t) = R_0 \int_0^\infty \phi(u) \nu(t, u) du. \quad (6.15)$$

Hence, an Euler-Lotka Equation for the growth rate λ is derived for exponential behaviour of ν :

$$R_0 = \int_0^\infty \phi(u) e^{-\lambda u} du. \quad (6.16)$$

If $R_0 > 1$, then $\nu^* > 0$ and Eq. (6.12) can be linearized as $u(x, t) = \nu(x, t) - \nu^*$

$$(\partial_t + \partial_z) u(t, x) = 0, \quad (6.17)$$

$$u(0, t) = \int_0^\infty \phi(u) u(t, u) du - \frac{R_0 - 1}{\int_0^\infty \Gamma(u) du} \int_0^\infty \Gamma(x) u(x, t) dx, \quad (6.18)$$

from which the Euler Lotka Equation is given by:

$$\int_0^\infty \phi(x) e^{-\lambda x} - \frac{R_0 - 1}{\int_0^\infty \Gamma(u) du} \int \Gamma(x) e^{-\lambda x} dx = 1. \quad (6.19)$$

It can be shown [102] that, for small increments in the average number of infection ($R_0 + \varepsilon$) the real roots (for the growth rate λ) are negative for sufficiently

small ε . In other words, if $R_0 < 1$, the asymptotic steady state uniquely exists and is globally asymptotically stable, while if $R_0 > 1$, the steady state is unstable, and a unique endemic steady state exists. The endemic steady state is locally asymptotically stable if $R_0 > 1$ and $|R_0 - 1|$ is sufficiently small [102]. This implies that the mechanism of infection-age dependency could explain the phenomenon of recurrent outbreaks. Indeed, sustained oscillations can be observed in the chronic-age-structured SIS model [35]. If R_0 becomes much larger than unity, it has been shown that the endemic steady state can lose its stability. A conjugate pair of complex characteristic roots then cross the imaginary axis into the right half plane with a positive speed, and a periodic solution bifurcates [20, 35, 102]. This type of bifurcation is often observed for epidemics with very long incubation periods. This implies that the mechanism of infection-age dependency could explain the phenomenon of recurrent outbreaks. Indeed, sustained oscillations can be observed in the chronic-age-structured SIS model [35].

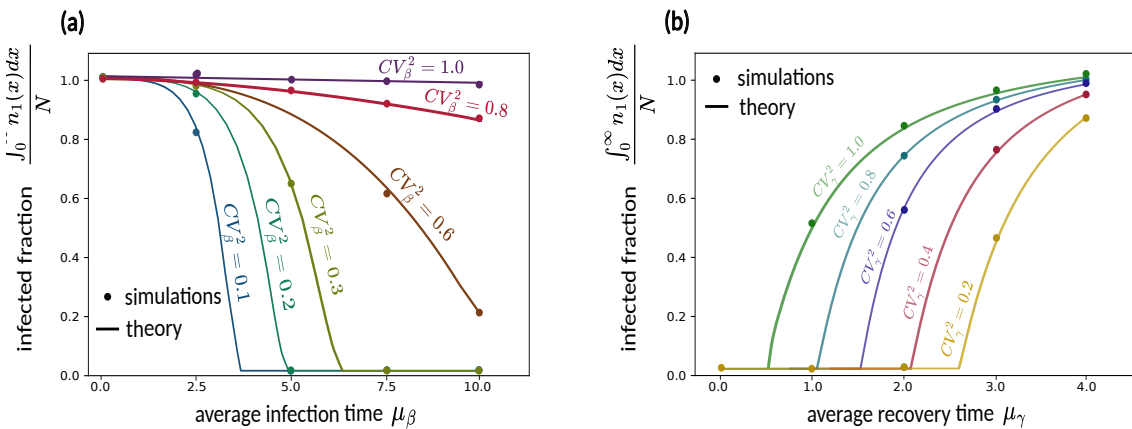


Figure 6.2: Age-induced fluctuations affect the epidemic asymptotic state. (a): The transition between the absence of infected agents and partial infection is shifted due to fluctuations in infection times. (b): The noise in the recovery times favours the endemic process. The infection and recovery times follow a Γ -distribution with parameters: $\mu_\gamma = 0.5$, $CV_\gamma^2 = 0.5$ and $N = 1000$ (a). $\mu_\beta = 10$, $CV_\beta^2 = 0.5$ and $N = 1000$ (b).

Despite the lack of an exact solution for the infected abundances $n_1(x, t)$, significant insights on the role of age-induced fluctuations can be derived, Fig. 6.2. A direct observation of the role of age-heterogeneity on the fate of an epidemic process is displayed in Fig. 6.2. In general, especially for large populations, the infection process is amplified by the non-linear propensities of the infection process; therefore, the average infection times μ_β can be greater than μ_γ and still the number of infected can collapse to zero. It can also be observed that the reduction of the fluctuation in the infection and recovery times from the

unstructured case $CV_{\beta}^2 = 1$ (Fig.6.2.(a)) or $CV_{\gamma}^2 = 1$ (Fig.6.2.(b)), highlights the age-induced effects on the epidemic spread. In fact, the transition between a partial infection ($\lim_{t \rightarrow \infty} \int_0^\infty n_1(x, t) dx > 0$) and a resolute scenario ($\lim_{t \rightarrow \infty} \int_0^\infty n_1(x, t) dx = 0$) is influenced by the age-induced noise in the recovery and infection times (Fig.6.2). Fig.6.2.(a) shows how the fluctuations in the infection times are empowered by the number of couples infected-susceptible, leading to an endemic state. On the contrary, Fig.6.2.(b) portrays the role played by noise in the recovery process and its relationship with the transition between partial and total recovery of the population.

Before introducing the aforementioned set of methods to study the stochastic evolution of the SIS, a few words also need to be spent on the simulations framework developed. Adopting an object-oriented approach, two agent classes were defined: infected and susceptible (Fig.6.3). Each infected agent is provided with an age and a recovery time, while each susceptible exhibits a set of possible infection times whose cardinality is equal to the number of infected agents (Fig.6.3.(a) initialization). Then, the minimum recovery times (overall, the infected agents) are sampled, and the minimum infection time is selected from a pool of possible infection times as large as the couples of infected-susceptible in the populations. After infection, a susceptible agent turns into an infection one with age $x = 0$, and the infection time list (susceptible agent attribute) is updated. After a recovery, instead, infected agents turn into susceptible ones and the new list of possible infection times is initialized while the infection time list of the other susceptible is updated. Regarding the sampling method used for the recovery and infection times, this last paragraph focuses on the relation between the system size and the fluctuations from the deterministic results. Fig.6.3.(b) displays the rejection-acceptance principle of the Thinning sampling method discussed in Ch.3. Despite the availability of different packages to sample random variables (for instance, Γ -distributed), the model requires to sample infection or recovery times for agents with age is not zero, which forced us to a sample from a rate function whose argument is translated (Fig.6.3.(b), right). In this context, the Thinning methods stands as a valuable tool which allows to sample from a Non-Homogeneous Poisson process independently on the initial age. In addition, we can observe that the fluctuation from the deterministic results clearly decreases with a higher number of individuals (which reduces the correlation between individuals), and smaller fluctuations in the infection and

recovery time promote dynamics closer to the deterministic picture, Fig.6.3.(c).

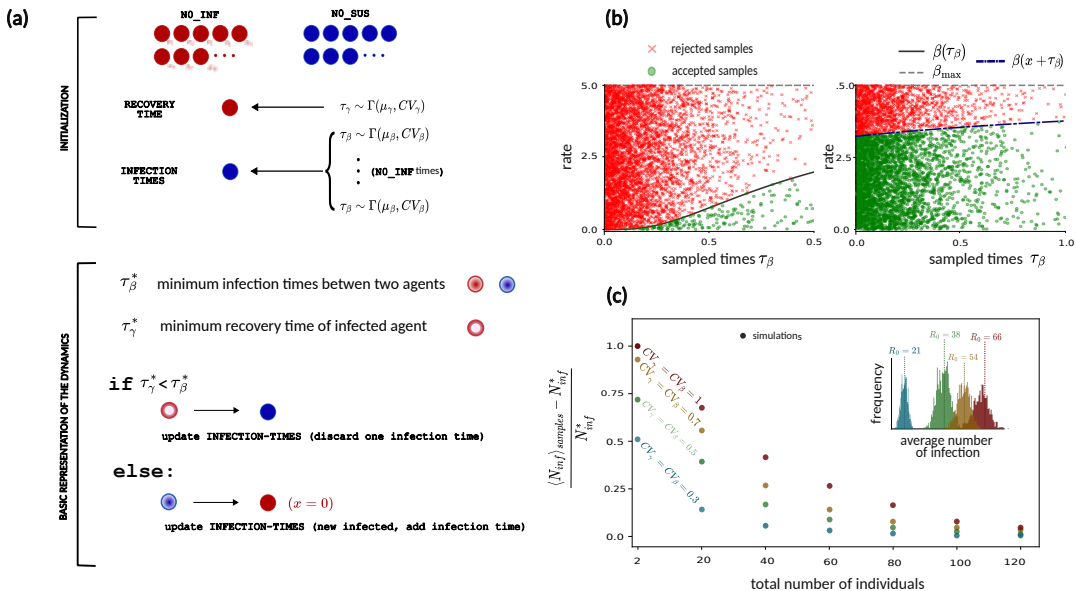
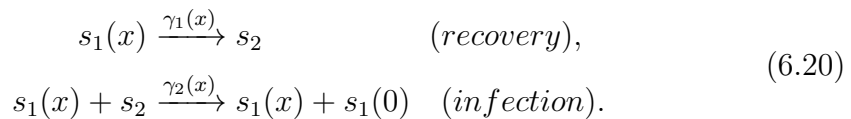


Figure 6.3: Simulations framework, time sampling and system size. (a): Framework of the simulations algorithm. The initialization panel sketches the different attributes of the susceptible and infected agent classes. The dynamics panel show how the increments in time are implemented. (b): The thinning method is a rejection-acceptance Monte Carlo method. Its utility is proven to sample infection times for agents with age different from zero. The sample times are Γ -distributed with $\mu_\beta = 2$. (c): The efficiency of the deterministic framework increases with smaller fluctuations. The fluctuations are also reduced by the total number of individuals. The simulations also allow the sample of the average infection number R_0 (insert panel (c)). The scattered points were sampled with infection and recovery time, which are Γ -distributed with means: $\mu_\gamma = 1$ and $\mu_\beta = 3$.

6.2 Stochastic SIS Model

Here, I consider a few results of Ch. 2 as potential candidates to study the model. First of all, the reaction network for an SIS model can be expressed as follows:



Moreover, the infection stoichiometric functions are given by $\nu_1^-[x] = \delta_{i,1}\delta_x$ and $\nu_1^+[x] = \delta_{i,2}$. Instead the recovering process can be encoded in: $\nu_1^-[x] = \delta_{i,1}\delta_x$ and $\nu_1^+[x] = \delta_{i,2}$.

Moreover, the *age-structured* Chapman-Kolmogorov differential Equations can be obtained:

$$\begin{aligned}\mathcal{D}_t \mathcal{P}[n, t] &= \int_0^\infty \gamma_1(x)(\varepsilon_1^{-1}(0)\varepsilon_2^{+1} - 1)n_1(x)n_2 \mathcal{P}[n, t] dx + \\ &\quad + \int_0^\infty \gamma_2(x)(\varepsilon_1^{+1}(x)\varepsilon_2^{-1} - 1)n_1(x) \mathcal{P}[n, t] dx,\end{aligned}\quad (6.21)$$

where the propensities of infection (γ_2) and recovery (γ_1) are not of the same order in n . The integral Backward Chapman-Kolmogorov Equation helps decompose the dynamics in the possible outcomes of the next closest time step; therefore, the functional probability $\mathcal{P}[n_1, n_2, t|m_1, m_2, 0]$ is equal to:

$$\begin{aligned}&\Pi_{n_1, n_2}(t)\delta_{[m_1, n_1^{+t}]} \delta_{[m_2, n_2^{+t}]} + \\ &+ \int_0^\infty (n_1(x) + 1) \int_0^t \gamma_1(x-u) \Pi_{n_1, n_2}(u) \mathcal{P}[n_1^{+u} - \delta_{x-u}, n_2 - 1, u|m, 0] du dx + \\ &+ \int_0^\infty (n_1(x) - \delta_x)(n_2 + 1) \int_0^t \gamma_2(x-u) \Pi_{n_1, n_2}(u) \mathcal{P}[n_1^{+u} - \delta_0, n_2 + 1, u|m, 0] du dx.\end{aligned}\quad (6.22)$$

As a final observation, I did not express the integral equation in terms of the generating functional \mathcal{Z} (as in Ch. 4 and 5). This decision relies on the fact that this is not a branching process, and the generating functional does not provide a representation as useful as the one for \mathcal{P} (Sec. 2.5).

Eq. (6.22) allows us to express the functional probability as a linear system of Volterra's equation. The following section accounts for potential ways to study these systems of integral equations.

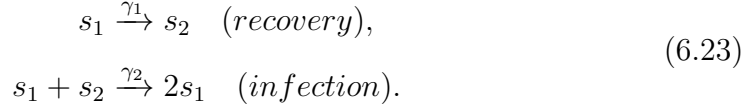
6.3 Linear Coupled Volterra's Equations

The stochastic dynamics of age-structured models can always be encoded in a (finite or infinite) system of linear equations for the state functional probability (Sec. 2.4). Here, I exploit the fact that the dynamics do not affect the total number of individuals. To be more clear, the total abundance conservation allows the encoding of the dynamics in a linear finite system of Volterra's equations. Here, I propose a few ideas on how this system of integral equations can be studied.

As an introduction, I first consider the *unstructured* SIS model, and then, I move to an *age-structured* generalisation.

6.3.1 Unstructured SIS as System of Renewal Equations

The *unstructured* formulation of the SIS reaction network can be obtained by neglecting the age-drifting process in Eq. (6.20):



Due to the independence from the age, Eq. (6.22) can be expressed as a system of renewal equation:

$$\begin{aligned} \mathcal{P}(n_1, n_2, t | m_1, m_2, 0) &= \Pi_{m_1, m_2}(t) \delta_{(n_1, m_1)} \delta_{(n_2, m_2)} + \\ &+ m_1 \gamma_1 (\Pi_{m_1, m_2} * \mathcal{P}(n_1, n_2 | m_1 - 1, m_2 + 1, 0))(t) \\ &+ \gamma_2 m_1 m_2 (\Pi_{m_1, m_2} * \mathcal{P}(n_1, n_2 | m_1 + 1, m_2 - 1, 0))(t), \end{aligned} \tag{6.24}$$

where the symbol $*$ labels the convolution product. Eq. (6.24) allows to cast the dynamics in a closed system of renewal equations because the total number of individuals is conserved:

$$m_1 + m_2 = n_1 + n_2. \tag{6.25}$$

Regardless of the initial conditions, the SIR dynamics can always be encoded in a system of renewal equations (Eq. (6.24)), and the system has a rank equal to $m_1 + m_2 + 1$.

Moreover, the Laplace Transform [169] of the probability returns

$$P(n_1, n_2, s | m_1, m_2, 0) = \int_0^\infty e^{-st} \hat{\mathcal{P}}(n_1, n_2, t | m_1, m_2, 0) dt, \tag{6.26}$$

so that the whole dynamics can be described by a linear system:

$$\mathbf{P}(s) = \mathbb{Q}\mathbf{P}(s) + \vec{b}(s). \tag{6.27}$$

To be clear, $(\mathbf{P}(s))_{m_1, m_2} = P(n_1, n_2, s | m_1, m_2, 0)$ and it evolves as Linear system where \mathbb{Q} is a $M \times M$ matrix and \vec{b} array of functions with M elements. This result is extremely compact and allows a fast computation. The introduction of age leads to a more complex scenario since the state composition is not encoded only in the number of individuals.

6.3.2 Age-Structured SIS Models Are not Renewal Processes

The introduction of the age structure leads to a functional generalisation of the unstructured case. The functional equation can now express the integral system (6.22):

$$P[n, t|m, 0] = \mathcal{B}[n, t, m] + (\mathcal{L}_+ + \mathcal{L}_-)[\mathcal{P}][n, t|m, 0], \quad (6.28)$$

where the variable n and m without lower or upper index are used to intend the tuple representation $n = (n_1, n_2)$ and $m = (m_1, m_2)$. The quantity labelled as \mathcal{B} is given by $\mathcal{B}[n, t|m, 0] = \Pi_{m_1, m_2}(t) \delta_{[n_1, m_1^{-t}]} \delta_{[n_2, m_2^{-t}]}$. and the operators \mathcal{L}_\pm are linear operators on \mathcal{P} defined as follows:

$$\begin{aligned} \mathcal{L}_-[\mathcal{P}][n, t|m, 0] &= \\ &= \int_0^\infty m_1(x) \int_0^t \Pi_{m_1, m_2}(y) \gamma_1(x+y) \mathcal{P}[n, t-y|m_1^{-y} - \delta_{x+y}, m_2 + 1], 0] dy dx, \end{aligned} \quad (6.29)$$

$$\begin{aligned} \mathcal{L}_+[\mathcal{P}][n, t|m, 0] &= \\ &= \int_0^\infty m_1(x) m_2 \int_0^t \Pi_{m_1, m_2}(y) \gamma_2(x+y) \mathcal{P}[n, t-y|m_1^{-y} + \delta_0, m_2 - 1, 0] dy dx \end{aligned} \quad (6.30)$$

In contrast to the unstructured case, the evolution cannot be expressed in terms of renewal equations, and the use of the Laplace Transform would not be useful for our purposes. This difference is induced by some kind of age inheritance in the infection process. In general, Eq. (2.46) can be turned into a renewal system only when the ages of the products do not depend on the ages of reactants.

Eq. (6.28) can still be suitable for the computational analysis. Let us cast the ageing process as discrete, i.e. as a jumping process with an age-threshold x_Q such that the age has to be $x(t) \leq x_Q$ for each individual. Under this assumption, the functional probability can be expressed as: $\mathcal{P} \in \mathbb{R}^{Q \times M \times M}$ so that the operators L_\pm are represented by a tensor of rank $Q \times M \times M \times Q \times M \times M$.

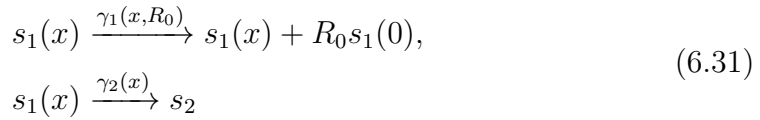
To conclude, the evolution of *age-structured* SIR models can always be represented with a system of integral equations. The main difference between the *unstructured* and the *age-structured* case regards the convolution property of

the system. Once the age is not neglected, the system of equations can not be written as a series of convolution products.

6.4 The Initial Spread

In Sec. 6.1, the basic reproduction number was introduced and labelled R_0 . This quantity is central to determining the evolution of an epidemic in real scenarios because it allows to model the system as a branching process. It substantially informs on the average number of new infected. Especially in the first stage of epidemics, the dynamics of disease spread can be modelled as a branching process. Here, I discuss the theoretical framework to approximate the stochastic dynamics of the SIS model on a mean-field level.

I assume a given randomicity for R_0 with distribution $\Phi(R_0)$. Therefore, if the infection process can approximated as a branching process, the reaction network is given by:



Comparing the above reaction network with the one proposed for the original *age-structured* SIS model (Eq. 6.20), the reader might object that such approximation might lead to unrealistic analysis due to the absence of interactions. Nevertheless, in an epidemic scenario, most of the efforts are into characterising the first phase of the spreading [20]. In the initial stage, the number of susceptible individuals is way greater than the number of infected individuals and the susceptible abundances might be approximated as constants (at least in this preliminary phase). Following from the reaction network proposed in Eq. (6.31), the Backward Chapman-Kolmogorov Equation allows to express the functional probability $\mathcal{P}[n, t|m, 0]$ as:

$$\begin{aligned} &\Pi_m(t)\delta_{[n, m-t]} \\ &+ \int_0^\infty m_1(x) \int_0^t \Pi_m(y) \gamma_1(x+y) \mathcal{P}[n, t-y|m_1^{+y} - \delta_{x+y}, m_2 + 1, 0] dy dx \\ &+ \int \Phi(R_0) \int_0^\infty m_1(x) \int_0^t \Pi_m(y) \gamma_2(x+y, R_0) \mathcal{P}[n, t-y|m_1^{+y} + R_0 \delta_0, m_2, 0] dy dx dR_0, \end{aligned} \tag{6.32}$$

where the functions Π_{m_1, m_2} can be expressed in a logarithmic scale as:

$$-\int_0^\infty m_1(x) \int_0^t \gamma_1(x+u) du dx - \int_0^\infty m_1(x) \int_0^t \int \Phi(R_0) \gamma_2(x+u, R_0) dR_0 du dx.$$

The quantity $\Phi(R_0)$ labels the probability of observing a reaction where one infected individual leads to the creation of R_0 newborn infected. Moreover, the generating functional can be exploited to obtain:

$$\begin{aligned} \mathcal{Z}[h, t | \delta_x, 0, 0] &= \Pi_{\delta_x, 0}(t) h_1(t+x) \\ &\quad + \int_0^t \Pi_{\delta_x, 0}(y) \gamma_1(x+y) \mathcal{Z}[h, t-y | 0, 1, 0] dy \\ &\quad + \int \Phi(R_0) \int_0^t \Pi_{\delta_x, 0}(y) \gamma_2(x+y, R_0) \mathcal{Z}[h, t-y | \delta_{x+y} + R_0 \delta_0, 0, 0] dy dR_0, \end{aligned} \tag{6.33}$$

which is a recursive equation of the generating functional $\mathcal{Z}[h_1, h_2, t | \delta_0, 0, 0]$ which is given by:

$$\begin{aligned} &\Pi_{\delta_x, 0}(t) h_1(t+x) \\ &\quad + \int_0^t \Pi_{\delta_x, 0}(y) \gamma_1(x+y) \mathcal{Z}[h, t-y | 0, 1, 0] dy \\ &\quad + \int \Phi(R_0) \int_0^t \Pi_{\delta_x, 0}(y) \gamma_2(x+y, R_0) \mathcal{Z}[h, t-y | \delta_{x+y}, 0, 0] \mathcal{Z}^{R_0}[h, t-y | \delta_0, 0, 0] dy dR_0. \end{aligned} \tag{6.34}$$

The last equation is a generalisation of the division-death process and a similar method can be used to study this case. This results from an approximation where the number of susceptible is sufficiently higher than the number of infected.

6.5 Peaked Distributions of Recovery and Infection Times

Here, I propose a moment's derivation to quantify the fluctuations affecting the deterministic evolution of the SIS model. The Dynkin's Equation (2.51) for this

SIS model can be written as:

$$\begin{aligned} \partial_t \langle F[n, t] \rangle + \int_0^\infty \langle \partial_x n(x) \frac{\delta F[n]}{\delta n(x)} \rangle dx &= \\ = \int_0^\infty \gamma_1(x) \langle \left(F[n_1 + \delta_0, n_2 - 1] - F[n_1, n_2] \right) n_1(x) n_2 \rangle dx + \\ + \int_0^\infty \gamma_2(x) \langle \left(F[n_1 - \delta_x, n_2 + 1] - F[n_1, n_2] \right) n_1(x) \rangle dx. \end{aligned} \quad (6.35)$$

If I set $F[n] = n(z)$, the evolution of the mean is obtained:

$$\begin{aligned} \partial_t \langle n(z) \rangle + \int_0^\infty \langle \partial_x n(x) \frac{\delta n(z)}{\delta n(x)} \rangle dx &= \int_0^\infty \gamma_1(x) \langle \left(n(z) + \delta(z) - n(z) \right) n_1(x) n_2 \rangle dx + \\ + \int_0^\infty \gamma_2(x) \langle \left(n_1(z) - \delta(x-z) - n_1(z) \right) n_1(x) \rangle dx. \end{aligned} \quad (6.36)$$

Via trivial manipulations, the deterministic McKendrick-Kermack equation can be recalled:

$$(\partial_t + \partial_z) \langle n(z) \rangle = \delta(z) \int_0^\infty \gamma_1(x) \langle n_1(x) n_2 \rangle dx - \gamma_2(z) \langle n_1(z) \rangle.$$

To start quantifying the fluctuations, I consider the stochastic variable $F[n] = n(z)n(y)$:

$$\begin{aligned} \partial_t \langle n(z) n(y) \rangle + \int_0^\infty \langle \partial_x n(x) \frac{n(z) n(y)}{\delta n(x)} \rangle dx &= \\ (\partial_t + \partial_z + \partial_y) \langle n^t(z) n^t(y) \rangle. \end{aligned} \quad (6.37)$$

and manipulation of the other side:

$$\begin{aligned} (\partial_t + \partial_z + \partial_y) \langle n^t(z) n^t(y) \rangle &= \\ = \int_0^\infty \gamma_1(x) \left(\langle n_1(x) n_2 n_1(y) \rangle \delta(z) + \delta(y) \langle n_1(x) n_2 n_1(z) \rangle + \delta(z) \delta(y) \langle n_1(x) n_2 \rangle \right) dx + \\ - (\gamma_2(y) + \gamma_2(z)) (\langle n_1(z) n_1(y) \rangle - \frac{\delta(z-y)}{2} \langle n_1(z) \rangle). \end{aligned} \quad (6.38)$$

Then I define the mixed variances as: $V_{x,y} = \langle (n_1(x) - \langle n_1(x) \rangle)(n_1(y) - \langle n_1(y) \rangle) \rangle$

$$\begin{aligned} (\partial_t + \partial_y + \partial_z)V_{x,y}(t) &= \sum_{u=z,y} \delta(u) \int_0^\infty \gamma_1(x) (\langle n_1(u)n_1(x)n_2 \rangle - \langle n_1(x)n_2 \rangle) dx + \\ &\quad - (\gamma(y) + \gamma(z))V_{y,x} + \delta(z)\delta(y) \int_0^\infty \gamma_1(x) \langle n_1^t(x) \rangle dx. \end{aligned} \tag{6.39}$$

The interesting thing is that, for individuals with incubation period $x > 0$, the fluctuations follow the continuity equation:

$$(\partial_t + \partial_y + \partial_z)V_{x,y}(t) = -(\gamma(y) + \gamma(z))V_{x,y} \tag{6.40}$$

Being a first-order PDE, an exact expression for $V_{x,y}$ can be obtained. A small noise expansion could also be developed to study a specific case where the noise level is reduced and in the case of a large population.

6.6 Conclusions

This chapter is dedicated to the age-structured generalization of a well-known epidemic model: the SIS (Susceptible-Infected- Susceptible) model. Here, I proposed a set of methods to quantify and simulate the stochastic evolution of an epidemic scenario where the ages of infected individuals bias the infection and recovery probabilities. After recalling the main deterministic results on the topic, three different approaches were presented. The first one (Sec.6.3) is based on the integral representation of the Chapman-Kolmogorov equations, and it allows for expressing the evolution of the functional probability as a linear system of Volterra's equations. In principle, once the age is discretized, such a system could be resolved exactly, in addition to several available numerical methods [170]. The second way to approach the study of age-structured stochastic SIS models is its approximation in terms of branching processes. In fact, since an exponential function with positive roots and a sigmoid function must intersect at some point, a branching process framework should exactly coincide with the exact solution before diverging. In the initial times of the epidemic outbreak, the dynamics can be expressed as a branching process, and the integral representation collapses into functional equations similar to those of Bellman-Harris. The last approach is presented in Sec.6.5, where I consid-

ered an almost deterministic (small fluctuations) SIS age-structured model. I showed that it is coherent with the deterministic case and that the fluctuations can be quantified in Partial Differential Equations. These three strategies aim to tackle the complexity of an epidemic scenario, encoded in the infection propensity's non-linearity and the age heterogeneity. From a different perspective, such complexity can be observed in the non-linearity of the Functional Derivative Equation describing the evolution of the generating function. At the current state, such non-linear behaviour allows the encoding of the functional probability in Linear Volterra's equations, which can be studied numerically as the second-order FDE for the generating functional can be. Therefore, we need to reduce the system's degrees of freedom by some kind of approximation, which, in this chapter, was given by assuming a linear prosperity rate or dealing with small fluctuations. Luckily for us, infection and recovery rarely are exponentially distributed, instead, they follow a peaked bell-shaped distribution for the infection and recovery times, making the small noise approximation a reliable asset [33,34]. The inferences arising from this short research report suggest that there is not a unique, reliable way to study an age-structured SIS model. Instead, the investigation should rely on simulation, numerical and analytical approximation based on the data recovered from the phenomena investigated. The initial spread can be quantified once the average number of infections is evaluated and the evolution model as a branching process. Despite the numerical cost, a numerical solution of the Master Equation can lead to an exact portray of the sis dynamics. Finally, assuming low-fluctuating reaction times, the variance from the deterministic results can be estimated via the small noise approximation portrayed in Sec.6.5. On top of this, the simulations approach can lead to a solid representation of the main properties of the SIS model. Additional time and effort will be dedicated to enlarging this work in the following months. A more detailed comparison between the different approaches still needs to be discussed and its coherency should be finally tested against real data.

Chapter 7

Conclusions

In this thesis, I proposed a theoretical framework to study jumping processes undergoing Liouville's drift and I used it to model the evolution of age-heterogeneous populations. As cases of study, I considered the growth of cancer and bacterial cells, and the dynamics of epidemic spreads.

The analytic derivation of the Chapman-Kolmogorov Equations (differential and integral) provides a formal ground on which the age-structured dynamics can be quantified. For branching processes, different results are presented (e.g. age-structured Galton-Watson Theory, Subsec. 2.5) and the sharpness of these results is discussed in comparison to the Bellman-Harris framework (Ch.2).

The theoretical framework was then applied to a division-death scenario where I explored how age variability introduces broader dynamics compared to the unstructured case. The introduction of persistent or dormant states allowed the adaptation of this model to the study of fractional killing in cancer treatments. The study of this application led to the description of an articulated interplay between heterogeneity and fluctuations.

For continuous treatments, I showed how to quantify the survival probability and proposed a biological interpretation of how the cell-cycle dependence (of division and death times) can be tuned to enhance the survival frequency. Moreover, a potential model was proposed to account for possible cell-cycle variations during the dormancy-awakening cycle. In Ch. 5, I referred to this model as *inheriting process* which appears to be a promising research path given its possible generalisation to other applications.

Later, I investigated the evolution of age-heterogeneous cells during periodic treatments. We drew several insights and encountered an undocumented phenomenon: *survival resonance*. This phenomenon is characterised by frac-

tional killing abruptly enhanced by specific combinations of noise, treatment lengths and survival strategies of cells (persistence and dormancy). This suggests that non-genetic mechanisms may contribute to some instances towards the incidence of cancer relapse. The encounter of *stochastic resonances* is also theoretically relevant, as the height of survival resonances is not monotonic in the noise (stochastic resonance, Sec. 4.4.2). In general, stochastic resonances are a universal phenomenon allowed by persistence or dormancy and rising in periodically forced age-structured branching processes (which are ubiquitous in biology).

As last remark on survival resonances, let me just observe that they might not be unique of their kind. To support such a statement, let me outline the relationship holding between survival resonances and drug selection, i.e. the ability of a drug to affect a particular population (gene, protein, signalling pathway, or cell) [171]. In general, the work presented in Ch.4 can be extended to a pool of initial cells with an arbitrary age distribution. Therefore, further investigations should concern possible resonance processes between the pool's initial age distribution and the treatment time intervals. It can not be excluded that possible synchronization between the initial age distribution and the treatment framework can lead to periodic survival pockets. This potential event might be interestingly linked with selection in cell populations and it might help to improve the current perspective on the topic.

At the end of this work, a second application was presented to study an interacting age-structured reaction network (Ch. 6) to model an epidemic scenario (SIS model). The theoretical framework sets up possible paths to study the SIS model. Ch. 6 is not a solid research proposal yet but offers a preview of the basic methods that can be developed using the integral Chapman-Kolmogorov Equations. In addition, the application to the unstructured SIS model could be considered a significant result (Subsec. 6.3.1). It suggests that the unstructured dynamics can always be encoded in a system of renewal equations which can be expressed in a matrix form as shown for the SIS model.

This thesis suggests several future research directions. *In primis* the inheritance process, in which the age of products cells can adjust the metabolic cycle from one state to another (e.g. dormant to non-dormant) or during division age-process. This topic follows under a wider theoretical class of model, where the ages of products and reactants depend on each other. If inheritance is ab-

sent, the theoretical framework allows the expression of the integral CKE as a system of renewal equations. However, in the case of inheritance, the framework returns the integral operator (over time) applied to the initial condition and the time of the functional probability, breaking the renewal symmetry. This shortcoming is a significant limitation of this theory. I suggested a possible solution to study inheritance processes (Subsec. 5.2.3) which is potentially extendable to division with age-inheriting newborns.

Therefore, a detailed analysis of age inheritance in age-structured branching processes is required and its implementation could also be extended to a general structured process. In fact, the ageing process was encoded in a linear drift but it can be extended to a general deterministic drift $\frac{dx_i(t)}{dt} = g_i(x)$ (for the i -th species) such that the Liouville's drift operator is:

$$\mathcal{D}_{n,t} = \partial_t + \sum_{i=1}^M \int_0^\infty dx g_i(x) \partial_x n_i(x) \frac{\delta}{\delta n_i(x)} \quad (7.1)$$

The combination of the inheritance dynamics and a general Liouville's drift would open a new path to a general stochastic theory for structured models.

A few additional observations regard the unstructured SIS process (Subsec. 6.3.1). The same kind of renewal formulation can be recalled for any Markov unstructured process. I am not currently aware of similar results, however it might not be an original result. This formulation allows a fast numerical implementation and several theoretical methods can be exploited due to its linearity [172].

Further efforts are also required to map and fully understand survival and extinction resonances in the dormancy-death-division process. Here, I showed that persistence (as defined in Chs. 4 and 5) substantially enhances the survival probability but does not change the dynamics of the process. Instead, this is observed for stochastic dormant times which lead to detect novel properties of the system as the extinction resonances. Dormancy does not shift the survival resonance positions but can be modelled in a more flexible way than persistence. If the inheritance is also accounted for, I would also expect non-monotonic behaviour of survival probabilities while varying the properties (mean and fluctuations) of the event times distribution.

In conclusion, this thesis provides a set of ingredients to study the stochastic dynamics of age-heterogeneous populations. The results presented were devel-

oped in three stages: analytic derivation, simulations comparison and application to real case scenarios. I proposed original analytical results and investigated two biological scenarios. I demonstrated the plasticity of the theoretical framework and pursued a physical investigation where novel phenomena of potential biological relevance were detected.

Appendix A

Derivation of The Integral Chapman-Kolmogorov Equations

The integral formulation of the Chapman-Kolmogorov Equations is a representation of a stochastic process in terms of the last (forward) or first (backward) reaction times. Here, I present a detailed derivation of the integral formulation of Chapman-Kolmogorov equations presented in Section 2.4. The derivation of the Integral Backward Chapman-Kolmogorov equation is discussed in Section A.1 while the Integral Forward Chapman-Kolmogorov equation is address in Section A.2. Such derivations are based on the application of Characteristic Curves Methods (CCM) [110] to the Differential Chapman-Kolmogorov Equation. CCM is a strong and powerful method to manipulate (and possibly solve) First Order Partial Differential Equations. CCM allows to express the function in tangent space but it does not allow to extract physical insights on the Integral formulation. In mere terms, why is it possible to decompose a Markov process in terms only of the first or last reaction time? To answer this question, I proposed a third intuitive derivation based on the Total Probability Theorem (Section A.2.1). This latter derivation is only proposed for the Backward Chapman-Kolmogorov equation and presents few similarities with the one proposed by Bellman and Harris [56].

For generality, I derive the equations for a general time dependent case where each rate is age and time dependent $\gamma(\vec{x}, t)$.

A.1 Integral Chapman-Kolmogorov Backward Equation

For the purpose of this Chapter, the Backward Master Equation (2.18)):

$$D_{m,t_0} \mathcal{P}[\cdot|m, t_0] = \int \mathcal{W}[q|m; t_0] \mathcal{P}[\cdot|m, t_0] - \mathcal{W}[q|m; t_0] \mathcal{P}[\cdot|q, t_0] \mathcal{D}q. \quad (\text{A.1})$$

Here, the variable n and m refers to the state of a multispecies population and are given by vectors of functions $n = (n_1, \dots, n_M)$ and $m = (m_1, \dots, m_M)$, Employing the Characteristic curves methods, latter equation can be expressed in terms of the parametric equation of the characteristic curves. The characteristic curves are described by a system of ODEs and a set of M PDEs:

$$\dot{t}_0(s_2) = 1, \quad (\text{A.2})$$

$$(\partial_{s_2} + \partial_x) m_i(x, s_2) = 0 \quad \forall i = 1, \dots, M, \quad (\text{A.3})$$

$$\begin{aligned} \frac{d}{ds_2} \mathcal{P}[\cdot|m(s_2), t_0(s_2)] &= \int \mathcal{W}[q|m(s_2); t_0(s_2)] \mathcal{P}[\cdot|m(s_2), t_0(s_2)] + \\ &\quad - \mathcal{W}[q|m(s_2); t_0(s_2)] \mathcal{P}[\cdot|q, t_0(s_2)] \mathcal{D}q. \end{aligned} \quad (\text{A.4})$$

Let us first observe that (A.3) evolves accordingly with continuity equation. From (A.3) follows that $m(x, s_2) = m(x - s_2, 0) = m^{-s_2}(x, 0)$. The functional $\mathcal{P}[\cdot|m(s_2), t_0(s_2)]$ evolves along the characteristic curves as:

$$\begin{aligned} \frac{d}{ds_2} (\Pi_m(s_2) \mathcal{P}[\cdot|m(s_2), t_0(s_2)]) &= \\ &= - \int \Pi_m(s_2) \mathcal{W}[q|m(s_2); t_0(s_2)] \mathcal{P}[\cdot|q, t_0(s_2)] \mathcal{D}q, \end{aligned} \quad (\text{A.5})$$

where we defined $\Pi_m(s_2) = e^{-\int_0^{s_2} \mathcal{W}[q|m(s'); s'] \mathcal{D}q ds'} = e^{-\int_0^{s_2} \mathcal{W}[q|m^{-s'}(0); s'] \mathcal{D}q ds'}$.

Integrating equation (A.5), the following steps follows:

$$\begin{aligned} \int_0^{s_2} \frac{d}{ds} (\Pi_m(s) \mathcal{P}[\cdot|m(s), t_0(s)]) ds &= \\ &= - \int_0^{s_2} \int \Pi_m(s) \mathcal{W}[q | \underbrace{m(s)}_{m^{-s}(0)}; t_0(s)] \mathcal{P}[\cdot|q, t_0(s)] \mathcal{D}q ds \end{aligned} \quad (\text{A.6})$$

$$\begin{aligned} \Pi_m(s_2) \mathcal{P}[\cdot | \underbrace{m(s_2)}_{m^{-s_2}(0)}, t_0(s_2)] - \mathcal{P}[\cdot|m(0), t_0(0)] &= \\ &= - \int \int_0^{s_2} \Pi_m(s) \mathcal{W}[q|m^{-s}(0); t_0(s)] \mathcal{P}[\cdot|q, t_0(s)] \mathcal{D}q. \end{aligned} \quad (\text{A.7})$$

Finally, we get back to the original set of variables involved in the FDE m, t and notice that $t_0(s_2) = s_2 + t_0$ $s_2 \in [0, t - t_0]$, we obtain

$$\begin{aligned} & \Pi_m(t - t_0) \underbrace{\mathcal{P}[\cdot | m^{-(t-t_0)}, t]}_{\delta[n - m^{-(t-t_0)}]} - \mathcal{P}[\cdot | m, t_0] = \\ &= - \int_0^{t-t_0} \int \Pi_m(y) \mathcal{W}[q | m^{-y}, y] \mathcal{P}[\cdot | q, t_0 + y] \mathcal{D}q dy. \end{aligned} \quad (\text{A.8})$$

Then, I employ the formalism introduced in Section 2.2 to observe that: $q = q_{m,r}(\vec{x}, y) = m^{-y} + \nu_r[\vec{x}]$. Therefore, we can switch between the functional to a semi-discrete representation $\int \mathcal{D}q \rightarrow \int_{\vec{x}} \sum_{r=1}^R$:

$$\begin{aligned} & \mathcal{P}[\cdot | m, t_0] = \\ &= \Pi_m(t - t_0) \delta[n - m^{-(t-t_0)}] + \sum_{r=1}^R \int_0^{t-t_0} \int_{\vec{x}} \Pi_{m,\gamma_r}(y, \vec{x}) \mathcal{P}[\cdot | q_{m,r}(\vec{x}, y), t_0 + y] d\vec{x} dy, \end{aligned} \quad (\text{A.9})$$

where we defined the function Π_{m,γ_r} as $\Pi_{m,\gamma_r}(t-t_0, \vec{x}) = \Pi_m(t-t_0) \gamma_r[\vec{x}] \Phi_r[m^{-t-t_0}, \vec{x}]$. The function Π_{m,γ_r} represents the probability density functions of observing (as first reaction) the $r-th$ reactions involving ages $\vec{x} = (x_1, \dots)$ given an initial age density $m(x)$.

A.2 Forward Integral Derivation

The derivation of the Integral Forward equation (2.15) follows symmetrically with the derivation of the backward:

$$D_{n,t} \mathcal{P}[n, t | \cdot] = \int \mathcal{W}[n | q, t] \mathcal{P}[q, t | \cdot] - \mathcal{W}[q | n, t] \mathcal{P}[n, t | \cdot] \mathcal{D}q. \quad (\text{A.10})$$

We parametrize the Characteristic curves for the Forward equation with the variable s_1 . The characteristic curves rising from the Forward Equation are described by a system of ODEs and one PDE:

$$\dot{t}(s_1) = 1, \quad (\text{A.11})$$

$$(\partial_x + \partial_{s_1})) n_i(x, s_1) = 0 \quad \forall i = 1, \dots, M, \quad (\text{A.12})$$

$$\begin{aligned} \frac{d\mathcal{P}[n(s_1), t(s_1) | \cdot]}{ds_1} &= \int \mathcal{W}[n(s_1) | q; t(s_1)] \mathcal{P}[q, t(s_1) | \cdot] \\ &\quad - \mathcal{W}[q | n(s_1); t(s_1)] \mathcal{P}[n(s_1), t(s_1) | \cdot] \mathcal{D}q. \end{aligned} \quad (\text{A.13})$$

The ODE regarding $\mathcal{P}[n(s_1), t(s_1)]$ can be expressed as:

$$\begin{aligned} \frac{d}{ds_1} & \left(\Pi_n(s_1) \mathcal{P}[n(s_1), t(s_1)|\cdot] \right) = \\ & = \int \Pi_n(s_1) \mathcal{W}[n(s_1)|q; t(s_1)] \mathcal{P}[q, t(s_1)|\cdot] \mathcal{D}q. \end{aligned} \quad (\text{A.14})$$

Before moving ahead, we observe that the PDE (A.12) is a transport function. Therefore we can propagate the values along the characteristic curves in term of the functions $n_i(x, s_1)$: $n_i(x, s_1) = n_i(x + t - t_0 - s_1, t) = n_i^{+t-t_0-s_1}(x, t)$. Once defined the functions $\Pi_n(s_1) = e^{\int \int_0^{s_1} \mathcal{W}[q|n(s'); s'] ds' \mathcal{D}q} = e^{\int \int_0^{s_1} \mathcal{W}[q|n^{+s'}(0); s'] ds' \mathcal{D}q}$. The functional probability \mathcal{P} along the characteristic curves can be expressed as:

$$\begin{aligned} \Pi_n(s_1) \mathcal{P}[n(s_1), t(s_1)|\cdot] - \mathcal{P}[n(0), t(0)|\cdot] &= \\ &= \int_0^s \int \Pi_n(s_1) \mathcal{W}[n(s_1)|q; t(s_1)] \mathcal{P}[q, t(s_1)|\cdot] \mathcal{D}q ds_1 \end{aligned} \quad (\text{A.15})$$

and

$$\begin{aligned} \Pi_n(t) \mathcal{P}[n, t|\cdot] - \underbrace{\mathcal{P}[n^{+t}, t_0|\cdot]}_{\delta_{n^{+t}-m}} &= \\ &= \int_0^{t-t_0} \int \Pi_n(s) \mathcal{W}[n^{t-s_1}|q; t(s_1)] \mathcal{P}[q, t(s_1)|\cdot] \mathcal{D}q ds_1 \end{aligned} \quad (\text{A.16})$$

Thank to the stochastic formalism introduce in Ch. 2, we can note that: $q = p_{n,r}(\vec{x}, y) = n^{t-y} - \nu_r[\vec{x}]$. As in the backward derivation, we can switch to semi-discrete representation $\int \mathcal{D}q \rightarrow \int_{\vec{x}} \sum_{r=1}^R$:

$$\begin{aligned} \mathcal{P}[n, t|\cdot] &= \\ &= \Pi_n(t) \delta[n^{+t} - m] + \sum_{r=1}^R \int_{\vec{x}} \int_0^{t-t_0} \int \Pi_{n,\gamma_r}(s) \mathcal{W}[n^{t-s_1}|q; t(s_1)] \mathcal{P}[q, t(s_1)|\cdot] \mathcal{D}q ds_1 = \\ &= \Pi_n(t) \delta[n^{+t} - m] + \sum_{r=1}^R \int_{\vec{x}} \int_0^{t-t_0} \int \Pi_{n,\gamma_r}(s) \mathcal{P}[p_{n,r}(\vec{x}, s), t - s_1|\cdot] d\vec{x} ds, \end{aligned} \quad (\text{A.17})$$

where the functions $\Pi_{n,\gamma_r}(s) = \gamma_r(\vec{x}) \Phi_r[n] e^{-\sum_{r=1}^R \int_{\vec{x}} \gamma(\vec{x}) \Phi_r[n^{t-s}; \vec{x}] d\vec{x} ds'}$ is the probability that no reaction will happen for a time-length s after that a given reaction (r -th with \vec{x} -ages reactants) happened at time $t - s$.

A.2.1 Derivation Based on the Total Probability Theorem

The last two (backward and forward) derivations do not provide an intuitive idea. Now, we provide an alternative and more intuitive derivation based on the law of total probability in its discrete form: $\mathcal{P}(A) = \sum_n \mathcal{P}(A|B_n)\mathcal{P}(B_n)$ where $\{B_n\}_{n=1,\dots}$ is countably infinite set of a finite or measurable partitions of a sample space A . W.l.o.g we focus on the derivation related to backward integral, Section A.1. The scenario investigated is still described by a stochastic process starting with density m at time t_0 and reaching a density n at time t , such that $A = (n, t|m, t_0)$. The first reaction time (after time t_0) is labelled with t^* so that the population switch from an initial density m to density q at time t^* . The stochastic couple (q, t^*) is made by a random density and a stochastic time. In relation with the law of total probability, the possible paths $(m, t_0) \rightarrow (q, t^*) \rightarrow (n, t)$ represent the partition of the sample space $A = (n, t|m, t_0)$. Therefore, we define the probability of observing (q, t^*) as $\Pi[q, t^*|m, t_0]$ and we obtain::

$$\mathcal{P}[n, t|m, t_0] = \int \int_0^{t-t_0} \mathcal{P}[n, t|q, t^*] \Pi[q, t^*|m, t_0] \mathcal{D}q dt^*. \quad (\text{A.18})$$

Eq. (A.18) is an integral Chapman-Kolmogorov equation that bridges on a stochastic time t^* . This stochastic time represents the first events in the evolution of the process $(n, t|m, t_0)$. The integral over the possible first new state $\int \mathcal{D}q$ can be parametrized in terms of the reaction-index r and the ages of the reactants \vec{x} . In fact, the only possible states at time t^* are the ones equal to $q_{r,m}(\vec{x}) = m + \nu_r[\vec{x}]$. Moreover, we have to account the chance of observing no reactions at time t^* so that $q = m = n$. This possible path is simply given by the probability of observing no reactions under the constraint $n = m$. It follows that Eq. (A.18) is given by:

$$\begin{aligned} \mathcal{P}[n, t|m, t_0] &= \delta[n - m] \Pi(m, t|m, t_0) + \\ &\sum_{r=1}^R \int_{\vec{x}} \int_0^{t-t_0} \mathcal{P}[n, t|q_{r,m}(\vec{x}), t^*] \Pi[q_{r,m}(\vec{x}), t^*|m, t_0] d\vec{x} dt^*. \end{aligned} \quad (\text{A.19})$$

We now want to include the ageing process in Eq.(A.19). In order to keep the notation as compact as possible, let us set $t_0 = 0$ and define f^{t^*} as the

shifted function f : $f^{t^*}(x) = f(x + t^*)$. In the range of time $[0, t^*]$, the ageing drift is a deterministic process and does not overlap with any stochastic events. Consequently, the bridging point $(m + \nu_r[\vec{x}], t^*)$ has to be adjusted since the density at time t^* is equal to the initial density m translated by t^* . It follows that the possible states at time t^* will depend on t^* itself: $q_{r,m}(x, t^*) = m^{t^*} + \nu_r[\vec{x}^{+t^*}]$. Therefore, Eq.(A.19) becomes:

$$\begin{aligned} \mathcal{P}[n, t|m, 0] &= \delta[n - m^{+t}] \Pi(m^{+t}, t|m, t_0) + \\ &\sum_{r=1}^R \int_{\vec{x}} \int_0^{t-t_0} \mathcal{P}[n, t|q_{m,r}(x, t^*), t^*] \Pi[q_{m,r}(x, t^*), t^* | m, t_0] d\vec{x} dt^*. \end{aligned} \quad (\text{A.20})$$

At this stage of the derivation, we focus on the probability $\Pi[m + \nu_r[\vec{x}], t^* | m, 0]$. Following from Non Homogeneous Poisson process theory, we observe that $\Pi[m + \nu_r[\vec{x}], t^* | m, 0]$ can be expressed as a products between three terms: the rate of the $r - th$ reaction with ages \vec{x} ($\gamma_r(\vec{x})$), the number of individuals able to perform such reaction ($\Phi_r[m; \vec{x}]$) and, as a third term, the probability of no other reaction before time t^* ($\Pi_m[t^*]$) which is:

$$\ln(\Pi_m(t^*, \vec{x})) = - \sum_r \int_{\vec{x}} d\vec{x} \int_0^t dt^* \Phi_r[\tilde{m}_r^{t^*}] \gamma_r(\vec{x}) \quad (\text{A.21})$$

and we label the product of these three quantities as:

$$\Pi_{m,\gamma_r}(t^*, \vec{x}) = \Phi_r[x; \vec{x}] \gamma_r(\vec{x}) \Pi_m(t^*, \vec{x}) \quad (\text{A.22})$$

. In conclusion, Eq.(A.20) becomes:

$$\mathcal{P}[n, t|m, 0] = \Pi_m(t) \delta[n - m^{+t}] + \quad (\text{A.23})$$

$$+ \sum_{r=1}^R \int_{\vec{x}} \int_0^t \mathcal{P}[n, t|q(\vec{x}, t^*), t^*] \Pi_{m,\gamma_r}(t^*, \vec{x}) d\vec{x} dt^*. \quad (\text{A.24})$$

For completeness, we also show that Eq.(A.23) can be expressed in term of the generating functional \mathcal{P} :

$$\mathcal{Z}[h, t|\delta_{x_0}] = \Pi(\vec{x}, t) \Gamma_{m^{+t}}[h] + \sum_{r=1}^R \int_0^t \Pi_{\gamma_r}(\vec{x}, u) \mathcal{Z}[h, t-u|q(\vec{x}, u)] du d\vec{x}. \quad (\text{A.25})$$

Appendix B

A Recursive Solution for the Division-Death Model

Instead of relying on the generating functional (Eq. (4.13)), we consider the integral Chapman-Kolmogorov Backward equation for the functional probability (Eq. (4.14)):

$$\begin{aligned} \mathcal{P}[n, t|m, 0] &= \Pi_m(t)\delta_{[n, m^{-t}]} + \\ &+ \int_0^\infty m(x) \int_0^t \Pi_m(y) \gamma_1(x+y) \mathcal{P}[n, t-y|m^{-y} + 2\delta_0 - \delta_{x+u}, 0] dy dx. \end{aligned} \quad (\text{B.1})$$

We observe that equation (B.2) is a linear integral equation for functional probability with shift initial conditions:

$$\begin{aligned} \mathcal{P}[n, t|m, 0] &= \Pi_m(t)\delta_{[n, m^{-t}]} + \\ &+ \int_0^\infty m(x) \int_0^t \Pi_m(y) \gamma_1(x+y) \mathcal{P}[n, t-y|m^{-y} + 2\delta_0 - \delta_{x+u}, 0] dy dx. \end{aligned} \quad (\text{B.2})$$

Since the number of elements in the system cannot decrease, we show that functional probability, with initial condition (e.g. $m = \delta_0$) is described by a system of integral equations:

$$\mathcal{P}[n, t|\delta_0, 0] = \Pi_{\delta_0}(t)\delta_{[n, \delta(t)]} + \int_0^t \Pi_{\delta_0}(y) \gamma_1(y) \mathcal{P}[n, t-y|2\delta_0, 0] dy dx, \quad (\text{B.3})$$

$$\mathcal{P}[n, t|2\delta_0, 0] = \Pi_{2\delta_0}(t)\delta_{[n, 2\delta(t)]} + 2 \int_0^t \Pi_{2\delta_0}(y) \gamma_1(y) \mathcal{P}[n, t-y|\delta_y + 2\delta_0, 0] dy dx, \quad (\text{B.4})$$

$$\begin{aligned}
\mathcal{P}[n, t - y | \delta_y + 2\delta_0, 0] &= \Pi_{\delta_y + 2\delta_0} \delta_{[n, \delta_y + t + 2\delta_t]} + \\
&\quad + 2 \int_0^t \Pi_{\delta_y + 2\delta_0}(u) \gamma_1(u) \mathcal{P}[n, t - u | 2\delta_0 + \delta_u + \delta_{y+u}, 0] du + \\
&\quad + \int_0^t \Pi_{\delta_y + 2\delta_0}(u) \gamma_1(y + u) \mathcal{P}[n, t - u | 2\delta_0 + 2\delta_u, 0] du, \\
&\quad \vdots \quad \vdots \quad \vdots \quad \vdots \\
&\quad \vdots \quad \vdots \quad \vdots \quad \vdots
\end{aligned} \tag{B.5}$$

Furthermore, by plugging equation (B.3), (B.4), (B.5) and the upcomings next, one into the other, we can obtain an explicit solution for the functional probability or for the probability of the total abundances. For instance, we can show that the probability of all the number of individuals N , at time t is given by:

$$\begin{aligned}
P(N, t) &= \delta_{N,1} \Pi_{\delta_0} + \\
&\quad + \delta_{N,2} \int_0^t \Pi_{\delta_0}(y) \gamma_1(y) \Pi_{2\delta_0}(y) dy + \\
&\quad + \delta_{N,3} \int_0^t \Pi_{\delta_0}(y) \gamma_1(y) \int_0^y \Pi_{2\delta_0}(u) \gamma(u) \Pi_{\delta_u + 2\delta_0} du dy + \dots
\end{aligned} \tag{B.6}$$

In conclusion, it is potentially possible to solve exactly equation (B.3), especially if divisions happen with slow frequency.

Appendix C

Constant Rates in Time-Dependent Environments

We discuss the age-independent branching processes in a periodic on-off environment. Constant rates imply exponentially distributed division and death times with $w_d = w_\gamma = 1$. For simplicity, we assume $T_{\text{on}} = T_{\text{off}} = T$.

In a constant environment, an exact solution of the generating function can be obtained [143]:

$$\mathcal{Z}(h, T|1, 0) = \frac{d + d(h - 1)e^{(\gamma-d)T} - \gamma h}{d + \gamma(h - 1)e^{(\gamma-d)T} - \gamma h}, \quad (\text{C.1})$$

where d and γ are the age-independent death and division rates (respectively equal to the inverse of the average death time μ_d and average division time μ_γ) and h is the age-independent auxiliary variable. The condition $|1, 0$ represents the initialisation of the system with one individual at time $t = 0$. From comparison with Eq. (5.26), we find the survival probability from Eq. (C.1): $p_{\text{surv}} = 1 - \lim_{T \rightarrow \infty} \mathcal{Z}(h = 0, T|1, 0) = \frac{\gamma-d}{\gamma} \Theta\left(\frac{\gamma-d}{\gamma}\right)$, where Θ is the Heaviside function.

We now move to time-dependent environment characterised by a fixed division rate γ and a periodically switching death rate $d(t)$. The asymptotic extinction probability function p_{surv} solves the following fixed point equation: $1 - p_{\text{surv}} = \mathcal{Z}_{\text{on}}(\mathcal{Z}_{\text{off}}(1 - p_{\text{surv}}, T|1, 0), T|1, 0)$, where \mathcal{Z}_{on} and \mathcal{Z}_{off} labels the generating function for on- and off-environments. This gives:

$$p_{\text{surv}} = 1 - \frac{d(e^{2\gamma T} - e^{(d+\gamma)T})}{de^{dT} - de^{(d+\gamma)T} - \gamma(e^{dT} + e^{2\gamma T})}. \quad (\text{C.2})$$

As shown in Fig. C.1, we observe a phase transition between extinction (blue, $p_{\text{surv}} = 0$) and fractional killing (red shading, $p_{\text{surv}} > 0$). In contrast to age-dependent results, the survival probability is monotonic in $\frac{\mu_d}{\mu_\gamma}$ and $\frac{T}{\mu_\gamma}$ and there are no survival resonances.

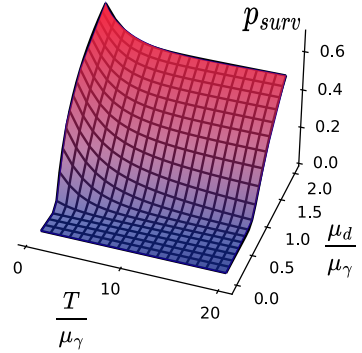


Figure C.1: Survival resonances are absent for constant division and death rates. Asymptotic, age-independent survival probability in a periodic time-dependent environment, Eq. (C.2).

Appendix D

Inheritance and Dormancy

I proposed an implementation of the dormancy-model where the cycle dormant-awaken cell is characterised by a scaling of the age 5.2.3. The stoichiometric reaction network can be expressed as follows:



where $\alpha, \beta \in \mathbb{R}$. To provide an additional prospective on the stoichiometric reaction network, we include the stoichiometric functions for the reactions listed in equation (D.1):

$$\nu_\gamma[\vec{x}] = 2\delta_0\delta_{i,1} - \delta_x\delta_{i,1}, \quad (\text{D.5})$$

$$\nu_d[\vec{x}] = -\delta_{i,1}\delta_x, \quad (\text{D.6})$$

$$\nu_{c_{1,2}}[\vec{x}] = -\delta_x\delta_{i,1} + \delta_{\alpha x}\delta_{i,2}, \quad (\text{D.7})$$

$$\nu_{c_{2,1}}[\vec{x}] = -\delta_x\delta_{i,2} + \delta_{\alpha x}\delta_{i,1}, \quad (\text{D.8})$$

In a deterministic context, the dynamics can be encoded in a generalised form of the McKendrick-Von Forster Partial Differential Equation. We label the number of non-dormant (dormant) cells with age x at time t : $n_1(x, t)$ ($n_2(x, t)$). The dynamics is described by a coupled set of PDEs, one raising for the first

species:

$$(\partial_t + \partial_x) n_1(x, t) = -(\gamma(x) + d(x) + c_{1,2}(x))n_1(x, t) + c_{2,1}(\frac{x}{\beta})n_2(\frac{x}{\beta}, t) \quad (\text{D.9})$$

$$n_1(0, t) = 2 \int_0^\infty \gamma(u) e^{-\int_0^u \gamma(x) + d(x) + c_{1,2}(x)} n(u, t) du \quad (\text{D.10})$$

and one for the second species:

$$(\partial_t + \partial_x) n_2(x, t) = c_{1,2}(\frac{x}{\alpha})n_1(\frac{x}{\alpha}, t) \quad (\text{D.11})$$

$$1 = 2 \int_0^\infty e^{-\lambda x} \gamma(x) e^{-\int_0^x (\gamma(u) + d(u)) du} + \int_0^\infty e^{-\lambda x} c(x) e^{-\int_0^x (\gamma(u) + d(u)) du}. \quad (\text{D.12})$$

We now introduce the framework to study the stochastic dynamics of the models. The stochastic process $(n, m) = (n_1, n_2, t | m_1, m_2, 0)$ is the process starting with initial distribution m_1 (for the first species) and m_2 (for the second species), leading to a state (n_1, n_2) at time t . For brevity, we name functional probability associated with the process , is described by the forward Chapman-Kolmogorov Equation:

$$\begin{aligned} \mathcal{D}_{n_1, n_2, t} \mathcal{P}[n, t | m, 0] &= \int_0^\infty \gamma(x)(\varepsilon_1^{+1}(x)\varepsilon_1^{-2}(0) - 1)n_1(x)\mathcal{P}[n, t | m, 0]dx \\ &\quad + \int_0^\infty d(x)(\varepsilon_1^{+1}(x) - 1)n_1(x)\mathcal{P}[n, t | m, 0]dx + \\ &\quad + \int_0^\infty c_{1,2}(x)(\varepsilon_1^{+1}(x)\varepsilon_2^{-1}(\alpha x) - 1)n_1(x)\mathcal{P}[n, t | m, 0]dx + \\ &\quad + \int_0^\infty c_{2,1}(x)(\varepsilon_2^{+1}(x)\varepsilon_1^{-1}(\beta x) - 1)n_2(x)\mathcal{P}[n, t | m, 0]dx. \end{aligned} \quad (\text{D.13})$$

Since we aim to present the integral formulation of the Master Equation, we first observe that the evolution of the first and of the second species can be categorised as branching process. It follows that the generating functional for

an initial non dormant cell ($m_1 = \delta_x, m_2 = 0, 0$) is given by:

$$\begin{aligned} \mathcal{Z}[h, t | \delta_x \delta_{i,1}, 0] \Pi(x) &= \Pi(t + x) h_1(t + x) + \\ &+ \int_0^t \Pi_d(u + x) du \\ &+ \int_0^t \Pi_\gamma(u + x) \mathcal{Z}^2[h, t - u | \delta_0 \delta_{i,1}, 0] du \\ &+ \int_0^t \Pi_{c_{1,2}} \mathcal{Z}[h, t - u | \delta_{\alpha(u+x)} \delta_{i,2}, 0](u + x) du, \end{aligned} \quad (\text{D.14})$$

where the quantity $\Pi(x) = \exp(-\int_0^x (\gamma(u) + d(u) + c_{1,2}(u)) du)$ represents the probability for a newborn non-dormant cells to survive, i.e. not dividing or dying or going dormant. Therefore, the probabilities the probabilities of dividing, dying or going dormant in an age-range $[x, x + dx)$ are respectively given by: $\Pi_\gamma(x) = \gamma(x)\Pi(x)$, $\Pi_d(x) = d(x)\Pi(x)$ and $\Pi_{c_{1,2}}(x) = c_{1,2}(x)\Pi(x)$.

On the other hand, the generating functional for a dormant cells with age x , i.e. ($m_1 = 0, m_2 = \delta_x$, is given by:

$$\begin{aligned} \mathcal{Z}[h, t | \delta_x \delta_{i,2}, 0] \pi(x) &= \pi(t + x) h_2(t + x) + \\ &+ \int_0^t \pi_{c_{1,2}}(u + x) \mathcal{Z}[h, t - u | \delta_{\beta(u+x)} \delta_{i,1}, 0](u + x) du. \end{aligned} \quad (\text{D.15})$$

The quantity $\pi(x) = \exp(-\int_0^x c_{2,1}(u) du)$ is the probability of remaining dormant for a dormant cell with age $x = 0$, while $\pi_{c_{2,1}}(x) = c_{2,1}(x)\pi(x)$ is the probability awake in at age $x \in [x, x + dx)$.

The main interest is in quantifying the number of non-dormant cell, therefore we note that equations (D.14) and (D.15) can be combined to obtain a recursive function the generating functional associate with the initial condition $m = (m_1 = \delta_x, m_2 = 0, 0)$. To do that, we derive the integral recursive equation for the generating functional associated with the stochastic process $(n_1, n_2, t - u | m_1 = 0, m_2 = \delta_{\alpha(u+x)})$, 0:

$$\begin{aligned} \mathcal{Z}[h, t - u | \delta_{(\alpha(x+u))} \delta_{i,2}, 0] &= \frac{\pi(t - u + \alpha(x + u))}{\pi(\alpha(x + u))} h_2(\alpha(x + u) + t - u) + \\ &+ \int_0^{t-u} \frac{\pi_{c_{1,2}}(y + \alpha(x + u))}{\pi(\alpha(x + u))} \mathcal{Z}[h, t - u - y | \delta_{\beta(\alpha(x+u)+y)} \delta_{i,1}, 0] dy. \end{aligned} \quad (\text{D.16})$$

The last term on the RHS side of equation (D.14) can then expressed as:

$$\begin{aligned} & \int_0^t \Pi_{c_{1,2}}(u) \mathcal{Z}[h, t-u | \delta_{\alpha(u+x)} \delta_{i,2}, 0](u+x) = \\ &= \int_0^t \Pi_{c_{1,2}}(u) \left[\frac{\pi(t-u+\alpha(x+u))}{\pi(\alpha(x+u))} h_2(\alpha(x+u)+t-u) \right] du + \\ &+ \int_0^t \Pi_{c_{1,2}}(u) \left[\int_0^{t-u} \frac{\pi_{c_{1,2}}(y+\alpha(x+u))}{\pi(\alpha(x+u))} \mathcal{Z}[h, t-u-y | \delta_{\beta(\alpha(x+u)+y)} \delta_{i,1}, 0] dy \right] du. \end{aligned} \quad (\text{D.17})$$

As last, we simply note that equation (D.17) becomes a renewal equation under the assumptions $\alpha = 0, \beta = 0$. The final results is given by a recursive equation for the generating functional:

$$\begin{aligned} \mathcal{Z}[h, t | \delta_x \delta_{i,1}] \Pi(x) &= \Pi(x+t) h_1(x+t) + \\ &+ \int_x^{t+x} \Pi_{c_{1,2}}(u) \frac{\pi(t-u+x+\alpha u)}{\pi(\alpha u)} h_2(t-u+x+\alpha u) dx + \\ &+ \int_0^t \Pi_\gamma(u+x) \mathcal{Z}^2[h, t-u | \delta_0 \delta_{i,1}] du + \int_0^t \Pi_d(u+x) du \\ &+ \int_x^{t+x} \Pi_{c_{1,2}}(u) \int_0^{t-x-u} \frac{\pi_{c_{2,1}}(y+\alpha u)}{\pi(\alpha u)} \mathcal{Z}[h, t-x-y-u | \delta_{\beta(y+\alpha u)} \delta_{i,1}] dy du. \end{aligned} \quad (\text{D.18})$$

The extinction probability $p(x) = \lim_{t \rightarrow \infty} \mathcal{Z}[0, t | \delta_x \delta_1]$:

$$\begin{aligned} p(x) \Pi(x) &= \int_x^\infty \Pi_\gamma(u) du p^2(0) + \int_x^\infty \Pi_d(u) du \\ &+ \int_x^\infty \frac{\Pi_{c_{1,2}}(u)}{\Pi(x)} \left[\int_0^\infty \frac{\pi_{c_{2,1}}(y+\alpha u)}{\pi(\alpha u)} p_{ND}(\beta(y+\alpha u)) dy \right] du. \end{aligned} \quad (\text{D.19})$$

Finally, we define the operator:

$$\mathcal{L}_{\alpha,\beta}[p_{ND}](x) = \frac{1}{\Pi(x)} \int_x^\infty \frac{\Pi_{c_{1,2}}(u)}{\pi(\alpha u)} \left[\int_{\beta \alpha u}^\infty \frac{\pi_{c_{2,1}}(y)}{\beta} p_{ND}(y) dy \right] du. \quad (\text{D.20})$$

Therefore, we obtain that:

$$p(x) = \sum_{k=0}^{\infty} (\mathcal{L}_{\alpha,\beta}^k [\nu_\gamma])(x) p^2(0) + \sum_{k=0}^{\infty} (\mathcal{L}_{\alpha,\beta}^k [\nu_d])(x), \quad (\text{D.21})$$

where the composition of the operator $\mathcal{L}_{\alpha,\beta}$ on a function f is: $(\mathcal{L}_{\alpha,\beta}^k f)(x) = (\mathcal{L}_{\alpha,\beta} \circ \mathcal{L}_{\alpha,\beta}^{k-1} f)(x)$. The geometric series in the last equation is Neuman Series:

$$p(x) = p^2(0) (1 - \mathcal{L}_{\alpha,\eta})^{-1} [\nu_\gamma](x) + (1 - \mathcal{L}_{\alpha,\beta})^{-1} [\nu_d](x) \quad (\text{D.22})$$

Equation (D.21) display the dormancy dynamics for $\alpha \neq 0$ as an expansion

of the division probability and death probability in terms of dormant-awakening cycles. In fact, the term $\mathcal{L}_{\alpha,\beta}^k[\nu_\gamma](x)$ ($\mathcal{L}_{\alpha,\beta}^k[\nu_d](x)$), is the effective division (death) probability that an initial awaken cell (with age x) will divide in the future, conditioned on the probability that the cell has already went in the dormant-awaken cycle k-times.Pausch

Bibliography

- [1] C. M. Dobson. Biophysical techniques in structural biology. *Annual review of biochemistry*, 88(1):25–33, 2019.
- [2] W. Lohmann w. Hoppe, H. Markl, and H. Ziegler. *Biophysics*. Springer Science & Business Media, 2012.
- [3] C.W. Gardiner et al. *Handbook of stochastic methods*, volume 3. Springer Berlin, 1985.
- [4] S. De Marchi and S. E. Page. Agent-based models. *Annual Review of political science*, 17(1):1–20, 2014.
- [5] J.S. Kim D. Wirtz E.B. Stukalin, I. Aifuwa and S.X. Sun. Age-dependent stochastic models for understanding population fluctuations in continuously cultured cells. *Journal of the royal society interface*, 10(85):20130325, 2013.
- [6] N.J. Roberts N. London Jr M.E. Pittman M.C. Haffner A. Rizzo A. Baras B. Karim A. Kim C. Tomasetti, J. Poling et al. Cell division rates decrease with age, providing a potential explanation for the age-dependent deceleration in cancer incidence. *Proceedings of the National Academy of Sciences*, 116(41):20482–20488, 2019.
- [7] G. Kronenberg A. Bick-Sander A. Garcia, B. Steiner and G. Kempermann. Age-dependent expression of glucocorticoid-and mineralocorticoid receptors on neural precursor cell populations in the adult murine hippocampus. *Aging cell*, 3(6):363–371, 2004.
- [8] A. Rozhok and J. DeGregori. A generalized theory of age-dependent carcinogenesis. *Elife*, 8:e39950, 2019.
- [9] S.R. Torborg E.A. Torre-B. Emert C. Krepler M. Beqiri K. Sproesser P. A. Brafford M. Xiao S.M. Shaffer, M.C. Dunagin et al. Rare cell variability

- and drug-induced reprogramming as a mode of cancer drug resistance. *Nature*, 546(7658):431–435, 2017.
- [10] D. A. Kessler and H. Levine. Phenomenological approach to cancer cell persistence. *Physical Review Letters*, 129(108101):108101, 2022.
- [11] J.W. Harper G. I. Shapiro et al. Anticancer drug targets: cell cycle and checkpoint control. *The Journal of clinical investigation*, 104(12):1645–1653, 1999.
- [12] W. Krzyzanski. Pharmacodynamic models of age-structured cell populations. *Journal of pharmacokinetics and pharmacodynamics*, 42:573–589, 2015.
- [13] K. Johnson M. Greenwood A.M. Weideman, M.A. Tapia-Maltos and Bibiana B.Bielekova. Meta-analysis of the age-dependent efficacy of multiple sclerosis treatments. *Frontiers in neurology*, 8:577, 2017.
- [14] R. Chait L. Kowalik N. Q. Balaban, J. Merrin and S. Leibler. Bacterial persistence as a phenotypic switch. *Science*, 305(1622):1622–1625, 2004.
- [15] J.G. Albeck J. M. Burke S. L. Spencer, S. Gaudet and P. K. Sorger. Non-genetic origins of cell-to-cell variability in trail-induced apoptosis. *Nature*, 459(7245):428–432, 2009.
- [16] A. Loewer W. C. Forrester A .L. Paek, J. C. Liu and G. Lahav. Cell-to-cell variation in p53 dynamics leads to fractional killing. *Cell*, 165(3):631–642, 2016.
- [17] J. Stewart-Ornstein N. Blüthgen S. Reber A. Jambhekar A.E. Granada, A. Jiménez and G. Lahav. The effects of proliferation status and cell cycle phase on the responses of single cells to chemotherapy. *Molecular Biology of the Cell*, 31(8):845–857, 2020.
- [18] M. Decollongny and S. Rottenberg. Persisting cancer cells are different from bacterial persisters. *Trends in cancer*, 2024.
- [19] S. Signorelli Y. Velappan and M.J. Considine. Cell cycle arrest in plants: what distinguishes quiescence, dormancy and differentiated g1? *Annals of Botany*, 120(4):495–509, 2017.

- [20] O Diekmann and R Montijn. Prelude to hopf bifurcation in an epidemic model: analysis of a characteristic equation associated with a nonlinear volterra integral equation. *Journal of mathematical biology*, 14(1):117—127, 1982.
- [21] N. Keyfitz and H. Caswell. *Applied mathematical demography*, volume 47. Springer, 2005.
- [22] D. D. Smith and N. Keyfitz. *Mathematical demography: selected papers*, volume 6. Springer Science & Business Media, 2012.
- [23] K.C. Land and A. Rogers. Multidimensional mathematical demography: an overview. *Multidimensional Mathematical Demography*, pages 1–4, 1982.
- [24] J.M. Cushing B. Dennis, R. Desharnais and R.F. Costantino. Nonlinear demographic dynamics: mathematical models, statistical methods, and biological experiments. *Ecological Monographs*, 65(3):261–282, 1995.
- [25] M. Iannelli. Mathematical theory of age-structured population dynamics, 1995.
- [26] N. Kubota and T. Fukuda. Genetic algorithms with age structure. *Soft Computing*, 1:155–161, 1997.
- [27] W.M. Schaffer. Selection for optimal life histories: the effects of age structure. *Ecology*, 55(2):291–303, 1974.
- [28] V. Ram and L.P. Schaposhnik. A modified age-structured sir model for covid-19 type viruses. *Scientific reports*, 11(1):15194, 2021.
- [29] S.G. Babajanyan and K.H. Cheong. Age-structured sir model and resource growth dynamics: A covid-19 study. *Nonlinear Dynamics*, 104:2853–2864, 2021.
- [30] H. Inaba. Threshold and stability results for an age-structured epidemic model. *Journal of mathematical biology*, 28:411–434, 1990.
- [31] M. Martcheva E. Shim, Z. Feng and C. Castillo-Chavez. An age-structured epidemic model of rotavirus with vaccination. *Journal of mathematical biology*, 53:719–746, 2006.

- [32] N. Bacaër. *A short history of mathematical population dynamics*, volume 618. Springer, 2011.
- [33] G. Chowell E. Undurraga and K. Mizumoto. Covid-19 case fatality risk by age and gender in a high testing setting in latin america: Chile, march–august 2020. *Infectious Diseases of Poverty*, 10, 12 2021.
- [34] X. Yu. Risk interactions of coronavirus infection across age groups after the peak of covid-19 epidemic. *International Journal of Environmental Research and Public Health*, 17(14), 2020.
- [35] F. Brauer and C. Castillo-Chavez. *Mathematical Models in Population Biology and Epidemiology*, volume 40 of *Texts in Applied Mathematics*. Springer New York, New York, NY, 2012.
- [36] H. Fort. Lotka–volterra models for multispecies communities and their usefulness as quantitative predicting tools. In *Ecological Modelling and Ecophysics*, pages 2–1 to 2–35. IOP Publishing, 2020.
- [37] J. Li. Dynamics of age-structured predator-prey population models. *Journal of mathematical analysis and applications*, 152(2):399–415, 1990.
- [38] M. Haddon. Frequency-dependent competitive success in an age-structured model. *The American Naturalist*, 120(3):405–410, 1982.
- [39] B. Ebenman. Competition between age classes and population dynamics. *Journal of Theoretical Biology*, 131(4):389–400, 1988.
- [40] Jim M Cushing and Mohamed Saleem. A predator prey model with age structure. *Journal of Mathematical Biology*, 14(2):231–250, 1982.
- [41] F. Gozzi G. Fabbri and G. Zanco. Verification results for age-structured models of economic–epidemics dynamics. *Journal of Mathematical Economics*, 93:102455, 2021.
- [42] A. Prskawetz G. Feichtinger and V.M. Veliov. Age-structured optimal control in population economics. *Theoretical Population Biology*, 65(4):373–387, 2004.
- [43] H.I. Cobuloglu-G.R. Houseman İ .Büyüktahatkın, E.Y. Kibis and J.T. Lampe. An age-structured bio-economic model of invasive species man-

- agement: insights and strategies for optimal control. *Biological invasions*, 17(9):2545–2563, 2015.
- [44] T. Chou Y. Chuang and M.R. D’Orsogna. Age-structured social interactions enhance radicalization. *The Journal of Mathematical Sociology*, 42(3):128–151, 2018.
- [45] A. Noymer. The transmission and persistence of ‘urban legends’: Socio-logical application of age-structured epidemic models. *Journal of Mathematical Sociology*, 25(3):299–323, 2001.
- [46] D. Soler J.C. Mico and A. Caselles. Age-structured human population dynamics. *Journal of Mathematical Sociology*, 30(1):1–31, 2006.
- [47] X. Zhu Z. Wang, Z. Wang and J.J. Arenzon. Cooperation and age struc-ture in spatial games. *Physical Review E—Statistical, Nonlinear, and Soft Matter Physics*, 85(1):011149, 2012.
- [48] J.M. Gaillard E. Chambon-Dubreuil, P. Auger and Khaladi M. Effect of aggressive behaviour on age-structured population dynamics. *Ecological modelling*, 193(3-4):777–786, 2006.
- [49] C. Bauch P.V. Souza, R. Silva and D.Girardi. Cooperation in a generalized age-structured spatial game. *Journal of theoretical biology*, 484:109995, 2020.
- [50] G.R. Conway. Mathematical models in applied ecology. *Nature*, 269(5626):291–297, 1977.
- [51] V. Grimm. Mathematical models and understanding in ecology. *Ecological modelling*, 75:641–651, 1994.
- [52] V.F. Krapivin. Mathematical model for global ecological investigations. *Ecological Modelling*, 67(2-4):103–127, 1993.
- [53] V.I. Gertsev and V.V. Gertseva. Classification of mathematical models in ecology. *Ecological Modelling*, 178(3-4):329–334, 2004.
- [54] A. G. McKendrick. Applications of mathematics to medical problems. *Proceedings of the Edinburgh Mathematical Society*, 44(1):98–130, 1926.

- [55] H. von Foerster. Some remarks on changing populations. In *The Kinetics of Cellular Proliferation*, pages 382–407. Grune and Stratton, New York, 1959.
- [56] T. Edward T. Harris and ot. *The theory of branching processes*, volume 6. Springer Berlin, 1963.
- [57] P.H. Leslie. On the use of matrices in certain population mathematics. *Biometrika*, 33(3):183–212, 1945.
- [58] E. Halley. Vi. an estimate of the degrees of the mortality of mankind; drawn from curious tables of the births and funerals at the city of breslaw; with an attempt to ascertain the price of annuities upon lives. *Philosophical Transactions of the Royal Society of London*, 17(196):596–610, 1693.
- [59] A.H. Cook. *Edmond Halley: Charting the Heavens and the Seas*. Clarendon Press, 1998.
- [60] K. Reich. Leonhard euler,‘introduction’to analysis (1748). In *Landmark Writings in Western Mathematics 1640-1940*, pages 181–190. Elsevier, 2005.
- [61] N. Keyfitz D.P. Smith and L. Euler. A general investigation into the mortality and multiplication of the human species. *Mathematical Demography: Selected Papers*, pages 83–91, 1977.
- [62] D. Bernoulli and S. Blower. An attempt at a new analysis of the mortality caused by smallpox and of the advantages of inoculation to prevent it. *Reviews in medical virology*, 14(5):275, 2004.
- [63] C. Gardiner. *Stochastic Methods: A Handbook for the Natural and Social Sciences*. Springer Series in Synergetics. Springer Berlin Heidelberg, 2009.
- [64] H. W. Watson and F. Galton. On the probability of the extinction of families. *The Journal of the Anthropological Institute of Great Britain and Ireland*, 4:138–144, 1875.
- [65] H. W. Watson and F. Galton. On the probability of the extinction of families. *The Journal of the Anthropological Institute of Great Britain and Ireland*, 4:138–144, 1875.

- [66] D. McFadden M. Fosgerau and M. Bierlaire. Choice probability generating functions. *Journal of Choice Modelling*, 8:1–18, 2013.
- [67] A. M. Neves and C. Moreira. Applications of the galton–watson process to human dna evolution and demography. *Physica A: Statistical Mechanics and its Applications*, 368(1):132–146, 2006.
- [68] J. Murray. *Mathematical Biology I: An Introduction*, volume 1. 01 2002.
- [69] W. Wanicharpichat. Explicit minimum polynomial, eigenvector and inverse formula of doubly leslie matrix. *Journal of applied mathematics & informatics*, 33(3-4):247–260, 2015.
- [70] R. E. Plant. A method for computing the elements of the leslie matrix. *Biometrics*, 42(4):933–939, 1986.
- [71] R. Bellman and T.E. Harris. On age-dependent binary branching processes. *Annals of Mathematics*, pages 280–295, 1952.
- [72] T. E. Harris. Branching Processes. *The Annals of Mathematical Statistics*, 19(4):474 – 494, 1948.
- [73] W. Feller. On the Integral Equation of Renewal Theory. *The Annals of Mathematical Statistics*, 12(3):243 – 267, 1941.
- [74] W. Feller. *An Introduction to Probability Theory and Its Applications*, volume 1. Wiley, January 1968.
- [75] A. Franceschetti and A. Pugliese. Threshold behaviour of a sir epidemic model with age structure and immigration. *Journal of mathematical biology*, 57:1–27, 08 2008.
- [76] M. Kot. *Elements of Mathematical Ecology*. Cambridge University Press, 2001.
- [77] P. Van den Driessche Pauline L.J.S. Allen, F. Brauer and J. Wu. *Mathematical epidemiology*, volume 1945. Springer, 2008.
- [78] M. Ausloos and M. Dirickx. *The Logistic Map and the Route to Chaos: From the Beginnings to Modern Applications*. Understanding Complex Systems. Springer Berlin Heidelberg, 2006.

- [79] E. Ott. *Chaos in Dynamical Systems*. Cambridge University Press, 2 edition, 2002.
- [80] D.T. Gillespie. Stochastic simulation of chemical kinetics. *Annual review of physical chemistry*, 58(1):35–55, 2007.
- [81] O. Watanabe and T. Zeugmann. *Stochastic Algorithms: Foundations and Applications*, volume 5792. 10 2009.
- [82] S. S. Asmussen and P.W. Glynn. *Stochastic Simulation: Algorithms and Analysis*. Stochastic Modelling and Applied Probability. Springer New York, 2007.
- [83] Y. T. Lin K. E. Erickson S. Feng R. Suderman, E. D. Mitra and W. S. Hlavacek. Generalizing gillespie’s direct method to enable network-free simulations, 2018.
- [84] S. Mwalili K.M. Kamina and A. Wanjoya. The modeling of a stochastic sir model for hiv/aids epidemic using gillespie’s algorithm. *Int. J. Data Sci. Anal*, 5(6):117, 2019.
- [85] M. Hanif M. Durad and M.N. Akhtar. Analysis of sir epidemic models. *VFAST Transactions on Software Engineering*, 3(1):1–6, 2015.
- [86] Z. Rui A. Ribeiro and S. Kauffman. A general modeling strategy for gene regulatory networks with stochastic dynamics. *Journal of computational biology : a journal of computational molecular cell biology*, 13:1630–9, 12 2006.
- [87] H. McAdams and A. Arkin. Stochastic mechanisms in gene expression. *Proceedings of the National Academy of Sciences of the United States of America*, 94 3:814–9, 1997.
- [88] L. Tsimring T. Lu, D. Volfson and J. Hasty. Cellular growth and division in the gillespie algorithm. *Systems biology*, 1(1):121–128, 2004.
- [89] B. Munsky and M. Khammash. The finite state projection algorithm for the solution of the chemical master equation. *The Journal of chemical physics*, 124(4):044104, 2006.

- [90] E. Giampieri A. Bazzani, G. Castellani and Claudia C. Sala. Master equation and relative species abundance distribution for lotka-volterra models of interacting ecological communities. *Master Equation and Relative Species Abundance Distribution for Lotka-Volterra Models of Interacting Ecological Communities*, pages 37–47, 2016.
- [91] U. Dieckmann and R. Law. The dynamical theory of coevolution: a derivation from stochastic ecological processes. *Journal of mathematical biology*, 34(5):579–612, 1996.
- [92] M. Iannelli. *The Basic Approach to Age-Structured Population Dynamics Models, Methods and Numerics*. Lecture Notes on Mathematical Modelling in the Life Sciences. Springer Netherlands, Dordrecht, 1st ed. 2017. edition, 2017.
- [93] J.M. Cushing. *An introduction to structured population dynamics*. Society for Industrial and Applied Mathematics SIAM, 3600 Market Street, Floor 6, Philadelphia, PA 19104, 1998.
- [94] P. Thomas. Making sense of snapshot data: ergodic principle for clonal cell populations. *Journal of The Royal Society Interface*, 14(136):20170467, 2017.
- [95] A. Ostling V. M. Savage J.P. O’Dwyer, J.K. Lake and J.L. Green. An integrative framework for stochastic, size-structured community assembly. *Proceedings of the National Academy of Sciences*, 106(15):6170–6175, 2009.
- [96] M. Gao. Age-structured population models with applications, 2016.
- [97] S. Karlin. On the renewal equation. *Pacific J. Math*, 5:229–257, 1955.
- [98] M. Buiatti and G. Longo. Randomness and multilevel interactions in biology. *Theory in Biosciences*, 132:139–158, 2013.
- [99] W.C. Wimsatt. Randomness and perceived-randomness in evolutionary biology. *Synthese*, 43:287–329, 1980.
- [100] T. Heams. Randomness in biology. *Mathematical Structures in Computer Science*, 24(3):e240308, 2014.

- [101] P.C. Bressloff. *Stochastic processes in cell biology*, volume 41. Springer, 2014.
- [102] I. C. Gohberg and I. A. Fel'dman. *Convolution equations and projection methods for their solution*. American Mathematical Society, Providence, R.I., 1974. Translated from the Russian by F. M. Goldware, Translations of Mathematical Monographs, Vol. 41.
- [103] N.G. Van Kampen. Master equation treatment of aging populations. *Reports on Mathematical Physics*, 11(1):111–122, 1977.
- [104] N.G. Van Kampen. *Stochastic Processes in Physics and Chemistry*. North-Holland Personal Library. Elsevier Science, 2011.
- [105] L. Duso and C. Zechner. Stochastic reaction networks in dynamic compartment populations. *Proceedings of the National Academy of Sciences*, 117(37):22674–22683, 2020.
- [106] R. Pasupathy. *Generating Nonhomogeneous Poisson Processes*. American Cancer Society, 2011.
- [107] M. Westcott. The probability generating functional. *Journal of the Australian Mathematical Society*, 14(4):448–466, 1972.
- [108] K. Lewin. Field theory, 1948.
- [109] G. Parisi and R. Shankar. Statistical field theory. 1988.
- [110] W.A. Strauss. *Partial Differential Equations: An Introduction*. Wiley, 2007.
- [111] P. Linz. *Analytical and numerical methods for Volterra equations*. SIAM, 1985.
- [112] T.E. Harris. *The theory of branching processes*, volume 6. Springer Berlin, 1963.
- [113] Y. Chen. Thinning algorithms for simulating point processes. 2016.
- [114] D. Luengo L. Martino and J. Miguez. *Accept–Reject Methods*, pages 65–113. 04 2018.

- [115] S. Asmussen and P.W. Glynn. *Stochastic Simulation: Algorithms and Analysis*, volume 57 of *Stochastic Modelling and Applied Probability*. Springer New York, 2007.
- [116] K. Sigman. *Professor Karl Sigman's Lecture Notes on Simulation*. 2007.
- [117] P.A.W. Lewis and G.S. Shedler. Simulation of nonhomogeneous poisson processes by thinning. *Naval Research Logistics Quarterly*, 26(3):403–413, 1979.
- [118] R. Grima M. Voliotis, P. Thomas and C.G. Bowsher. Stochastic simulation of biomolecular networks in dynamic environments. *PLOS Computational Biology*, 12(6):1–18, 06 2016.
- [119] P. Piho F. Puccioni, J. Pausch and P. Thomas. Noise-induced survival resonances during fractional killing of cell populations, 2024.
- [120] M. Kimmel and D.E. Axelrod. *The Bellman-Harris Process*, pages 87–102. Springer New York, New York, NY, 2002.
- [121] H. Von Foerster. Some remarks on changing populations. In *The kinetics of cellular proliferation*, pages 382–407. Grune and Stratton, 1959.
- [122] W. J. M. Hrushesky R. Demicheli, M.W. Retsky and M. Baum. Tumor dormancy and surgery-driven interruption of dormancy in breast cancer: learning from failures. *Nature Clinical Practice Oncology*, 4(12):699–710, 2007.
- [123] J.A. Aguirre-Ghiso. Models, mechanisms and clinical evidence for cancer dormancy. *Nature Reviews Cancer*, 7(11):834–846, 2007.
- [124] J. V. Frangioni. New technologies for human cancer imaging. *Journal of clinical oncology*, 26(24):4012–4021, 2008.
- [125] L. Preziosi. *Cancer modelling and simulation*. CRC Press, 2003.
- [126] I. Ronin I. Levin-Reisman C. Gabay N. Shoresh O. Biham Ofer E. Rotem, A. Loinger and N.Q. Balaban. Regulation of phenotypic variability by a threshold-based mechanism underlies bacterial persistence. *Proceedings of the National Academy of Sciences*, 107(28):12541–12546, 2010.

- [127] E. Ben-Jacob J. Feng, D. A. Kessler and H. Levine. Growth feedback as a basis for persister bistability. *Proceedings of the National Academy of Sciences*, 111(1):544–549, 2014.
- [128] M. S. Cuoco-L. Amir-Zilberstein H. F. Cabanos J.C. Hütter B. Hu P. I. Thakore M. Tabaka C. P. Fulco et al. Y. Oren, M. Tsabar. Cycling cancer persister cells arise from lineages with distinct programs. *Nature*, 596:576–582, 2021.
- [129] M. Kimmel and D. E. Axelrod. *Branching Processes in Biology*. Springer, New York, NY, 2nd edition, 2015.
- [130] Farshid Jafarpour, Charles S. Wright, Herman Gudjonson, Jedidiah Riebling, Emma Dawson, Klevin Lo, Aretha Fiebig, Sean Crosson, Aaron R. Dinner, and Srividya Iyer-Biswas. Bridging the timescales of single-cell and population dynamics. *Phys. Rev. X*, 8:021007, Apr 2018.
- [131] F. Jafarpou. Cell size regulation induces sustained oscillations in the population growth rate. *Physical Review Letters*, 122(11):118101, 2019.
- [132] T. Nozoe and E. Kussell. Cell cycle heritability and localization phase transition in growing populations. *Physical Review Letters*, 125(26):268103, 2020.
- [133] T. GrandPre E. Levien and A. Amir. Large deviation principle linking lineage statistics to fitness in microbial populations. *Physical Review Letters*, 125(4):048102, 2020.
- [134] P. Piho and P. Thomas. Feedback between stochastic gene networks and population dynamics enables cellular decision-making. *Science Advances*, 10:eadl4895, 2024.
- [135] A. L. Paek R. Ballweg and T. Zhang. A dynamical framework for complex fractional killing. *Scientific Reports*, 7(1):8002, 2017.
- [136] S. Chakrabarti, A. L. Paek, J. Reyes, K. A. Lasick, G. Lahav, and F. Michor. Hidden heterogeneity and circadian-controlled cell fate inferred from single cell lineages. *Nature Communications*, 9(5372):1–13, 2018.

- [137] L. Peliti A. Genthon, T. Nozoe and D..Lacoste. Cell lineage statistics with incomplete population trees. *Physical Review X Life*, 1:013014, Sep 2023.
- [138] X. Ma Y.Sun, Y. Liu and H. Hu. The influence of cell cycle regulation on chemotherapy. *International journal of molecular sciences*, 22(13):6923, 2021.
- [139] D.J. Dwyer M.A. Kohanski and Collins J.J. How antibiotics kill bacteria: from targets to networks. *Nature Reviews Microbiology*, 8(6):423–435, 2010.
- [140] R.L. Lock and E.J. Harry. Cell-division inhibitors: new insights for future antibiotics. *Nature Reviews Drug Discovery*, 7(4):324–338, 2008.
- [141] P. Ortega-Prieto-S. Desai-P. Thomas L.V. Fets S.J. Cutty, F.A. Hughes and A.R. Barr M. Secrier. Pro-survival roles for p21(cip1/waf1) in non-small cell lung cancer. *bioRxiv*, page 595102, 2024.
- [142] H. D. Dahmen, G. Jona-Lasinio, and J. Tarski. The method of characteristics for functional-derivative equations. *Nuovo Cimento A Serie*, 10(3):513–520, 1972.
- [143] D. G. Kendall. On the generalized birth-death process. *The Annals of Mathematical Statistics*, 19(1):1–15, 1948.
- [144] R. Garcia-Millan, J. Pausch, B. Walter, and G. Pruessner. Field-theoretic approach to the universality of branching processes. *Physical Review E*, 98:1–11, 12 2018.
- [145] Y.A. Neyfakh-M.P. Orlova B.F. Dibrov, A.M. Zhabotinsky and L.I. Churikova. Mathematical model of cancer chemotherapy. periodic schedules of phase-specific cytotoxic-agent administration increasing the selectivity of therapy. *Mathematical biosciences*, 73(1):1–31, 1985.
- [146] Xiaotian Wu, Fahima Nekka, and Jun Li. Analytical solution and exposure analysis of a pharmacokinetic model with simultaneous elimination pathways and endogenous production: The case of multiple dosing administration. *Bulletin of Mathematical Biology*, 81, 08 2019.

- [147] A. Prémaud J.B. Woillard, M. Labriffe and P. Marquet. Estimation of drug exposure by machine learning based on simulations from published pharmacokinetic models: The example of tacrolimus. *Pharmacological Research*, 167:105578, 2021.
- [148] P. Jung L. Gammaitoni, P. Hänggi and F. Marchesoni. Stochastic resonance. *Reviews of Modern Physics*, 70(1):223, 1998.
- [149] T.J. Mitchison. The proliferation rate paradox in antimitotic chemotherapy. *Molecular biology of the cell*, 23(1):1–6, 2012.
- [150] S.M. Gross L. Karginov J.C. Lagarde-L.M. Heiser F. Mohammadi, S.Visaga and A.S. Meyer. A lineage tree-based hidden Markov model quantifies cellular heterogeneity and plasticity. *Communications Biology*, 5(1):1258, 2022.
- [151] K.R Singleton M.A.R. Strobl R. Washart K.C. Wood K J. Maltas, S.T. Killarney and K.B. Wood. Drug dependence in cancer is exploitable by optimally constructed treatment holidays. *Nature Ecology & Evolution*, 8(1):147–162, 2024.
- [152] S. Bandara J.J. Sims H. Hudson D.Chai Diana J. Roux, M. Hafner and P.K. Sorger. Fractional killing arises from cell-to-cell variability in overcoming a caspase activity threshold. *Molecular Systems Biology*, 11(5):803, 2015.
- [153] John L Quinn, Samantha C Patrick, Sandra Bouwhuis, Teddy A Wilkin, and Ben C Sheldon. Heterogeneous selection on a heritable temperament trait in a variable environment. *Journal of Animal Ecology*, 78(6):1203–1215, 2009.
- [154] A.R. Barr F.A. Hughes and P. Thomas. Patterns of interdivision time correlations reveal hidden cell cycle factors. *eLife*, 11:e80927, 2022.
- [155] R. Chait K. Schneider F. Signorino-Gelo s. Leibler Y. Wakamoto, N. Dhar and J.D. McKinney. Dynamic persistence of antibiotic-stressed mycobacteria. *Science*, 339(6115):91–95, 2013.
- [156] T.J. Kobayashi and Y. Sugiyama. Fluctuation relations of fitness and information in population dynamics. *Physical Review Letters*, 115(23):238102, 2015.

- [157] H. Dhiman D. Ivanoiu N. Slaven-S.P. Hong A. Rocca S. Bravaccini S. Ravaioli R. Noberini T. Bonaldi D. Rosano, E. Sofyali and L. Magnani. Unperturbed dormancy recording reveals stochastic awakening strategies in endocrine treated breast cancer cells. *bioRxiv*, 2021.
- [158] M.L. Devitt and J.P. Stafstrom. Cell cycle regulation during growth-dormancy cycles in pea axillary buds. *Plant molecular biology*, 29:255–265, 1995.
- [159] W. Hamer. Epidemiology old and new. 1928.
- [160] R. Ross. *The Prevention of malaria*. J. Murray, 1910.
- [161] A.G. McKendrick W.O. Kermack and G.T. Walker. Contributions to the mathematical theory of epidemics. ii. —the problem of endemicity. *Proceedings of the Royal Society of London. Series A, Containing Papers of a Mathematical and Physical Character*, 138(834):55–83, 1932.
- [162] W. O. Kermack and A. G. McKendrick. Contributions to the mathematical theory of epidemics: V. analysis of experimental epidemics of mouse-typhoid; a bacterial disease conferring incomplete immunity. *Journal of Hygiene*, 39:271 – 288, 1939.
- [163] H. Abbey. An examination of the reed-frost theory of epidemics. *Human Biology*, 24(3):201–233, 1952.
- [164] F. Brauer, J. Wu P. Van den Driessche, and L.J.S. Allen. *Mathematical epidemiology*, volume 1945. Springer, 2008.
- [165] Roy M R. M. Anderson. Mathematical and statistical studies of the epidemiology of hiv. *Aids*, 3(6):333–346, 1989.
- [166] R.R. Sarkar S. Mandal and S. Sinha. Mathematical models of malaria-a review. *Malaria journal*, 10:1–19, 2011.
- [167] J. He B. Zhu F. Wang-L. Tang M. Kleinsasser D. Barker M. C. Eisenberg L. Wang, Y. Zhou and P. X. Song. An epidemiological forecast model and software assessing interventions on the covid-19 epidemic in china. *Journal of Data Science*, 18(3):409–432, 2020.

- [168] R. Ross. An application of the theory of probabilities to the study of a priori pathometry.—part i. *Proceedings of the Royal Society of London. Series A, Containing Papers of a Mathematical and Physical Character*, 92(638):204–230, 1916.
- [169] M.R. Spiegel. *Laplace transforms*. McGraw-Hill New York, 1965.
- [170] A. Feldstein and J.R. Sopka. Numerical methods for nonlinear volterra integro-differential equations. *SIAM Journal on Numerical Analysis*, 11(4):826–846, 1974.
- [171] S. Maxwell. Rational prescribing: the principles of drug selection. *Clinical medicine*, 16(5):459–464, 2016.
- [172] P.J. Antsaklis and A.N. Michel. *Linear systems*, volume 8. Springer, 1997.